International Workshop on

Structure and Dynamics of the Oceanic Lithosphere/Asthenosphere System

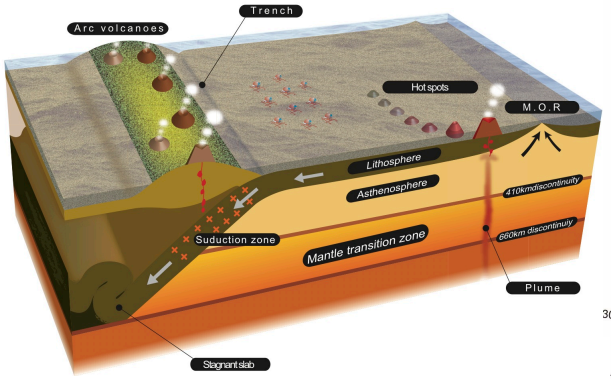

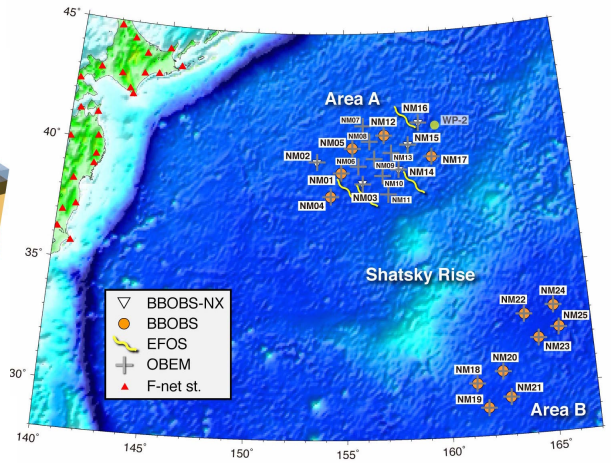

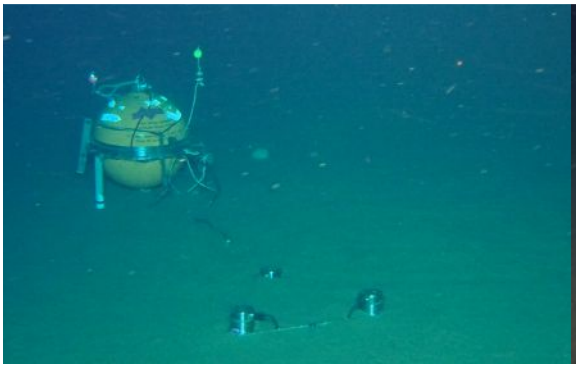

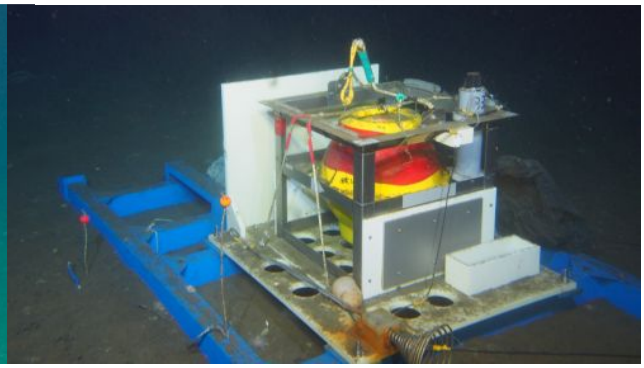

March 3-6, 2015
Hotel Matsushima Taikanso, Miyagi, Japan

EARTHQUAKE RESEARCH INSTITUTE
UNIVERSITY OF TOKYO

JAMSTEC

科研費
KAKENHI

International Symposium on

Structure and Dynamics of the Oceanic Lithosphere/Asthenosphere System

March 3-6, 2015

Hotel Matsushima Taikanso, Miyagi, Japan

March 3, 2015

Reception 16:00~ near the Hotel's Front Desk

Icebreaker 21:30~22:30 at Main Bar "*Grand Prix*" (1st Floor)

March 4, 2015

Breakfast 7:00~ at Restaurant "*La Ceres*" (B1 Floor)

- Session 1: NOMan Project (8:30-10:10) at "*Fuji-A*" (1st Floor)
[Max. 25 min/presentation including Q&A]
Chair: **Hitoshi Kawakatsu** (Earthquake Research Institute, University of Tokyo)

Hisashi Utada (Earthquake Research Institute, University of Tokyo)
Five years of Normal Oceanic Mantle Project

Akiko Takeo (Hokkaido University)
Seismic Anisotropy in the Oceanic Lithosphere/Asthenosphere System from Broadband Dispersion Survey

Yuki Abe (Earthquake Research Institute, University of Tokyo)
Receiver function analysis of NOMan BBOBS data: searching for seismic-LAB

Kiyoshi Baba (Earthquake Research Institute, University of Tokyo)
Thermal and compositional variety of the old oceanic upper mantle beneath the northwestern Pacific: Implications from electrical conductivity

Coffee Break (10:10-10:40)

- Session 2: Other Projects (10:40-12:00) at "*Fuji-A*" (1st Floor)
[Max. 25 min/presentation including Q&A]
Chair: **Daisuke Suetsugu** (JAMSTEC)

Pei-ying Lin (Lamont-Doherty Earth Observatory, Columbia University)
Anisotropic shear-velocity structure of the lithosphere-asthenosphere system in the central Pacific from the NoMelt experiment

Rob. L. Evans (Woods Hole Oceanographic Institution)
The Electrical Structure of the Central Pacific Upper Mantle Constrained by the NoMelt Experiment

Donald W. Forsyth (Brown University)
Lithospheric and Asthenospheric Structure Beneath Old, "Normal" Seafloor South of the Shatsky Rise, Western Pacific

Lunch 12:15~13:15 at Hall "*Chiyo*" (1st Floor)

-Session 3: OBS observations (13:30-15:10) at "*Fuji-A*" (1st Floor)
[Max. 25 min/presentation including Q&A]
Chair: **Hajime Shiobara** (Earthquake Research Institute, University of Tokyo)

Takehi Isse (Earthquake Research Institute, University of Tokyo)
Surface wave and P-wave tomography using BBOBS data of NOMan Project

Azusa Shito (Kyoto University)
Seismic structure of the oceanic lithosphere inferred from Po/So waves

Brian Kennett (Australian National University)
Po/So propagation in the Pacific and inferences on lithosphere heterogeneity

Nozomu Takeuchi (Earthquake Research Institute, University of Tokyo)
Scattering features of oceanic lithosphere and asthenosphere

Coffee Break (15:10-15:40)

-Session 4: Sunduction zones/Models (15:40-17:20) at "*Fuji-A*" (1st Floor)
[Max. 25 min/presentation including Q&A]
Chair: **Takehiko Hiraga** (Earthquake Research Institute, University of Tokyo)

Tim Stern (Victoria University of Wellington)
A high resolution seismic reflection image for the oceanic LAB (Lithosphere-Asthenosphere Boundary), beneath southern North Island, New Zealand

Teh-Ru Alex Song (University College London)
Subduction of lithosphere/asthenosphere system: insights from shear-wave splitting observations

Andrea Tommasi (Geosciences Montpellier, CNRS & Univ. Montopellier)
Heterogeneity and anisotropy in the shallow suboceanic mantle: constraints from observations in natural systems

Shun-ichiro Karato (Yale University)
Origin of the LAB (lithosphere-asthenosphere-boundary) and the MLD (mid-lithosphere discontinuity)

-Discussions (17:20~)

Banquet 19:00~ at Hall "*Chiyo*" (1st Floor)

March 5, 2015

Breakfast 7:00~ at Restaurant "*La Ceres*" (B1 Floor)

-Session 5: Boundaries/Anisotropy (8:30-10:10) at "*Fuji-A*" (1st Floor)
[Max. 25 min/presentation including Q&A]
Chair: **Takashi Tonegawa** (JAMSTEC)

Nicholas Schmerr (University of Maryland)
Imaging the Lithosphere-Asthenosphere Boundary with Underside Reflections

Catherine A. Rychert (University of Southampton)
Seismic imaging of lithosphere and melt beneath Iceland and other hotspots

Shuichi Kodaira (JAMSTEC)
Active-source seismic study in the Northwestern Pacific ocean basin

Jean-Paul Montagner (IPG Paris)
Mid-Lithospheric discontinuity below oceans from seismic surface waves

Coffee Break (10:10-10:40)

-Session 6: Rheology/Mechanics (10:40-12:00) at "*Fuji-A*" (1st Floor)
[Max. 25 min/presentation including Q&A]
Chair: **Satoru Honda** (Earthquake Research Institute, University of Tokyo)

Takehiko Hiraga (Earthquake Research Institute, University of Tokyo)
Diffusion creep of peridotite

Ben Holtzman (Lamont-Doherty Earth Observatory, Columbia University)
What can we infer about upper mantle thermodynamic state from the NOMELT shear velocity structure ?

Tomoo Katsura (University of Bayreuth)
Estimation of temperature, pressure, and water-content dependence of olivine creep from indirect observations

Photo 12:00~

Lunch 12:15~13:15 at Restaurant "*La Ceres*" (B1 Floor)

-Poster session (13:30-15:00)

Coffee Break (15:00-15:30)

-Session 7: Melt/Water/…. (15:30-17:10) at "*Fuji-A*" (1st Floor)
[Max. 25 min/presentation including Q&A]
Chair: **Kiyoshi Baba** (Earthquake Research Institute, University of Tokyo)

Fabrice Gaillard (CNRS-University of Orleans)
The Geodynamics of Melting in the Asthenosphere and its Geophysical Expression

Takashi Yoshino (Okayama University)
Electrical conductivity anisotropy in partially molten peridotite under shear deformation

Marc M. Hirschmann (University of Minnesota)
Small degree melting in the "normal" asthenosphere- models and challenges

Yasuko Takei (Earthquake Research Institute, University of Tokyo)
Temperature, grain size, and chemical controls on polycrystal anelasticity over a broad frequency range extending into the seismic range

-Discussions (17:10~)

Dinner/Reception 19:00~ at Main Dining "*Shiosai*" (7th Floor)

March 6, 2015

Breakfast 7:00~ at Restaurant "*La Ceres*" (B1 Floor)

-Session 8: Global/Deep earth perspectives (8:30-10:10) at "*Fuji-A*"
[Max. 25 min/presentation including Q&A]
Chair: **Hisayoshi Shimizu** (Earthquake Research Institute, University of Tokyo)

Daisuke Suetsugu (JAMSTEC)
Seismic discontinuities of the mantle transition zone beneath the northwestern Pacific Ocean

Pascal Tarits (Université de Bretagne Occidentale)
Is there a deep carbonatite signature beneath the East African Rift?

Göran Ekström (Lamont-Doherty Earth Observatory, Columbia University)
Oceanic Mantle Structure from Global Tomography

Thorsten Becker (University of Southern California)
Oceanic boundary layer structure and dynamics from seismological imaging and geodynamic modeling

Coffee Break (10:10-10:40)

-Session 9: Future directions (10:40-11:30) at "*Fuji-A*" (1st Floor)
[Max. 25 min/presentation including Q&A]
Chair: **Hisashi Utada** (Earthquake Research Institute, University of Tokyo)

Hajime Shiobara (Earthquake Research Institute, University of Tokyo)
BBOBS observations in the NOMan project and the future

Hitoshi Kawakatsu (Earthquake Research Institute, University of Tokyo)
Pacific Array

-Discussions (11:30~)

[Departure]

Posters [March 5, 13:30-15:00] at "*Fuji-B*" (1st Floor)

(P1 ~ P29)

P1. **Devesh Walia** (North-Eastern Hill University)
Tectonosphere over the NE Indian Region

P2. **Manabu Morishige** (Kyoto University)
A new type of 3D small-scale convection in the mantle wedge

P3. **Chris Havlin** (Lamont-Doherty Earth Observatory, Columbia University)
Melt migration beneath thinning lithosphere

P4. **Kosuke Yabe** (Earthquake Research Institute, University of Tokyo)
Synthesis and high-temperature creep experiments on polycrystalline Fe-bearing olivine

P5. **Takashi Tonegawa** (JAMSTEC)
Seismic structure for oceanic crust and sediment in the northwestern Pacific

P6. **Tim Stern** (Victoria University of Wellington)
Data and interpretation of the LAB beneath Wellington, New Zealand from the SAHKE experiment

P7. **Maki Hata** (Earthquake Research Institute, University of Tokyo)
Thermal structure and melt fraction distribution in a mantle wedge determined from the 3-D electrical conductivity structure beneath Kyushu in the Southwest Japan Arc

P8. **Sanae Koizumi** (Earthquake Research Institute, University of Tokyo)
Synthesis of textured olivine aggregate using colloidal processing under high magnetic field

P9. **Satoru Honda** (Earthquake Research Institute, University of Tokyo)
Tomographic slabs and simulated slabs

P10. **Hatsuki Yamauchi** (Earthquake Research Institute, University of Tokyo)
Elasticity, anelasticity, and viscosity of a polycrystalline material at near-solidus temperatures

P11. **Noriko Tada** (JAMSTEC)
Three-dimensional electrical conductivity structure in the upper mantle in the French Polynesia

P12. **Adam Sarafian** (Woods Hole Oceanographic Institution)
Experimental Determination of the H2O-undersaturated Peridotite Solidus

P13. **Emily Sarafian** (Woods Hole Oceanographic Institution)
The Electrical Structure of the Central Pacific Upper Mantle Constrained by the NoMelt Experiment

P14. **Tetsuo Matsuno** (Earthquake Research Institute, University of Tokyo)
Electromagnetic investigation into mantle transition zone by using the NOMan project data

P15. **Kenta Sueyoshi** (Earthquake Research Institute, University of Tokyo)
Continuous measurements of electrical conductivity and viscosity of synthesized lherzorite samples during partial melting under gradual temperature change

P16. **Tadashi Nakakoji** (Earthquake Research Institute, University of Tokyo)
High precision measurement of activation energy of creep of polycrystalline forsterite

P17. **Akane Ohira** (Yokohama National University)
Crustal and upper mantle structure in southeast of Shatsky Rise in the northwestern Pacific revealed from seismic reflection and refraction data

P18. **Genta Maruyama** (Earthquake Research Institute, University of Tokyo)
Observations of Grain- to Multi-Grain Scale Deformation: Mechanism of the Development of Crystal Preferred Orientation during Diffusion Creep

P19. **PeiYing Patty Lin** (Lamont-Doherty Earth Observatory, Columbia University)
Anisotropic shear-velocity structure of the lithosphere-asthenosphere system in the central Pacific from the NoMelt experiment

P20. **Celia Eddy** (Lamont-Doherty Earth Observatory, Columbia University)
Anisotropy in the Pacific upper mantle from inversion of a surface-wave dispersion dataset

P21. **Makoto Uyeshima** (Earthquake Research Institute, the University of Tokyo)
Electrical conductivity structure beneath backarc side of Chubu District, Central Japan, revealed by the Network-MT survey

P22. **Nobukazu Seama** (Kobe University)
Upper mantle electrical resistivity structures beneath the Indian Ocean and back-arc basins

P23. **Masahiro Osako** (National Museum of Nature and Science)
Thermal conductivity of omphacite, jadeite and diopside under pressure : Implication for the role of eclogite in subduction slab

P24. **Makoto Yamano** (Earthquake Research Institute, University of Tokyo)
Multiple-scale heat flow anomalies seaward of the Japan Trench associated with deformation of the incoming Pacific plate

P25. **Akira Yoneda** (ISEI, Okayama Univ.)
Single Crystal Elasticity of Iron Bearing Perovskite and Post Perovskite Analog

P26. **Naoto Ogawa** (Earthquake Research Institute, University of Tokyo)
Observation and modeling of SKS splitting parameters measured in Japan with Hi-net

P27. **Kazunori Yoshizawa** (Hokkaido University)
On the effects of parameterization for radial anisotropy constrained by Love and Rayleigh waves

P28. **Hiroshi Ichihara** (JAMSTEC)
A preliminary resistivity model of the back arc region in the NE Japan arc based on marine and island MT da**ta**

P29. **Hitoshi Kawakatsu** (Earthquake Research Institute, the University of Tokyo)
A new parameter characterizing radial anisotropy

P30. **Takehi Isse** (Earthquake Research Institute, the University of Tokyo)
Oceanic plate structures beneath the northwestern Pacific Ocean revealed by explosion experiments

P31. **Kiyoshi Baba** (Earthquake Research Institute, the University of Tokyo)
Possibility of anisotropic structure in electrical conductivity for the upper mantle beneath northwestern Pacific Ocean

Oral Presentations

Five years of Normal Oceanic Mantle Project

Hisashi Utada[1], Hitoshi Kawakatsu[1], Hajime Shiobara[1], Kiyoshi Baba[1], Takehi Isse[1], Daisuke Suetsugu[2], and the NOMan Project team

[1]Earthquake Research Institute, University of Tokyo, Japan,
[2]Japan Agency for Marine-Earth Science and Technology

The oceanic mantle is an important region to understand the Earth system, because more than 2/3 of the surface is covered by oceanic area. Normal Oceanic Mantle (NOMan) project focuses on the "normal oceanic mantle" in particular. Here the normal oceanic mantle can be defined as the oceanic mantle without disturbance by vertical motion of mantle flow such as mid oceanic ridges, subduction zones, or hotspots. In NOMan project, we try to solve a couple of most fundamental questions concerning the normal oceanic mantle as follows.

First question is on the cause of the asthenosphere, which is a lubricating layer below oceanic plate (lithosphere). Plate tectonics is based on a concept that a rigid lithosphere moves over a weaker asthenosphere, and thus the precise knowledge of its lubrication mechanism is fundamental to understand how our planet works.

Second question concerns the amount of water within the Earth, particularly in the mantle transition zone (MTZ) below the normal oceanic mantle. The presence of water is one of the properties characterizing the planet Earth. Because the MTZ minerals have very high water solubility (~ 3 wt.%) as compared with that of upper or lower mantle minerals (Inoue et al., 2010), accurate estimation of water content in the normal MTZ is essential to understand the Earth's total water budget. The water in the MTZ may also have significant contribution to the dynamics of the whole lithosphere asthenosphere system (e.g., Karato, 2012).

The NOMan project has been carried out for 5 years since 2010. It aims to solve these two questions from observational approach, collaborating with laboratory experimental and computational approaches. We selected two target areas (A and B) of similar seafloor age (about 130 and 140 Ma, respectively) in the northwestern Pacific Ocean (Fig. 1) where the mantle below is supposed to be normal. Area A is originally intended to be the main study area where mantle structure is estimated as accurately as possible by conducting long-term and highest quality seafloor observations. Area B is regarded as the sub-study area so as to generalize the result from area A by confirming the consistency. This presentation will give an overview of five years of the NOMan project, especially of its observational activities, and present a summary of preliminary results so far obtained.

In June 2010, we deployed a small array consisting of 5 (both seismic and EM) sites and started data acquisition from area A, which we call the NOMan pilot experiment. The main observation by long-term seafloor arrays in areas A and B was started by installation cruises carried out in November 2011 and in August 2012, deploying state-of-the-art ocean bottom seismic and electromagnetic instruments (BBOBS-NXs and EFOSs) in area A that are handled by ROV for installation and recovery (Fig. 2). Conventional instruments (BBOBS and OBEM of free-fall/self-pop-up type) were also deployed both in areas A and B. These instruments

were all originally developed by our group. Most of instruments of the pilot experiment were recovered by the cruise in August 2012. New type instruments (BBOBS-NXs and EFOSs) which were installed in 2012 were equipped with batteries sufficient for 2 years of deployment, but conventional instruments (BBOBSs and OBEMs) only for one year or so. Therefore, we conducted a cruise by W/V Kaiyu in August 2013 to maintain the observation array by recovering and re-deploying respective instruments. The Kaiyu cruise in 2013 provided us the first seafloor data from area B as well as those from the eastern part of area A. In June 2014, we conducted another W/V Kaiyu cruise, in which we recovered most of conventional instruments in area A after conducting a controlled source seismic experiment by using explosive sources. In September 2014, we completed a recovery cruise by R/V Kairei with ROV Kaiko-7000II. By these two cruises conducted in 2014, we have recovered instruments from all sites except only one site (NM03) where a few EM instruments were left and are still operating. Thus, we can say that NOMan project has completed its observation phase and entered into its analyzing phase.

The seafloor age of each study area varies approximately between 127 and 133 Ma in area A and between 135 and 145 in area B. So the age difference is only about 10 Ma, which was thought small enough for the temperature difference between two areas to be ignored at the first order approximation. We originally intended to generalize the results obtained in area A where we have plenty of high-quality data, by confirming that corresponding results in area B show close similarity to them. However, results of array analysis of the surface waves indicate significant difference in the lithosphere-asthenosphere structure between areas A and B. Results of other seismic analyses also suggest the presence of lateral heterogeneity between the areas and possibly within each array. Multi-station seafloor magnetotelluric (MT) data from these two areas also show different features. Furthermore, comparison with MT results in surrounding areas obtained by previous projects (Baba et al., 2010) implies the presence of further significant heterogeneity in the old oceanic mantle in the northwestern Pacific toward the subduction zone. For the moment, we are trying to invert each of NOMan geophysical dataset as accurately as possible so as to characterize the mantle structure and its lateral variation. Later we try to clarify the cause for these lateral variabilities, as it can be one of the key issues to understand the lithosphere-asthenosphere system in the old oceanic mantle.

The high-quality data obtained by the long-term seafloor observation of NOMan project are also used to investigate the MTZ structure. In particular, electric field data obtained by EFOS (with 2 km electrode separation) provide longer period responses with higher sensitivity to the electrical conductivity of the MTZ than OBEM data. Resulting MT (ratio of horizontal electric to magnetic fields variations) and GDS (ratio of vertical to horizontal magnetic field variations) responses are both roughly consistent with the NW Pacific semi-global 1-D model (Shimizu et al., 2010). This indicates that the MTZ structure below the study region has weak lateral variation (well approximated by a 1-D model) and is consistent with the conductivity of MTZ minerals containing about 0.1 wt.% water or less (Yoshino & Katsura, 2013). The seismic data will also be jointly used to constrain the amount of water in the same region.

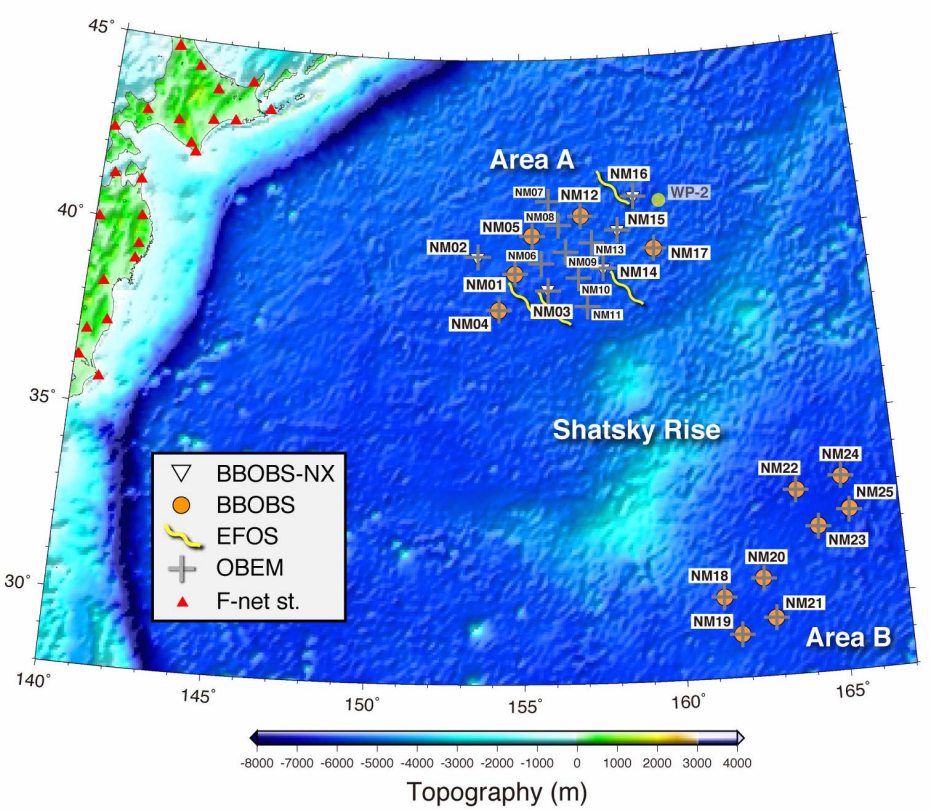

Fig. 1. Site distribution in the NOMan study areas A and B.

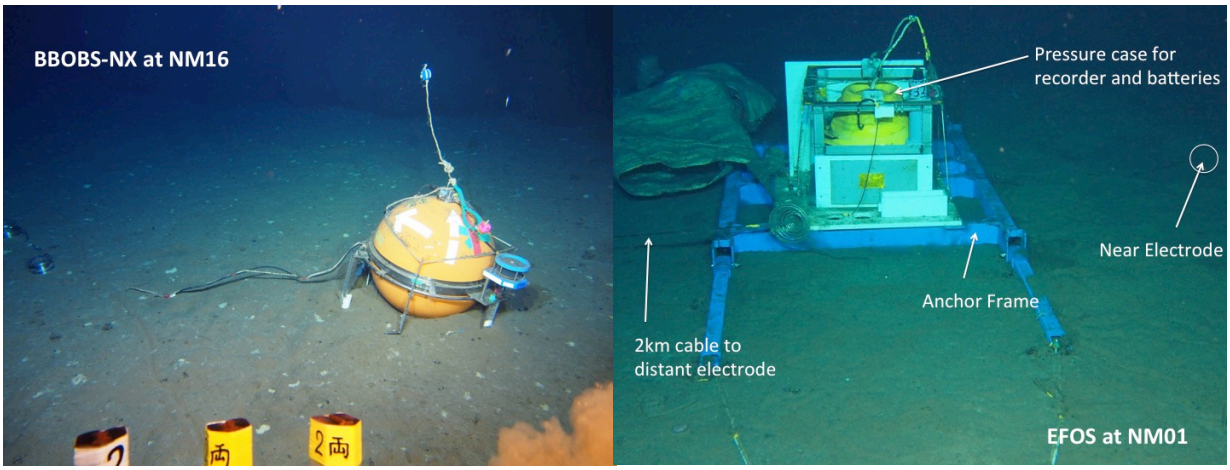

Fig. 2. BBOBS-NX installed at NM16 (left) and EFOS installed at NM01 (right).

Seismic Anisotropy in the Oceanic Lithosphere/Asthenosphere System from Broadband Dispersion Survey

Akiko Takeo[1], Takehi Isse[2], Kiwamu Nishida[2], Hitoshi Kawakatsu[2], Hajime Shiobara[2], Hiroko Sugioka[3], Aki Ito[3] and Hisashi Utada[2]

[1]Department of Natural History Sciences, Hokkaido University, Japan, [2]Earthquake Research Institute, University of Tokyo, Japan, [3]Japan Agency for Marine-Earth Science and Technology, Japan

Seismic structure in the oceanic uppermost mantle has been determined from 1960s to discuss the growth and dynamics of oceanic lithosphere/asthenosphere system. Recent studies have been especially focused on seismic anisotropy as the recorder of past deformations or the indicator of layered heterogeneity. In this study, we applied multi-band surface-wave analysis method to array records of broadband ocean bottom seismometers (BBOBSs) for the purpose of improving the depth resolution of the uppermost mantle structure and obtaining the intensity of seismic anisotropy, which are difficult for conventional tomography studies.

The BBOBS records are those obtained by the Normal Oceanic Mantle (NOMan) project from 2010 to 2014 in the northwest (area A) and southeast (area B) of Shatsky Rise, the northwest Pacific Ocean. For each array, we measured average phase velocities of Rayleigh and Love waves from ambient noise at a period range of 5-30 s and from teleseismic waveforms at a period range of 30-100 s (Takeo et al. 2013, 2014). The measurements were then used to obtain one-dimensional radially anisotropic model in each region. We also measured phase velocities of Rayleigh waves as a function of propagation azimuths to obtain one-dimensional azimuthally anisotropic model in each region.

The obtained radially anisotropic model for the area A shows 2-3% lower shear-wave velocity at a depth range of 70-150 km compared that for the area B. The velocities are almost same at shallower depths. Since the two areas have similar seafloor ages of 130 Ma and 140 Ma, plate-cooling models should give similar thermal structure and the seismic velocities for two areas. The observed difference indicates different potential temperature and/or composition for two areas less than 1000 km apart.

The intensity of radial anisotropy is estimated to be about 6% by assuming a constant value at a depth range of 10-150 km. The value is slightly large compared to that in the younger seafloor, the Shikoku Basin (Takeo et al. 2013). The peak-to-peak intensity of azimuthal anisotropy is ~5% at depth shallower than 40 km, and becomes 2% at deeper depth. An additional analysis shows stronger or similar radial anisotropy at depths deeper than 50 km compared to shallower depths. These results indicate that the intensities of radial and azimuthal anisotropies are almost same at top of the lithosphere, whereas the radial anisotropy is stronger than azimuthal anisotropy at deeper depths. The stronger radial anisotropy requires AG-type olivine or the apparent anisotropy due to layered heterogeneity.

Although the discussion is still diverse, this study shows the possibility of the "broadband dispersion survey" to determine radially and azimuthally anisotropic model in the uppermost mantle by deploying ~10 BBOBSs at the target seafloor like the refraction survey

to determine structure at depths shallower than ~20 km.

References

[1] Takeo, A., K. Nishida, T. Isse, H. Kawakatsu, H. Shiobara, H. Sugioka, and T. Kanazawa, Radially anisotropic structure beneath the Shikoku Basin from broadband surface wave analysis of ocean bottom seismometer records, J. Geophys. Res., 118(6), 2878–2892, doi:10.1002/jgrb.50219, 2013.

[2] Takeo, A., D. W. Forsyth, D. S. Weeraratne, and K. Nishida, Estimation of azimuthal anisotropy in the NW Pacific from seismic ambient noise in seafloor records, Geophys. J. Int., 199(1), 11–22, doi: 10.1093/gji/ggu240, 2014.

Receiver function analysis of NOMan BBOBS data: searching for seismic-LAB

Yuki Abe[1], Hitoshi Kawakatsu[1], Akiko Takeo[2], Hajime Shiobara[1], Takehi Isse[1], Hiroko Sugioka[3], Aki Ito[3] and Hisashi Utada[1]

[1]Earthquake Research Institute, University of Tokyo, Japan
[2]Natural History Sciences, Graduate School of Science, Hokkaido University, Japan
[3]Japan Agency for Marine-Earth Science and Technology, Japan

We have conducted seismic observation around the Shatsky Rise in the northwest Pacific Ocean at 18 stations equipped with a broadband ocean bottom seismometer (BBOBS) for understanding the structure of the Earth's interior and the mechanism of plate motion (Normal Mantle Project). It is important to estimate the upper mantle structure beneath these stations, for revealing existence of partial melt and/or water in the oceanic uppermost mantle. The upper mantle structure has been estimated from surface wave dispersion data of this project (Takeo, 2014, Thesis, Univ. Tokyo). However, it is difficult for such an analysis to detect sharp velocity change with depth. Therefore, we performed receiver function (RF) analyses for detecting sharp velocity change in the upper mantle.

We calculated P- and S-wave receiver functions (PRF, SRF) with waveform data obtained from the BBOBSs. We used teleseismic events occurring between June 2010 and September 2014, whose magnitudes are over 5.5. Epicentral distances of the events used for calculating PRF are between 30° and 90°, and those for calculating SRF are between 55° and 90°. Careful handling is required for analyzing the data obtained at stations northwest side of the Shatsky Rise (area A) because the data are largely affected by reverberations in the thick sediment layer. We applied a Gaussian low pass filter whose cut off frequency is 0.1 Hz to SRF because noise level of the observed waveforms in the frequency domain around 0.2 Hz is high. A Gaussian filter whose cut off frequency is 0.05 Hz was applied to PRF for preventing contamination by reverberations in the sediment layer. We averaged PRFs and SRFs for each station, and obtained a broad negative peak on averaged PRFs and a broad positive peak on averaged SRFs, between 5 s and 15 s. Both these peaks may be due to a velocity drop with depth in the upper mantle that possibly corresponds to seismic LAB. We synthesized PRF and SRF with a model, which contains a discontinuity at depths between 30 km and 150 km, where velocity decreases between 0% and 20% with depth, and search for a model that explains PRF and SRF obtained at each station.

Thermal and compositional variety of the oceanic upper mantle beneath the northwestern Pacific: Implications from electrical conductivity

Kiyoshi Baba[1], Noriko Tada[1,2], Tetsuo Matsuno[1], Hisayoshi Shimizu[1], Luolei Zhang[3], Pengfei Liang[1], and Hisashi Utada[1]

[1]Earthquake Research Institute, The University of Tokyo, Japan
[2]Japan Agency for Marine-Earth Science and Technology, Japan
[3]Tongji University, China

Oceanic upper mantle beneath the northwestern Pacific has large-scale lateral heterogeneity that is impossible to attribute to just an age-dependency of the thermal structure based on a cooling of homogeneous mantle with age. This surprising fact was revealed from seafloor magnetotelluric (MT) data collected in three areas, northwest (Area A) and southeast (Area B) of the Shatsky Rise, and off the Bonin Trench (Area C), through the Normal Oceanic Mantle Project and the Stagnant Slab Project. One-dimensional structures of electrical conductivity representing each area show significant difference in the thickness of the upper resistive layer that may be interpreted as cool lithosphere. The thickness of the layer that is more resistive than 0.01 S m^{-1} is ~90 km for Area A, ~100 km for Area B, and ~180 km for Area C. The conductivity below the resistive layer is similar to ~0.03 S m^{-1} for all areas. The thermal structures for the lithospheric age representing the areas (130, 140, and 147 Ma for Areas A, B, and C, respectively) predicted from a simple plate cooling model are almost identical and thus cannot reproduce such variations in electrical conductivity. Then, in this study, thermal and compositional states of the mantle beneath the three areas were investigated to discuss the cause of the variations. Combination of five model parameters, electrical conductivity of crust (σ_{crust}), mantle potential temperature (T_P), thickness of thermally conductive plate (h), and H_2O and CO_2 contents (C_{H2O} and C_{CO2}) in the asthenospheric mantle were searched by forward modeling and the $\chi 2$ misfit between the MT responses observed and predicted were assessed with 95% acceptable level. The possibility of partial melting was taken into account by a self-consistent manner comparing to the solidus of peridotite that is reduced by H_2O and CO_2. We assumed that the mantle conductivity may be represented by the mixture of hydrous olivine and hydrous carbonated melt. The results suggest a possible influence of a mantle up-welling associated with the formation of the Shatsky Rise to the mantle beneath Areas A and B although these areas are away from the bathymetric anomaly.

Session 2-1

Anisotropic shear-velocity structure of the lithosphere-asthenosphere system in the central Pacific from the NoMelt experiment

P.Y. Lin[1], J. B. Gaherty[1], G. Jin[1], J.A. Collins[2], D. Lizarralde[2], R. Evans[2], G. Hirth[3] and H. F. Mark[2]

[1]Lamont-Doherty Earth Observatory of Columbia University
[2]Woods Hole Oceanographic Institution
[3]Brown University

The Recent theoretical models of the seismic properties of mantle rocks predict seismic velocity profiles for mature oceanic lithosphere that are fundamentally inconsistent with the best observations of seismic velocities in two ways. Observations of strong positive velocity gradients with depth, and a very sharp and very shallow low-velocity asthenosphere boundary (LAB), both suggest that non-thermal factors such as bulk composition, mineral fabric, grain size, and dehydration play important roles in controlling the formation of the lithosphere, and thus the underlying LAB. There is little consensus on which of these factors are dominant, in part because observations of detailed lithosphere structure are limited. To address this discrepancy, we conducted the NoMelt experiment on ~70 Ma Pacific lithosphere between the Clarion & Clipperton fracture zones. The experiment consists of a 600x400 km array of broad-band ocean bottom seismometers (OBS) and magnetotelluric instruments, and an active-source reflection/refraction experiment. Here we characterize the shear-velocity structure and its seismic anisotropy across the lithosphere-asthenosphere system beneath the array using surface-wave dispersion from ambient noise and earthquake-generated Rayleigh waves. Of the 27 deployed instruments, 21 were recovered, all of which produced useful data on the seismometer and the differential pressure gauge in the 20-200 s period band. Energetic, high S/N Rayleigh waves and useful love waves are observed from over 19 and 7 events with Mw > 6.5 respectively. Models of shear velocity as a function of depth derived from intra-array Rayleigh-wave phase velocities are characterized by a thin lid with high velocity overlying a modest low velocity zone and can pretty well fit the dry-olivine with a simple cooling model with no melt adding in. The Rayleigh-wave phase velocities show remarkable strong and clear evidence of azimuthal anisotropy with fast-directions parallel to fossil spreading (78^{o} azimuth) at periods of 14-60 seconds. The anisotropy appears to weaken slightly at intermediate periods, before strengthening and rotating slightly towards a more EW direction at the longest periods. The model of seismic anisotropy as a function of depth suggests strong seafloor-spreading fabric in the upper 60 km and the strength is relatively week in the asthenosphere. In addition to azimuthal anisotropy from shear velocity variations, the result from P-wave refraction data suggest that the upper 10-15 km of the mantle are strongly anisotropic, with velocities in the direction of fossil seafloor-spreading ~8% faster

than in the ridge-parallel direction. Love waves are difficult to observe on OBS data due to the higher noise levels generated observed on the horizontal components. We have measured the average phase velocity in the frequency band between 20-60 sec. Love-wave propagation in the ocean basins produces a complex multi-mode wavefield. The relatively contributions of fundamental and higher modes are strongly frequency dependent for the oceanic upper mantle.

The Electrical Structure of the Central Pacific Upper Mantle Constrained by the NoMelt Experiment

Rob. L. Evans[1], Emily Sarafian[2], John Collins[1], Jimmy Elsenbeck[1], Glenn Gaetani[1], James B. Gaherty[3], Greg Hirth[4], Daniel Lizarralde[1]

[1]Geology and Geophysics, Woods Hole Oceanographic Institution, Woods Hole, MA
[2]MIT-WHOI Joint Program, Woods Hole Oceanographic Institution, Woods Hole, MA
[3]Lamont-Doherty Earth Observatory of Columbia University, Palisades, NY
[4]Geological Sciences Department, Brown University, Providence, RI

The NoMelt Experiment imaged the mantle beneath 70 Ma Pacific seafloor with the aim of understanding the transition from the lithosphere to the underlying convecting asthenosphere. Seafloor magnetotelluric data from four stations were analyzed using 2-D regularized inverse modeling. The preferred electrical model for the region contains an 80 km thick resistive (>10^3 Ωm) lithosphere with a less resistive (~50 Ωm) underlying asthenosphere. The preferred model is isotropic and lacks a highly conductive (≤10 Ωm) layer under the resistive lithosphere that would be indicative of partial melt. We first examine temperature profiles that are consistent with the observed conductivity profile. Our profile is consistent with a mantle adiabat ranging from 0.3 °C/km-0.5°C/km. A choice of the higher adiabatic gradient means that the observed conductivity can be explained solely by temperature. In contrast, a 0.3°C/km adiabat requires an additional mechanism to explain the observed conductivity profile. Of the plausible mechanisms, H_2O, in the form of hydrogen dissolved in olivine, is the most likely explanation for this additional conductivity. Our profile is consistent with a mostly dry lithosphere to 80 km depth, with bulk H_2O contents increasing to between 25 and 400 ppm by weight in the asthenosphere with specific values dependent on the choice of laboratory dataset of hydrous olivine conductivity and the value of mantle oxygen fugacity. The estimated H_2O contents support the theory that the rheological lithosphere is a result of dehydration during melting at a mid-ocean ridge.

Session 2-3

Lithospheric and Asthenospheric Structure Beneath Old, "Normal" Seafloor South of the Shatsky Rise, Western Pacific

Donald W. Forsyth[1] and Dayanthie Weeraratne[2]

[1]Department of Earth, Environmental and Planetary Sci., Brown University, Providence, US
Department of Geological Sciences, California State University, Northridge, CA, US

South of the Shatsky Rise, the oldest identifiable magnetic anomalies (150-160 Ma) form a magnetic bight with the two limbs of the bight perpendicular to each other. The perpendicularity makes this an ideal location to distinguish between fossil azimuthal anisotropy frozen into the lithosphere and anisotropy created by shear deformation below the plate. In addition, the seafloor in this area is largely unaffected by subsequent Cretaceous volcanism, with original abyssal hill topography still evident, so it may form an end member example of very old, "normal" oceanic mantle.

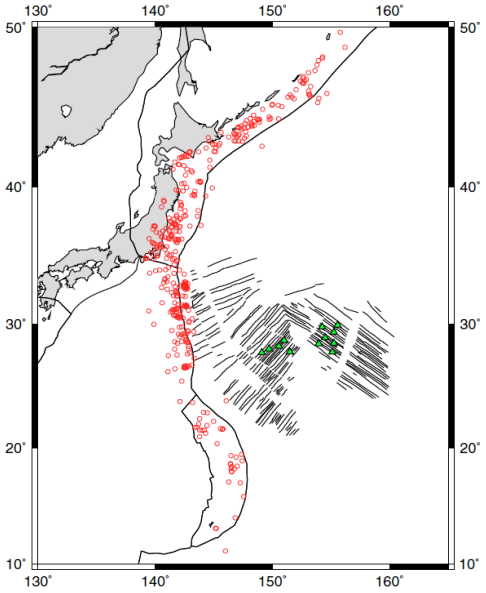

To study the upper mantle structure in this area, we deployed 16 broadband, ocean bottom seismometers for one year, separated into arrays of 8 OBSs on each limb of the magnetic bight. Although the failure of several of the instruments compromised some aspects of the experiment, we were able to use P and Pn (or Po) phases from nearby subduction zone events, ambient noise, and Rayleigh waves generated by teleseismic earthquakes to constrain anisotropic velocity structure and attenuation. The dominant anisotropic effects are clearly related to the fossil seafloor spreading direction on each limb. Pn anisotropy is strong (~ 10% peak-to-peak variation with azimuth θ) with the fastest direction rotated about 15° counterclockwise from the spreading direction on both limbs. Surprisingly, the 4θ variation is almost as strong as the 2θ variation (Figure 2), which cannot be explained with simple orthorhombic symmetry.

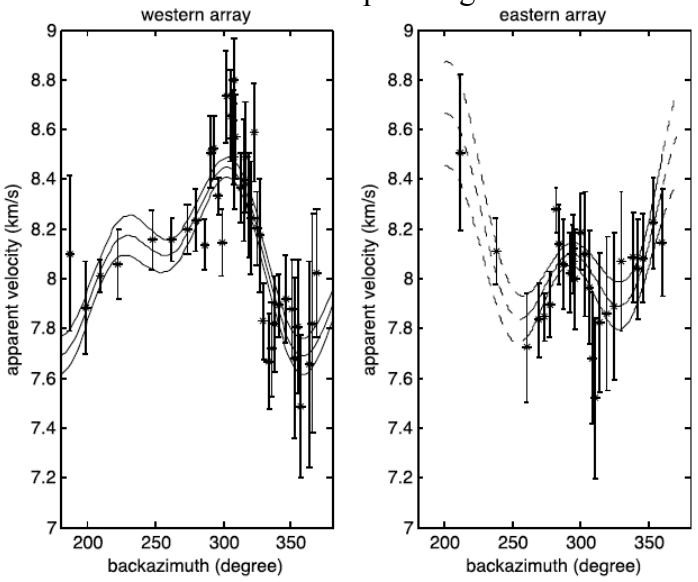

We speculate that there must be a change in orientation with depth.

Rayleigh waves also are azimuthally anisotropic. The fast directions on the two limbs are roughly perpendicular to each other, but rotated somewhat more from the spreading direction than the Pn fast direction. Unfortunately, the long period data (>50 s) is not good enough to really resolve the depth extent of the azimuthal anisotropy. The azimuthal anisotropy is smaller on the eastern limb than the western limb, perhaps because there is a much bigger difference between absolute plate motion direction and spreading direction on the eastern limb.

Rayleigh wave dispersion requires azimuthally averaged shear velocities in the uppermost mantle lithosphere to be on the order of 4.80 km/s. This high velocity is distinctly different than the relatively uniform 4.65 km/s in the upper 50 km found by Nishimura and Forsyth (1989) for seafloor older than 110 Ma. The difference is probably due to the inclusion of hot spot or Cretaceous flood basalt influenced regions with thickened crust or altered upper mantle in N&F.

Attenuation of P waves finds Q values in the asthenosphere that are quite low, on the order of values found in the asthenospheric wedge above subducting plates. The attenuation is required to be frequency dependent, although the favored coefficient of frequency dependence is not compatible with the Rayleigh wave attenuation at longer periods. Either the frequency coefficient needs to be at the limit of acceptable values for P, or there is an absorption peak or the P attenuation is strongly affected by scattering.

Surface wave and P-wave tomography using BBOBS data of NOMan Project

Takehi Isse[1], Masayuki Obayashi[2], Hajime Shiobara[1], and NOMan project team

[1]Earthquake Research Institute, University of Tokyo, Japan,
[2]Japan Agency for Marine-Earth Science and Technology, Japan

The oceanic mantle is an important region to understand the Earth system, because more than 2/3 of the surface is covered by oceanic area. Since 1990s, seafloor observations by using newly developed long-term broadband ocean seismometers (BBOBSs) have been operated in the northwestern and center part of the Pacific Ocean. These observations have revealed the structures in and around the subduction zone in the Pacific Ocean and in the Pacific superswells, respectively. However, we have no observation and result in the normal oceanic regions.

Our “Normal Oceanic Mantle Project” (NOMan project) focuses on the ‘normal oceanic mantle’ in particular to reveal that (a) "What is the physical condition for the lithosphere-asthenosphere boundary (LAB)?" and (b) "Is the mantle transition zone (MTZ) a major water reservoir of the Earth?" The "normal" ocean floor is the best window to approach these questions as it allows us to see the inside of the Earth through it without the disturbance due to the thick and heterogeneous continental crust. The NOMan project is carried out for 5 years from 2010. It aims to solve these two questions from observational approach in two target areas in the northwestern Pacific Ocean where the mantle supposed to be normal. Hereafter, one target area at the northwestern side of the Shatsky Rise is called as 'Area A', and the other is 'Area B'.

We have determined the three-dimensional upper mantle structure in the northwestern Pacific Ocean by using surface wave tomography technique and P-wave tomography technique.

We have used a surface wave tomography technique in which multimode phase speed of the Rayleigh wave are measured and inverted for a 3-D shear wave speed structure by incorporating the effects of finite frequency and ray bending.

In this method, we consider the ray bending so that we analyze the whole Pacific Ocean. We obtained a new upper mantle seismic structure from surface wave using data of permanent seismic station, previous BBOBS observations and NOMan project. The preliminary results suggest that upper mantle structures in Area A and B are not similar. Average 1-D shear wave velocity structure in Area A is consistent with Nishimura & Forsyth (1989), where as that in Area B is faster than that.

In P-wave tomography, we measured differential travel times of P-waves as the function of frequency between any two stations from the BBOBSs of the NOMan project and the land stations in the vicinity. Then we obtained a new P-wave tomography model by adding the data to the previous model (Obayashi et al., 2013) and taking the finite frequency effect into account for the frequency-depended differential travel times. This model shows slow

anomalies in the depth range between about 100 and 300 km near the Area A while no anomaly or slightly fast anomalies are observed near the Area B. These characteristics that the Area B is faster than the Area are consistent with the result of the surface wave tomography. Slow anomalies are observed below the Shatsky rise as well.

Session 3-2

Seismic structure of the oceanic lithosphere inferred from Po/So waves

Azusa Shito[1], Daisuke Suetsugu[2], and Takashi Furumura[3]

[1]Institute for Geothermal Science, Kyoto University, Japan,
[2]Department of Deep Earth Structure and Dynamics Research, JAMSTEC, Japan,
[3]Earthquake Research Institute, University of Tokyo, Japan,

Po/So waves which have high-frequency content, large amplitude, and long-duration travel through the oceanic lithosphere for large distance (up to 3000 km). The Po/So waves are developed by multiple forward scattering of P and S waves due to small-scale heterogeneities in the oceanic lithosphere. In order to study the origin of the small-scale heterogeneities, the Po/So waves are analyzed in the Philippine Sea Plate.

The Philippine Sea is one of the marginal seas of the Pacific Ocean. It is fundamentally divided into two regions bounded by the Kyushu-Palau Ridge, each is considered to have formed in different episodes of back-arc spreading and that western part (45-60 Ma) is older than eastern part (15-30 Ma) [e.g., Seno and Maruyama, 1984]. The comparison of the Po/So waves propagation in the different ages of the oceanic lithosphere is expected to reveal the origin of the small-scale heterogeneities.

Seismological observations using BBOBSs was conducted in the Philippine Sea from 2005 to 2008 as a part of the Stagnant Slab Project [Fukao et al., 2009], and high-quality Po/So waves from earthquakes in subducting Philippine Sea plate were recorded very clearly. The findings from the observed Po/So waves in the Philippine Sea plate are summarized as follows [Shito et al., 2014]. (1) The Po/So waves propagate even in youngest oceanic lithosphere (15 Ma) near the past spreading center of the Shikoku Basin. (2) The Po/So waves propagate much more effectively in older western part than younger eastern part of the Philippine Sea.

We investigate the mechanism of this propagation efficiency using numerical a Finite Difference Method simulations of 2-D seismic wave propagation. The comparison of the observed and calculated Po/So waves indicates that the age-dependence can be explained by the thickness of the heterogeneous lithosphere. The estimated thicknesses of the oceanic lithosphere are consistent with those obtained by a previous study based on receiver function analysis [Kawakatsu et al., 2009].

The results suggest that the oceanic lithosphere including the small-scale heterogeneities thicken with age. These small-scale heterogeneities may form continuously in oceanic lithosphere from the time of its formation at a spreading ridge, via the solidification of melts distributed in the asthenosphere.

Po/So propagation in the Pacific and inferences on lithosphere heterogeneity

B.L.N. Kennett[1] and T. Furumura[2]

[1] Research School of Earth Sciences, The Australian National University, Canberra, Australia
[2] Earthquake Research Institute, University of Tokyo, Japan,

In many parts of the ocean high-frequency seismic energy is carried to very great distances from the source. The onsets of the P and S energy travel with speeds characteristic of the mantle lithosphere. The complex and elongated waveforms of such Po and So waves and their efficient transport of high frequencies (> 10 Hz) implies a strong scattering environment. A critical role is played by shallow reverberations in the water and sediments, which link to propagation in a heterogeneous mantle. The nature of the Po and So phases are consistent with pervasive stochastic heterogeneity in the oceanic lithosphere with a horizontal correlation length (~10 km) much larger than the vertical correlation length (~0.5 km), with a similar "millefeuille" character to that proposed for the asthenosphere, by Kawakatsu et al. (2009).

In the western Pacific high-frequency seismic energy is carried to very great distances from the source. High frequency waves are often still visible more than 4000 km from the source. However, in the eastern part of the Pacific basin, equivalent paths show muted Po and weak, or missing, So. Weaker guided phases are also found across the younger Philippine Sea plate.

Once established, it is hard to eliminate such guided high-frequency Po and So energy in the mantle lithosphere by purely structural effects. Even sharp changes in lithospheric thickness or complex transitions at fracture zones only weaken the mantle ducted wavetrains, but Po and So remain distinct. In contrast, the effect of attenuation is much more severe and can lead to suppression of the So phase to below the noise level after passage of a few hundred kilometres. The differing characteristics of Po and So across the Pacific can therefore be related directly to the thermal state via the enhanced attenuation in hotter regions, such as spreading ridges and back-arc regions.

Scattering Features of Oceanic Lithosphere and Asthenosphere

Nozomu Takeuchi[1]

[1]Earthquake Research Institute, University of Tokyo, Japan,

Waveforms of scattered waves contain information for small-scale heterogeneities and intrinsic attenuation that cannot be resolved by seismic tomography. Analyses of scattered waves (i.e., coda envelopes) are therefore considered important, however, in many of previous studies, parameter search has been conducted by trial-and-error and was not very systematic (e.g, Shearer and Earle, 2004).

In this study, we develop a waveform inversion method of coda envelopes. The method allows us to systematically and fully exploit information included in the waveforms. We compute synthetic envelopes by Monte Carlo simulation that can take the effects of multiple scattering into account. The drawback was huge requirements for computational resources especially for computing partial derivatives with respect to model perturbations (i.e., computation of synthetic envelopes for various perturbed models), however we developed an efficient method for computing partial derivatives. The most time-consuming step is ray-tracing, but out method computes partial derivatives using the rays computed for the initial model. We therefore have to trace rays just once in the inversion, which greatly reduces the required CPU time.

We applied our method to data observed by NOMan BBOBS (i.e., data sampling an oceanic region) and data observed by NESSSArray (sampling a subduction zone). The envelopes observed by NOMan have unique features that cannot be observed in those by NECESSArray. First, in the vertical component of waveforms for closer distance (less than 15 degrees), we can observe very large S-coda that is probably caused by strong scattering in the oceanic lithosphere. Second, the amplitudes of coda envelopes fast decrease with distance, which is probably caused by low-Q in the oceanic asthenosphere. The results of our waveform inversion also support this interpretation.

References

Share, P.M. & Earle, P.S., 2004. The global short-period wavefield modelled with a Monte Carlo seismic phonon method, *Geophys. J. Int.*, **158**, 1103-1117.

A high resolution seismic reflection image for the oceanic LAB (Lithosphere-Asthenosphere Boundary), beneath southern North Island, New Zealand

Tim Stern[1], S.H. Henrys[2], D.A. Okaya[3], M.K. Savage[1], H. Sato[4], R. Sutherland[1,2], T. Iwasaki[4], J. Louie[5]

[1]Institute of Geophysics, Victoria University, Wellington, 6140, New Zealand

(tim.stern@vuw.ac.nz)

[2]Institute of Geological and Nuclear Sciences, Lower Hutt, 5010, New Zealand

[3]Department of Earth Sciences, University of Southern California, Los Angeles, CA 90210, USA

[4]Department of Earth Sciences, Tokyo University, Tokyo, 12345, Japan

[5]Seismological Laboratory, University of Nevada, Reno, NV 89557, USA

We present the first high-resolution, multichannel, seismic-reflection image for the base of an oceanic plate. There are three main findings from this experiment: i/ the existence of 10 km channel of rocks with reduced Vp (8-10% reduction) at the base of the plate, ii/ the sharp transition into the channel, and iii/ a measured thickness for the plate of 73 ± 1 km.

Our seismic reflection image is based on an 85 km-long, ~ 900 station deployment across the lower North Island of New Zealand. 12 x 500 kg explosive shots were used as seismic sources. Strong reflections at a two way travel time of 9-12 s define the top of the plate that dips to the NW at ~ 12-15 degrees. Between 27-32 s we identify a pair of reflections on some shot gathers that are interpreted to come from a reflection 90-100 km deep, that dips to the NW at 15 degrees. We interpret the reflection pair as marking a Lithosphere-Asthenosphere Boundary (LAB) zone at the base of the Pacific plate. Using all 12 shots we made a CDP-stacked image (maximum fold = 15) that shows the LAB as a double event (2-3 s apart) dipping roughly parallel to the top of the plate and Benioff zone. Shot quality varies but the highest frequencies we record from the base of the plate are ~ 14 Hz, suggesting a boundary zone < 1 km thick. Seismic amplitude attributes, calibrated to the reflection from the top of the plate, indicate P-wave speed drops off at least 8% across the LAB boundary. The double reflection at the LAB is interpreted to be a 10 km-thick layer of low seismic wave speed. Because it is so sharp it cannot be a thermal boundary and must represent some form of mechanical change. Previous attempts to explain the abruptness of seismic wave speed changes at the LAB have appealed to layered zones of ponded melt, or anelastic relaxation due to water accumulating beneath the LAB. Both mechanisms may explain our observations and both would point to low viscosity below the LAB. However, the fact we see a ~ 10 km thick channel, with strong acoustic impedances each side of the channel, suggests a shear zone where plate motion (~ 9 cm/y in hotspot reference frame) is taken up and strain rates of ~3 x 10^{-13} s^{-1} are generated. This interpreted, low wave-speed, low-viscosity, shear zone appears to be a key factor in allowing plates to slide with little resistance and therefore to allow plate tectonics to work.

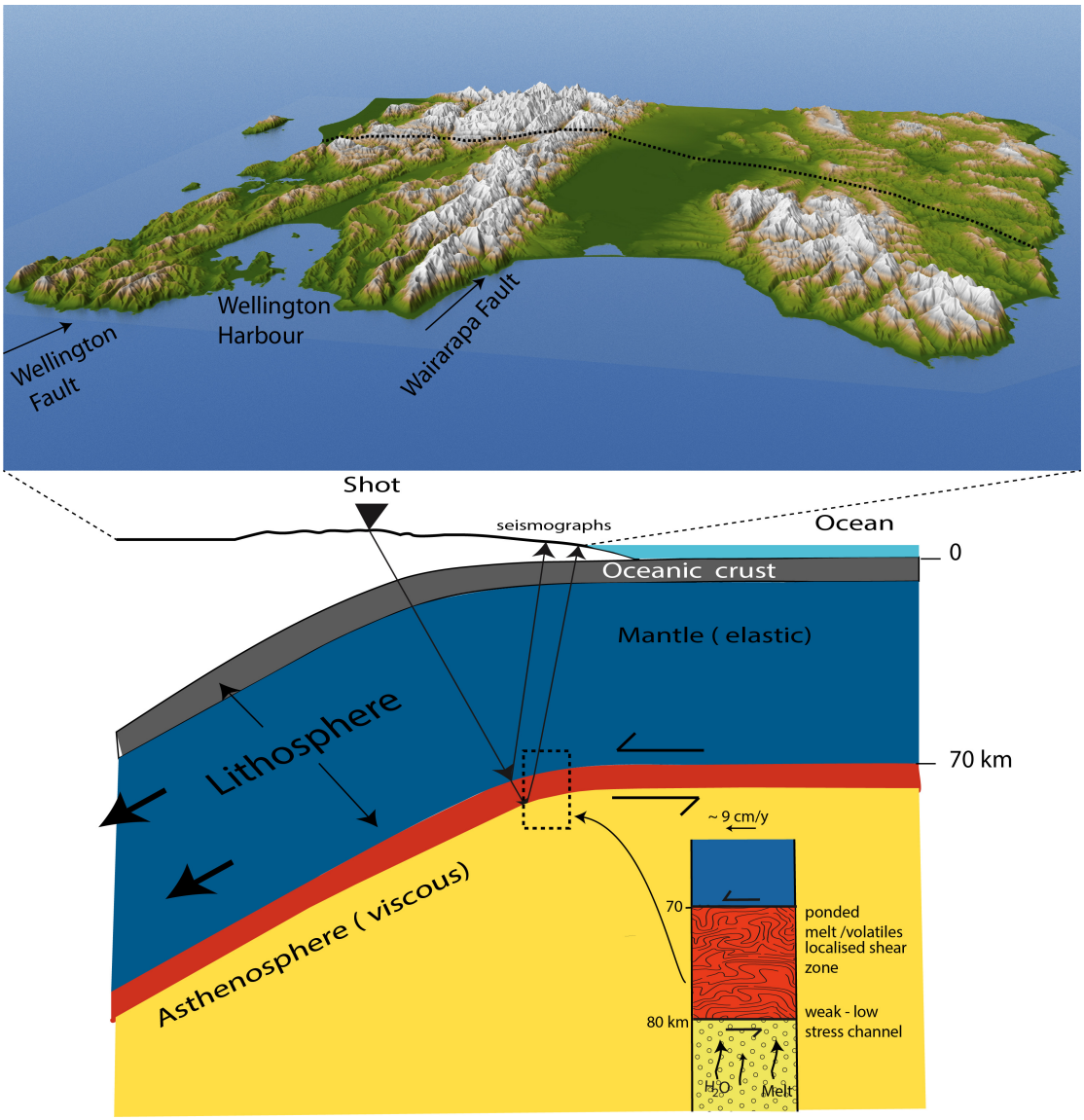
Wellington Fault
Wellington Harbour
Wairarapa Fault
Shot
seismographs
Ocean
0
Oceanic crust
Mantle (elastic)
Lithosphere
70 km
~ 9 cm/y
70
ponded melt /volatiles localised shear zone
80 km
weak - low stress channel
H2O
Melt
Asthenosphere (viscous)

Session 4-2

Subduction of lithosphere/asthenosphere system: insights from shear-wave splitting observations

Teh-Ru Alex Song[1] and Hitoshi Kawakatsu[2]

[1]Seismological Laboratory, Department of Earth Sciences, University College London, UK
[2]Earthquake Research Institute, the University of Tokyo, Japan

Subduction of oceanic asthenosphere is a simple concept to link the nature of oceanic asthenosphere, subduction zone flow field as well as mantle fabric. Among all, the fundamental of this scenario relies on the details of anisotropy symmetry in the oceanic asthenosphere and sub-slab mantle and how it modulates seismic observables such as multiple S waves radial anisotropy, surface wave radial anisotropy, azimuthal anisotropy and shear wave splitting. On the basis of global as well as regional SKS splitting dataset, Song and Kawakatsu (2012, GRL; 2013, EPSL) recently demonstrated the effect of strong radial anisotropy of oceanic asthenosphere in dictating sub-slab fast splitting pattern. Since subduction of oceanic asthenosphere predicts that the splitting pattern is incidence angle dependent, fast splitting directions and splitting times derived from the near-vertical SKS wave and the more oblique teleseismic S wave can be quite different in a given subduction zone, strongly depending on the back azimuth, incidence angle, and the inclination of symmetry axis in the sub-slab mantle, or slab dip.

We examine latest global source-side S wave splitting observations (Lynner and Long, 2014a) against asthenospheric anisotropy fabric highlighted by Song and Kawakatsu (2012). To emphasize the asthenospheric fabric and to avoid complex anisotropy associated with potential 3D mantle flows near small plates of high curvature, we first focus on observations near large subducting plates. As predicted, subducting asthenosphere reconciles two major conflicts among SKS and source-side S splitting observations: 1. Source-side S splitting direction in the slab up-dip direction is often at a high angle to the SKS splitting direction, which is generally parallel or sub-parallel to the trench. 2. Source-side S splitting time is often substantially larger than SKS splitting time.

However, there are cases where subduction of oceanic asthenosphere alone does not do well in predicting source-side S wave splitting observations, particularly where the age of the subducting slab is old (Lynner and Long, 2014b), e.g., Japan and Tonga subduction zones. Motivated by the success/failure of subducting asthenosphere against SKS and source-side S wave splitting observations, as well as observed anisotropy in the oceanic lithosphere, we re-examine SKS and source-side S wave splitting pattern through a subduction of lithosphere/asthenosphere system, a dipping two-layer anisotropy. In the oceanic lithosphere, we construct orthorhombic anisotropy elastic tensor consistent with radial anisotropy and azimuthal anisotropy imaged by recent global/regional surface wave tomography.

Our result indicates that, when the fast azimuthal anisotropy direction in the oceanic lithosphere is sub-parallel to the present day plate motion direction, subducting lithosphere can appear relatively “invisible” and the fast splitting direction is predominantly dictated by the subducting asthenosphere. In the cases where azimuthal anisotropy in the oceanic

lithosphere is strong and fast azimuth anisotropy direction is at an acute angle to the present day plate motion direction, subducting lithosphere and asthenosphere contribute to the apparent fast splitting direction.

In summary, subducting lithosphere/asthenosphere system can largely reconcile SKS and teleseismic source-side splitting patterns observed in large subducting plates without invoking complicated flow geometry. Strong anisotropy in the old oceanic lithosphere appears consistent with latest observations (e.g., Kodaira et al., 2014; Takeo et al., 2013, 2014) where the paleo-spreading is very fast (e.g., Song and Kim, 2012). Finally, we will discuss lithosphere/asthenosphere anisotropy symmetry constructed in this report against olivine petrofabric data summarized by Song and Kawakatsu (2013) and speculate on the change of mantle fabric in the oceanic lithosphere/asthenosphere system.

Session 4-3

Heterogeneity and anisotropy in the shallow suboceanic mantle: constraints from observations in natural systems

Andréa Tommasi[1]

[1]Geosciences Montpellier, CNRS & Univ. Montpellier, France

Geophysical observations indicate that the suboceanic mantle lithosphere and asthenosphere are both anisotropic and heterogeneous. Seismic anisotropy data is in general consistent with olivine crystal preferred orientations (CPO) formed by dislocation creep, with dominant [100] glide, in response to a velocity gradient between the plate and the deep mantle and progressively frozen in the plate by cooling. However, observations such as the apparent isotropy of SKS observed in some island stations, the high variability in delay time in SKS data, the small angular deviation of fast Pn propagation directions relative to fossil spreading directions, or the strong 4Θ component in Pn data in the western Pacific cannot be explained by this simple model. On the other hand, the clear SP conversions observed at depths corresponding to the lithosphere-asthenosphere boundary even beneath plunging slabs or the scattering of guided waves in the oceanic lithosphere call for a better understanding of the processes that may produce sharp velocity contrasts in the shallow mantle. The analysis of observations in ophiolites and mantle xenoliths from oceanic environments brings some constraints on the processes producing and destroying heterogeneity and anisotropy in the mantle. Ophiolites sample significant volumes of the very shallow oceanic mantle (uppermost 5 km). These data highlight the role of ridge-related processes in the formation of anisotropy and heterogeneity in the shallow mantle lithosphere and the feedbacks between deformation and melt in shallow LABs. Xenoliths, on the other hand, sample the entire mantle lithosphere, but in a discontinuous way and in domains which have been modified by plume activity. The analysis of a xenolith suite, which samples the entire mantle lithosphere beneath the Ontong Java plateau, corroborates numerical models that show minor erosion of the mantle lithosphere atop a plume. These data also highlight a variation in seismic anisotropy and the possible presence of a peridotite- pyroxenite layering formed mainly by reactive melt percolation in the mantle lithosphere. Calculation of seismic properties for these rocks indicate that although such a compositional layering does not produce anisotropy, in the garnet stability field it might produce significant velocity contrasts (>5%), which might explain some seismic observations such as the scattering of guided waves. It also shows that a change in orientation of the structures may result in seismic reflections or conversions, but only in limited situations. In addition, data in OJP mantle xenoliths also indicate that H contents in olivine are not solely controlled by partial melting and that metasomatism may effectively hydrate the lithospheric mantle, destroying the initial stratification formed in response to partial melting at the ridge. Caution should therefore be used in interpreting seismic conversions as due to variation in the hydration state of the mantle.

Origin of the LAB (lithosphere-asthenosphere-boundary) and the MLD (mid-lithosphere discontinuity)

Shun-ichiro Karato

Yale University, Department of Geology & Geophysics
New Haven, CT USA

In terms of geodynamics, the lithosphere-asthenosphere boundary (LAB) is essentially a rheological boundary, but inferring the rheological boundary from geophysical observations is challenging. Therefore geophysicists use either seismological methods or electromagnetic induction (e.g., MT) to obtain some hints as to the transition in the physical properties across the LAB with a hope to locate the rheological boundaries. However, in many cases, the properties that geophysicists could infer from their observations are only indirectly linked to the long-term rheological properties. Consequently, it is important to evaluate the advantages and the limitations of various geophysical tools in view of the micro-physics underlying these processes (elastic, non-elastic deformation, electrical conductivity) to understand how these geophysical observables are connected to the long-term rheological properties.

Among the most important and surprising observations that recent high-resolution (short wavelength) body-wave seismology brought to us is the occurrence of a substantial velocity drop at relatively low temperatures (~900 C with some regional variations). And in some localities, high and highly anisotropic electrical conductivity was inferred in the shallow asthenosphere. I will present a brief discussion on the interpretation of these observations with an aim to obtain some clue as to the link between these observations and long-term rheological properties.

I will show that a majority of these observations (seismological and electromagnetic induction observations) can be explained by sub-solidus mechanisms involving various crystalline defects (e.g., grain-boundaries, hydrogen-related point defects). These analyses show that a link between velocity reduction and long-term viscosity is indirect: a large velocity reduction can occur without a large reduction in long-term viscosity, and a large reduction in long-term viscosity can occur without a large reduction in seismic wave velocities. High and highly anisotropic electrical conductivity can be attributed to hydrogen-enhanced conduction. The link between geophysical observations and the long-term viscosity is more direct for electrical conductivity. My model predicts little change in electrical conductivity at the MLD, but a large change in conductivity at the continental LAB where seismic wave velocity changes little. Partial melting is nearly ubiquitous in the upper mantle but it does not change the physical properties so much because the melt content is limited in most cases.

Imaging the Lithosphere-Asthenosphere Boundary with Underside Reflections

Nicholas Schmerr[1]
Catherine A. Rychert[2], Nicholas Harmon[2], and Caroline Beghein[3]

[1]Department of Geology, University of Maryland, College Park, MD, USA
[2]Ocean and Earth Sciences University of Southampton, Southampton, SO14 3ZH, UK
[3]Department of Earth, Planetary, and Space Sciences, UCLA, Los Angeles, CA, USA

The lithosphere-asthenosphere boundary (LAB) separates the upper thermal boundary layer of a rigid, conductively cooling plate from the underlying ductile, convecting mantle. Many different mechanisms have been proposed over the years to explain the origins of this transition, but the boundary still remains enigmatic. The oceanic plates are ideal for testing hypotheses regarding the nature and evolution of a plate since they make up 70% of Earth's surface area and have a relatively simple geological histories. In addition, numerous studies have detected a regional, sharp seismic discontinuity near 30-120 km depth beneath the oceans (the Gutenberg, or G discontinuity), roughly coincident with the expected depth of the LAB. If associated with the LAB, this discontinuity enables direct seismic investigation of the changes in properties from the lithosphere to the asthenosphere.

Recent studies with SS precursors, receiver functions, surface waves, and ScS reverberations have expanded sampling of oceanic regions, with increased resolution and provocative results. Several possible explanations for the seismic properties of the G discontinuity have been proposed over the years, including aligned melts, anisotropy, volatile enrichment/depletion, and/or high asthenospheric temperatures. Here we use observations of the SS precursors to examine some of these possibilities, exploring the hypothesis that a strong sharp discontinuity may be caused by lateral variations in anisotropic structure, either from melt alignment, preserved anisotropic fabrics, or other mechanisms. To examine the anisotropy hypothesis, we stack a dataset of broadband SS waveforms (>30,000 seismograms) with bounce points sampling the central Pacific into azimuthal bins, with a particular focus on the regions underlying the Normal Oceanic Mantle (NOMan) Project deployment.

This analysis reveals azimuthal variation in the amplitude of the precursory waveforms in some regions, but a clear picture remains elusive owing to non-uniform azimuthal sampling of the Pacific by SS. In well-sampled regions, the negative polarity precursor associated with the lithosphere-asthenosphere transition appears where source-receiver paths are oriented perpendicular to the dominant direction of asthenospheric mantle flow. This observation suggests frozen in anisotropy in the lithosphere and/or anisotropic alignment of minerals or melt in the asthenosphere is capable of producing the necessary shear wave velocity reductions. Thus there appears there may be a strong azimuthal anisotropy component to the oceanic LAB discontinuity.

In the vicinity of the NOMan project, where absolute plate motion and fossil spreading directions are close to 90º, SS does not detect a negative seismic discontinuity, though in some stacks there exists evidence for a weak positive discontinuity. Given the

limited range in azimuthal sampling of this region, further investigations with other methods and new data are needed. Anisotropy is a likely factor necessary for forming discontinuities near LAB depth in oceanic regions and as suggested in other work, beneath and within the continental lithosphere.

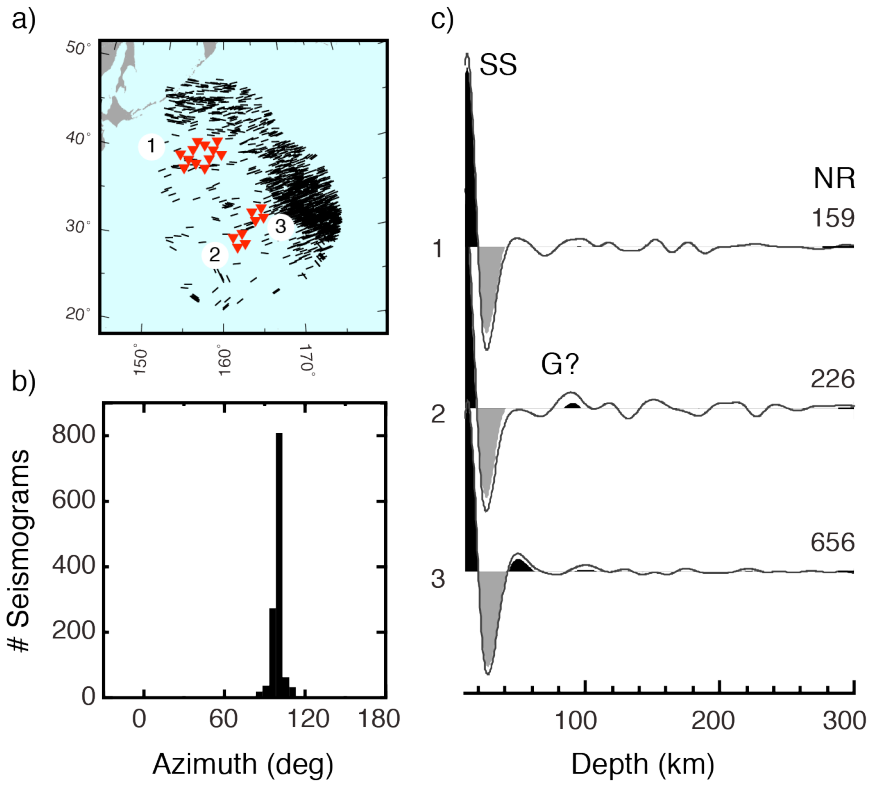

Figure 1. SS precursor results for upper mantle structure lying beneath the NOMan Project array. a) Location and orientation of SS bouncepoints halfway between the sources and receivers that sample within 1000 km of the NOMan Project ocean bottom observatories. b) Histogram of the SS bouncepoint azimuths sampling the region. c) Stacks for each subarray of stations, NR-number of records, with 95% confidence intervals from a bootstrap resampling shown as black shading for positive amplitudes, and gray for negative amplitudes.

Seismic imaging of lithosphere and melt beneath Iceland and other hotspots

Catherine A. Rychert[1] and Nicholas Harmon[1]

[1]National Oceanography Centre, Southampton, University of Southampton

Mid-ocean ridges and hotspots are ideal environments to constrain the definition of the lithosphere-asthenosphere boundary (LAB). LAB depth is expected to be significantly different in these regions depending on the definition of the plate. A purely thermal definition should deepen with age and distance from the ridge and shallow in the presence of a thermal plume anomaly. Whereas, compositional boundaries could exist at constant depth, possibly deepened by a thermal plume anomaly. We use S-to-P receiver functions to image upper mantle discontinuities beneath Iceland. We image a strong velocity decrease with depth at 45 – 80 km depth that is likely associated with the LAB. The phase undulates in depth, shallowest beneath the ridge, deeper in adjacent regions near ~9 My old seafloor, and shallow again at great distances from the ridge. The depth variations do not show simple thickening with seafloor age, even when effects of thermal plume anomalies are taken into account. The phase is also deeper and its magnitude greater than predictions for a thermal plate based on experimental constraints. The observation is better explained by a compositionally defined lithosphere with thickness dictated by temporal variation in thermal plume anomaly magnitude. Indeed, periodic plume pulsing has been hypothesized to explain variations in crustal thickness and gravity at the nearby Reykjanes Ridge. Our model suggests that thicker lithosphere is created at the ridge during times of plume pulsing, e.g., ~9 My. The thickened plate is subsequently rifted apart and thinner lithosphere is created until another pulse occurs. Comparison to experimental predictions for half-space cooling adjusted for regional crustal thickness suggests melt is likely required beneath the discontinuity to explain large velocity drops (~10 – 15%). Indeed, a velocity increase with depth is imaged at 160 km depth just east of Iceland that is likely the base of the melt rich layer. This suggests the plume approaches the island from the east, consistent recent eastward ridge jumps. Comparisons with other hotspot environments including Galapagos, Hawaii, and Afar suggest compositional components to the definition of the lithosphere, plume ascents that are non-vertical, and melt residence in the mantle at time and length scales that are seismically imageable.

Session 5-3

Active-source seismic study in the Northwestern Pacific ocean basin

Shuichi Kodaira[1,2] Akene Ohira[2] Gou Fujie[1] Yasuyuki Nakamura[1] Ryuta Arai[1] Seiichi Miura[1] Mikiya Yamashita[1] Takeshi Sato[1] Tsutomu Takahashi[1] Narumi Takahashi[1]

[1]R&D Center for Earthquake and Tsunami, JAMSTEC, Japan,
[2]Yokohama National University, Japan,

In order to understand structure, dynamics and alternation process of oceanic lithosphere in the older Pacific plate in the Northwestern Pacific, JAMSTEC have been acquiring active-source seismic data from the ocean basin to the outer rise region off the Japan – Kuril trench. Active-source seismic data obtained off the Kuril Trench, we observed very high P-wave velocities (Vp = 8.5–8.6 km/s) and strong anisotropy (8.5–9.8%) in the uppermost mantle immediately below oceanic crust in which lower crustal dipping reflectors (LCDRs) are seismically imaged with dominantly uniform dip and spacing. Our observations constrain interpretations of the origin of LCDRs and show that the LCDRs and anisotropy formed from shear in the ductile lower crust due to a drag force at the base of the crust caused by mantle flow moving faster than the spreading rate. Another data set acquired along 1130 km-long seismic profile in the ocean basin at the south of the Shatsky Rise show a remarkably different seismic characters from those we observed from the off-Kuril profile. Moho reflection along this profile is only clearly imaged at the southern end of the profile, but it's obscure or even not imaged in the most of the profile. Although we only deploy five OBSs along the Shatsky profile, the seismic velocity of the uppermost mantle is as high as we observed along the Kuril profile (i.e., ~ 8.5 km/s). It should be noted that most striking observation from the Shatsky data is strong deep mantle reflections; i.e., in a tentative model, we modeled the deep reflectors at 40 – 65 km deep in the mantle. We have not had a conclusive interpretation of this reflector, but further amplitude modeling may help to understand an origin of this reflector. In this presentation, we will review the active-source seismic study we have done off the Japan-Kuril trench and will present preliminary results from the Shatsky profile. (There is an accompanied poster presentation, Ohira et al., in this symposium. Details of the data from the Shatsky profile are shown in the poster.)

Session 5-4

Mid-Lithospheric discontinuity below oceans from seismic surface waves.

Jean-Paul Montagner[1], Gaël Burgos[1]
[1]Institut de Physique du Globe, Paris, France

The nature of Lithosphere-Asthenosphere boundary (LAB) is controversial according to different types of observations. Using a massive dataset of surface wave dispersions in a broad frequency range (15-300s), we have developed a 3D anisotropic tomographic model of the upper mantle at the global scale. It is used to derive maps of LAB from the resolved elastic parameters.

We investigate LAB distributions primarily below oceans according to three different proxies which correspond to the base of the lithosphere from the vertically polarized shear velocity variation at depth, the top of the radial anisotropy positive anomaly and from the changes in orientation of the fast axis of azimuthal anisotropy. The LAB depth determinations of the different proxies are basically consistent for each oceanic region. The estimates of the LAB depth based on the shear velocity proxy increase from thin (20 km) lithosphere in the ridges to thick (120-130 km) old ocean lithosphere. The radial anisotropy proxy presents a very fast increase of the LAB depth from the ridges, from 50 km to older ocean where it reaches a remarkable monotonic subhorizontal profile (70-80km).LAB depths inferred from azimuthal anisotropy proxy show deeper values for the increasing oceanic lithosphere (130-140 km).

The results present two types of pattern of the age of oceanic lithosphere evolution with the LAB depth. The shear velocity and azimuthal anisotropy proxies show age-dependent profiles in agreement with thermal plate models while the LAB based on radial anisotropy is characterized by a shallower depth, defining a subhorizontal interface with a very small age dependence for all three main oceans (Pacific, Atlantic and Indian). These different patterns raise questions about the nature of the LAB in the oceanic regions, of the formation of oceanic plates, and of the existence of a mid-lithospheric discontinuity within the oceanic lithosphere.

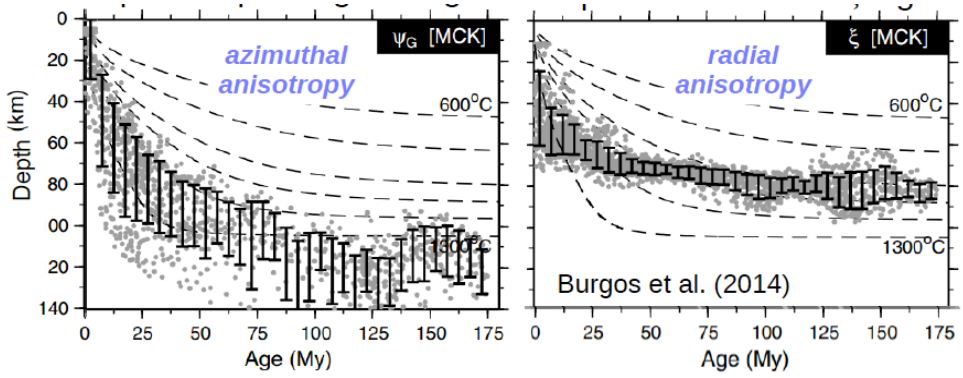

Diffusion creep of peridotite

Takehiko Hiraga[1], Genta Maruyama[1], Kousuke Yabe[1], Tomonori Miyazaki[1], Tadashi Nakakoji[1], Kenta Sueyoshi[1] and Sanae Koizumi[1]

[1]Earthquake Research Institute, University of Tokyo, Japan,

Recently, we have shown that a significant crystallographic preferred orientation (CPO) of forsterite develops during Newtonian flow of the forsterite aggregate (Miyazaki et al., 2013). Since the aggregate also exhibits (i) superplasticity (>>100 % tensile strain) (Hiraga et al. 2010), (ii) the same phase aggregation at the direction of compression (Hiraga et al. 2013) and (iii) essentially no change in grain shape before and after the deformation, we concluded that grain boundary sliding (GBS) should have accommodated a majority of the sample strain. We found that the preexisting grain shape, which is controlled by crystallography of forsterite, controls the CPO development and its pattern. Based on these results, we estimated that the preferential GBS at the boundary parallel to the specific crystallographic plane (i.e., low-index plane grain boundary) resulted in CPO. To examine this hypothesis, we imposed line markers to the lateral surface of samples which were subsequently deformed. Absence of intragranular deformation, significant grain boundary sliding and grain rotation were identified. Further, we found that the grain rotation was well reproduced by shear stress applied to the low-index plane boundary (see also Maruyama's poster). Based on these results, we propose that CPO can develop during diffusion creep at the condition where low-index plane boundaries develop in the rock. Such condition was examined in the mantle and was compared to the depth profile of seismic anisotropy.

Olivine aggregates synthesized from San Carlos olivine crystal and from reagents using sol-gel method show 1-2 orders of magnitude difference in their flow rate at the same stress condition during diffusion creep (Faul and Jackson 2007; Hirth and Kohlstedt 1995; Hansen et al. 2011). Such discrepancy yields an uncertainty for applying an experimentally determined flow law to nature. We applied a different technique to fabricate olivine aggregates with similar Fe content with the previous studies. Nano-sized highly pure powders were used to prepare ~100 nm grain size mineral powders through solid state reaction at high temperature condition. Such powders were sintered to obtain highly dense and fine-grained olivine aggregate. We deformed such aggregates under a control of oxygen fugacity showing the similar strength with the aggregate from sol-gel method. Further, our Fe-free aggregate exhibits the similar strength (see also Yabe and Nakakoji's posters).

Diffusion creep of olivine aggregate has been understood based on classic models of Nabarro-Herring or Coble creep and also based on point defect chemistry mainly controlled by ferric iron. We will present that such classic view on diffusion creep of peridotite may require alternative models.

What can we infer about upper mantle thermodynamic state from the NOMELT shear velocity structure ?

Ben Holtzman, Chris Havlin, Pei-ying Lin, James Gaherty
Lamont Doherty Earth Observatory, Columbia University

Inferring the thermal-mechanical structure of oceanic plates and the shallow upper mantle informs our understanding of the thermal evolution of the mantle and the driving forces for plate tectonics. Despite many efforts on this problem, open questions remain: What is the mantle potential temperature? Is there an ambient melt fraction? What is the thermo-mechanical origin and geodynamic meaning of the low velocity zone (between about 100-200 km)? How coupled are the plates to the immediately underlying asthenosphere-- and to the deeper convecting mantle? Is there small scale convection beneath oceanic lithosphere? If so, at what distance from the ridge does the onset of this convection occur? How does this convection affect melt and heat extraction from the upper mantle? The NOMELT experiment was designed to address aspects of the evolution of oceanic lithosphere that the MELT experiment could not, and is a fortuitous companion study to the NOMAN experiment.

In this preliminary work, we present efforts to forward model the isotropic Vs structure, with the aim of characterizing the uncertainty that each aspect of this problem bring to the interpretation of thermodynamic state. We start with a series of thermal models for the upper mantle, the classic half-space cooling model and plate models. We include variations with (a) constant thermal properties (heat capacity, thermal expansivity, thermal conductivity) and (b) pressure and temperature dependent thermal properties and thus density. We then calculate the effects of thermodynamic state variables on the mechanical properties including anharmonic elastic, steady state viscous and anelastic. We include effects of melt on the elastic modulus from Takei, 1998. From these, we calculate the unrelaxed and relaxed Vs, using the Andrade model scaling (Jackson and Faul, 2010; hereon JF10) and soon the Maxwell scaling approach (e.g. Takei et al., 2014). We include effects of melt that induce rapid change in viscosity and anelasticity at very small melt fractions (<<1%), demonstrated by recent experimental results on olivine (Faul and Jackson, 2007) and Borneol rock analog (McCarthy and Takei, 2011), incorporated into the JF10 Andrade model. Thus, we can explore the potential effects of melt and temperature on Vs and thus the interpretation of thermodynamic state, due to their strong trade-offs.

We find that (a) can nicely fit the NOMELT Vs profile, while in the more realistic case (b) a single potential temperature cannot fit both the plate structure (~20-100km) and the underlying upper mantle structure (200-325 km)-- the plate appears to have emerged from a lower potential temperature than the current state of the deep region. However, this discrepancy in potential temperature can be reconciled by including only a small amount of melt (<1%), providing one possible solution. We will build on these results by incorporating the Maxwell scaling model for attenuation, and effects of grain size. Eventually, grain size, melt distribution, stress and other properties will be coupled self-consistently in the forward models to a greater degree. With the current limited range of models, we cannot infer the presence or absence of small scale convection. In future work, receiver functions, body wave attenuation and electrical conductivity will all be predicted and compared to measurements to reduce the number of potential solutions.

Session 6-3

Estimation of temperature, pressure, and water-content dependence of olivine creep from indirect observations

Tomoo Katsura[1], Hongzhan Fei[1,2] and Wang Lin[1]

[1]Bayerisches Geoinstitut, University of Bayreuth, Japan
[2]Institute for Study of the Earth's Interior, Okayama University, Japan

Knowledge of rheological properties of mantle minerals is essential for understanding the mantle dynamics. Although a variety of information about them has been obtained by direct deformation experiments, the strain-rate conditions in laboratory deformation apparatus are by many orders of magnitude higher than in the nature. In addition, pressure and temperature conditions achievable by precise deformation apparatus are limited. Such gaps may cause misinterpretation about the mantle dynamics. For this reason, it is necessary to examine the results of deformation experiment by independent techniques. Results of 4 series of experiments to help us estimate temperature (T), pressure (P), and water content (C_{H_2O}), dependence of olivine creep are presented in this talk.

1) Measurement of Si lattice diffusion coefficient (${D_{Si}}^{Latt}$) of forsterite

The ${D_{Si}}^{Latt}$ is the most basic information to investigate rheological properties of silicate minerals. We measured ${D_{Si}}^{Latt}$ of synthetic-forsterite single crystal as a function of T, P, and C_{H_2O}, and obtained activation energy of ${\Delta E_{Si}}^{Latt}$ =410±50 kJ/mol, activation volume of ${\Delta V_{Si}}^{Latt}$ = 2±2 cm^3/mol, and the C_{H_2O} exponent of ${r_{Si}}^{Latt}$=0.32±0.03. Thus, the P and C_{H_2O} dependences of olivine creep are expected to be small.

2) Measurement of Si grain-boundary diffusion coefficient (${D_{Si}}^{GB}$) of forsterite

The ${D_{Si}}^{GB}$ is essential to investigate the Coble diffusion creep of silicate minerals. We measured ${D_{Si}}^{GB}$ of fine-grained (300-400 nm) polycrystalline forsterite also a function of T, P, and C_{H_2O}, and obtained ${\Delta E_{Si}}^{GB}$ =220±30 kJ/mol, ${\Delta V_{Si}}^{GB}$ = 4±2 cm^3/mol, and ${r_{Si}}^{GB}$ = 0.26±0.07. The C_{H_2O} dependence of ${D_{Si}}^{GB}$ is even smaller than ${D_{Si}}^{Latt}$. The Coble creep is not expected effectively enhanced by water incorporation.

3) Dislocation recovery of olivine deformed in the [100](010) and [001](010) slip systems

The dislocation creep under high-T and low strain-rate ($\dot{\varepsilon}$) conditions is expected controlled by dislocation climb. We conducted dislocation recovery experiment to olivine single crystals with C_{H_2O} up to 30 ppm deformed in the [100](010) and [001](010) slip systems to estimate T and P dependences of dislocation climb mobility (${k^{climb}}$). We obtained ${\Delta E_{[100](010)}}^{climb} = 400 \pm 30$ and ${\Delta E_{[001](010)}}^{climb} = 410 \pm 40$ kJ/mol, ${\Delta V_{[100](010)}}^{climb} = 2.7 \pm 0.2$ and ${\Delta V_{[001](010)}}^{climb} = 2 \pm 1$ cm^3/mol. Thus, the T and P dependences are found comparable in these two slip systems. The ${\Delta E^{climb}}$'s are found identical to ${\Delta E_{Si}}^{Latt}$. The ${\Delta V^{climb}}$'s are slightly higher than ${\Delta V_{Si}}^{Latt}$, but lower than ${\Delta V_{Si}}^{GB}$. Hence, it is expected that the dislocation creep should dominate the Coble diffusion creep in deeper regions.

4) Formation of sub-grain boundary of olivine deformed in the [100](010) slip system

Dislocation glide could be essential for olivine creep even under high-T and low-$\dot{\varepsilon}$ conditions corresponding to the deep upper mantle. In order to estimate T and P dependence of dislocation-glide mobility (k^{glide}), we observe the trapping rate of dislocations by sub-grain boundaries in olivine deformed in the [100](010) slip system. The preliminary results show $\Delta E_{[100](010)}{}^{\mathrm{glide}} = 550 \pm 50$ kJ/mol and $\Delta V_{[100](010)}{}^{\mathrm{glide}} = 7 \pm 2$ cm^3/mol. These values are significantly larger than $\Delta E_{[100](010)}{}^{\mathrm{climb}}$ and $\Delta V_{[100](010)}{}^{\mathrm{climb}}$, respectively.

The Geodynamics of Melting in the Asthenosphere and its Geophysical Expression

Fabrice Gaillard, Guillaume Richard, Malcolm Massuyeau, David Sifré, Leila Hashim, Emmanuel Gardes[1]

[1]Institut des Sciences de la Terre, Université d'Orléans, Orléans, France

The top of the asthenosphere is imaged as a global layer of S-wave velocity reductions that is well seen underneath oceanic lithospheres and yields an increasingly weak signal underneath increasing old and thick lithosphere. It remains to be investigated whether this is broadly observed or not, but this region of the Earth's mantle also appears to be a very good electrical conductor in contrast with the resistive lithosphere. In this presentation, recent advances in petrology, physical properties of melts and melt-peridotite aggregates are gathered to demonstrate that such geophysical signals are compatible with a small fraction of volatile-rich melts embedded in the peridotite.

These incipient melts are triggered by small amounts of water and carbon dioxide contained in the peridotite and these melts are exclusively stable in the P-T region defined by the Asthenosphere. These melts are extremely rich in incompatible and volatile elements, and are low in density and viscosity. They are formed at depths of ca. 300-150 km and are solidified at 50 km underneath young lithosphere and down to >200 km underneath cratons due to the well-known cooling with ages. Such a distribution of incipient melts perfectly matches the depths of the top of the asthenosphere identified by various geophysical surveys in different tectonic settings. Incipient melts therefore define a column of melting that varies from thick underneath oceanic lithosphere to very thin, almost elusive, underneath cratons, which is also what is deduced from geophysical observations.

Buoyant and low in viscosity, these melts can migrate at a rate faster than the convection of the solid mantle. Incipient melting in the convective asthenosphere must then naturally trigger melt accumulation at the upper bound of their stability, that is, at 50-70 km underneath the oceanic lithosphere and at 200 km underneath cratons. Two phase-flow computations (solid+liquid) in a convecting asthenosphere show a definitive enrichment in incipient melts at the Lithosphere-Asthenosphere Boundary at the level of the volume percent underneath oceanic lithospheres. Depending on the choice of the physical parameters (permeability, viscosity of the liquid & solid, initial melt fractions), the thickness of the melt-rich layer is at the level of 1 to 6 km, satisfying a broad series of geophysical observations. In addition of providing a natural mechanism for melt ponding at the LAB, this process also enriches in CO_2 the source region of intraplate magmatism.

Electrical conductivity anisotropy in partially molten peridotite under shear deformation

Takashi Yoshino[1] and Baohua Zhang[1,2]

[1]Institute for Study of the Earth's Interior, Okayama University, Japan
[2]Institute of Geochemistry, Chinese Academy of Sciences, Guiyang, Guizhou 550002, China

Ocean floor magnetotelluric (MT) investigations revealed a high-conductivity layer (HCL) with high anisotropy characterized by higher conductivity in the direction parallel to plate motion. This has been observed beneath the southern East Pacific Rise (Evans et al., 2005; Baba et al., 2006) and beneath the edge of the Cocos plate at the Middle America trench offshore of Nicaragua (Naif et al., 2013). To account anisotropic conductivity, two major hypotheses have been proposed, hydration of mantle minerals, especially olivine (Evans et al., 2005), and partial melting (Yoshino et al., 2006; Naif et al., 2013). Experimental studies on the conductivity of single crystal hydrous olivine (Yoshino et al., 2006; Poe et al., 2010; Yang, 2012) showed the small effect of water on electrical conductivity in olivine and the small magnitude of the conductivity anisotropy. In contrast Dai and Karato (2014) experimentally demonstrated that hydrous olivine has the large effect of water and the large conductivity anisotropy based on measurement at high temperatures. However, the low storage capacity of water in olivine coexisting with peridotite mineral assemblage at depth of the oceanic asthenosphere is around 50 ppm owing to partitioning with other mantle phases (Hirschmann et al., 2009; Férot and Bolfan-Casanova, 2012). Such small amount of water in olivine cannot significantly raise conductivity of the oceanic asthenosphere (Yoshino and Katsura, 2013). Thus, proton conduction seems to be insignificant for the large conductivity anisotropy observed in the oceanic asthenosphere near the Eastern Pacific Rise. Therefore, we consider the partial melting as reasonable hypothesis for the anisotropic HCL.

In this study, the electrical conductivity of partially molten peridotite was measured during deformation in simple shear at 1 GPa in a DIA type apparatus with a uniaxial deformation facility. To detect development of electrical anisotropy during deformation of partially molten system, the electrical conductivity was measured simultaneously in two directions of three principal axes: parallel and normal to the shear direction on the shear plane, and perpendicular to the shear plane. Impedance spectroscopy measurement was performed at temperatures of 1523 K for Fe-bearing and 1723 K for Fe-free samples, respectively, in a frequency range from 0.1 Hz to 1 MHz. To understand effect of partial melt on conductivity anisotropy, the conductivity measurement was also performed for the melt-free system during shear deformation. Melt fraction of partial molten sample was around 2 vol.%.

The electrical conductivity of partially molten peridotite parallel to shear direction increased to more than one order of magnitude higher than those normal to shear direction on the shear plane (Fig. 1). On the other hand, conductivity perpendicular to the shear plane decreased gradually after the initiation of shear and finally achieved a value close to that of olivine. The magnitude and development style of conductivity anisotropy was almost the

same for both Fe-bearing and Fe-free melt-bearing systems, and also independent of shear strain. However, such conductivity anisotropy was not developed in melt-free samples during shear deformation, suggesting that the conductivity anisotropy requires a presence of partial melting under shear stress. Microstructural observations of deformed partially molten peridotite samples demonstrated that conductivity anisotropy was attributed to the elongation of melt pockets parallel to the shear direction.

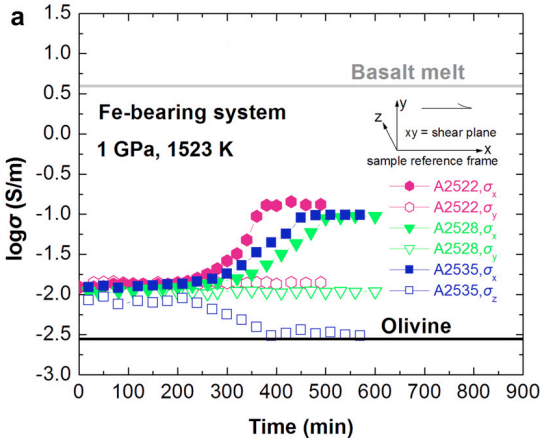

Fig. 1. Conductivity change of partial molten olivine-basalt mixture with time during shear deformation.

The magnitude of conductivity difference reaches around one order of magnitude, which is consistent with the observed conductivity anisotropy near the Eastern Pacific Rise. 2 vol.% of basaltic melt used in this study is consistent with that predicted in low seismic-velocity regions beneath the Eastern Pacific Rise. Thus, the high conductivity anisotropy observed at the top of asthenosphere can be explained by high degree of melt connectivity in the spreading direction coupled with relatively lower connectivity in the ridge parallel direction. A counterargument to the interpretation of smooth plate motion being caused by partial melting is that the partial melt should rapidly become segregated from the host peridotite because of the high permeability of melt in peridotite and the large density difference between melt and mantle minerals. However, extremely low conductivity normal to the shear plane could produce extremely low permeability in the gravitational direction. These observations suggest that partial melting can explain softening and the observed geophysical anomalies of asthenosphere. In summary, horizontal electrical conductivity anisotropy revealed by magnetotelluric surveys in the oceanic asthenosphere can be explained by the realignment of partial melt induced by shear stress.

References

Baba, K., Chave, A.D., Evans, R.L., Hirth, G., Mackie, R.L., 2006. J. Geophys. Res.111, B02101.

Dai, L., Karato, S., 2014. Earth Planet. Sci. Lett., 408, 79-86.

Evans, R.L., Hirth, G., Baba, K., Forsyth, D., Chave, A., Mackie, R., 2005. Nature437, 249–252..

Férot, A., Bolfan-Casanova, N., 2012. Earth Planet. Sci. Lett.349–350, 218–230.

Hirschmann, M.M., Tenner, T., Aubaud, C., Withers, A.C., 2009. Phys. Earth Planet. Inter.176, 54–68.

Karato, S., 2014. Phys. Earth Planet. Inter.228, 300–306.

Naif, S., Key, K., Constable, S., Evans, R.L., 2013. Melt-rich channel observed at the lithosphere–asthenosphere boundary. Nature495, 356–359.

Poe, B.T., Romano, C., Nestola, F., Smyth, J.R., 2010. Phys. Earth Planet. Inter.181, 103–111.

Yang, X.Z., 2012. Earth Planet. Sci. Lett.317–318, 241–250.

Yoshino, T., Matsuzaki, T., Yamashita, S., Katsura, T., 2006. Nature443, 973–976.

Yoshino, T., Katsura, T., 2013. Annu. Rev. Earth Planet. Sci.41, 605–628.

Small degree melting in the "normal" asthenosphere- models and challenges

Marc M. Hirschmann
Dept. of Earth Sciences, U. Minnesota, Minneapolis, MN USA

It is now well established that volatile-rich melts are thermodynamically stable in the oceanic mantle beneath the conductively cooled lithosphere, but the composition, distribution, and fraction of melt remains uncertain, as does the possible persistence of such melt in regions where active upwelling is not occurring. Melts *could* be present, but they may be in such small concentrations or they may have been removed by compaction, so that melts may not actually have appreciable influence on geophysical properties. Therefore, although the thermodynamic stability is a necessary condition if partial melts are responsible for observed geophysical anomalies, it does not necessarily follow that melts are in fact responsible for these geophysical observations.

Although both H_2O and CO_2 could contribute to stabilization of volatile-rich melt, it is C that likely plays the most important role owing to the absence of significant storage of C in predominant mantle silicates. This potentially allows formation of highly C-rich melts which can be stable at comparatively low temperatures. In extreme cases, carbonatite melts can be stable at low temperature conditions. However, owing to the inverse relationship between melt CO_2 concentration and melt fraction, regions where only extreme composition melts either have very low melt fractions or are anomalously C-rich, perhaps owing to local concentration of melts owing to permeability barriers.

An important limit on the fraction of melt potentially present in the convecting mantle is the concentration of C in normal "depleted" mantle. New experiments examining the partitioning behavior of C between mantle minerals and silicate melts confirms that CO_2 is highly incompatible during mantle melting, with a partition coefficient similar to Ba and smaller than that of Nb. Application of these partition coefficients to compositions of undegassed basalts indicate that the depleted mantle has 75±25 ppm CO_2, which is towards the low end of historical estimates. Thus, even under ideal circumstances, melt fractions in the asthenosphere and LAB beneath mature oceanic lithosphere must be small.

Temperature, grain size, and chemical controls on polycrystal anelasticity over a broad frequency range extending into the seismic range

Yasuko Takei[1] and Hatsuki Yamauchi[1]

[1]Earthquake Research Institute, University of Tokyo, Japan,

Rock anelasticity causes dispersion and attenuation of seismic waves. Therefore, for the quantitative interpretation of seismic low velocity and/or low Q regions in the upper mantle, understanding of rock anelasticity is necessary. Recent experimental studies have shown that anelasticity of polycrystalline materials is subject to the Maxwell frequency (f_M) scaling: $Q^{-1}(f/f_M)$ [e.g., 1,2]. However, its applicability to the seismic waves has not been guaranteed because experimental frequencies normalized to f_M of the laboratory samples are usually much lower than the seismic frequencies normalized to f_M in the upper mantle ($f/f_M = 10^6$ - 10^9). In this study, by using polycrystalline organic borneol as an analogue to the mantle rock, we measured anelasticity up to about $f/f_M = 10^8$ and found that the Maxwell frequency scaling is not fully applicable at $f/f_M > 10^4$ [3]. A closer examination of our data showed that each of the relaxation spectra obtained under various temperature, grain size, and chemical composition can be represented by the superposition of a background dissipation which is subject to the Maxwell frequency scaling and a peak dissipation which is always centered at $f/f_M = 10^3$ (Fig. 1). Significant increases of the peak amplitude and width with increasing temperature, grain size, and impurity (diphenylamine) content result in failure of the Maxwell frequency scaling at $f/f_M > 10^4$, where the peak dissipation dominates over the background dissipation. To quantitatively estimate the dispersion and attenuation of seismic waves, it is important to understand the behavior of the peak dissipation.

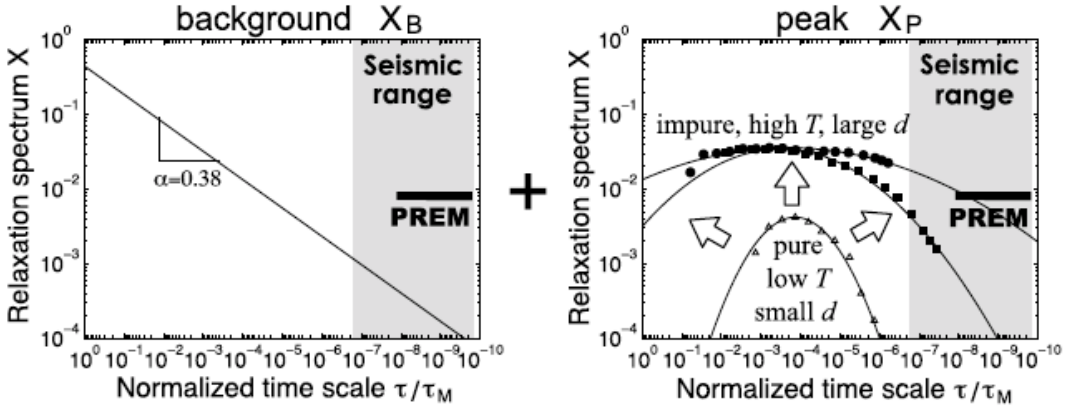

(left) Background and (right) peak dissipation along with the seismic range in the upper mantle. The background dissipation follows the Maxwell frequency scaling but the peak dissipation does not fully follow this scaling, because the amplitude and width of the peak increase with increasing temperature, grain size, and impurity (diphenylamine) content. [3]

The addition of impurity (diphenylamine) to borneol significantly reduces the melting (solidus) temperature from T_m = 477 K to T_m = 316 K. Therefore, we have speculated that the observed variation of the peak dissipation with impurity and temperature can be scaled by the normalized temperature T/T_m, such that the peak amplitude and width increase with increasing T/T_m. The significant broadening of the peak observed near, but below, the solidus temperature (T/T_m = 0.93) suggests that seismic velocity and Q can be lowered even without melt and would have important implications for upper mantle seismic structures. We further investigated the detailed behavior of the peak at near solidus temperatures (T/T_m = 0.88 - 1.01), and found that the peak amplitude saturates at about T/T_m = 0.95, but that the peak width continuously increases up to the supersolidus temperature T/T_m = 1.01 (Yamauchi, master thesis). The obtained result was formulated in terms of the two dimensionless parameters f/f_M and T/T_m and preliminarily applied to the seismic waves in the upper mantle. The result shows that low V and low Q occur at near solidus temperatures even without melt. At the onset of melting, seismic wave velocity shows a discrete reduction due to the poroelastic effect of melt, but the seismic attenuation does not show a discontinuous change.

Our experimental results are, at least qualitatively, consistent with those obtained by Jackson and co-workers [4,5]. However, the mechanism of the peak dissipation is so far poorly understood. Although the background dissipation is explained well by the model of ``diffusionally accommodated grain boundary sliding'', the peak dissipation cannot be explained by any existing model including the models of ``elastically accommodated grain boundary sliding'' and ``melt squirt flow''. Further experimental and theoretical studies are needed to obtain the formula to predict the quantitative effects of rock anelasticity on the seismic velocities and attenuation in the mantle.

References:

[1] McCarthy, C., Y. Takei, and T. Hiraga (2011), Experimental study of attenuation and dispersion over a broad frequency range: 2. The universal scaling of polycrystalline materials, J. Geophys. Res., 116, B09207, doi:10.1029/2011JB008384. [2] McCarthy, C., and Y. Takei (2011), Anelasticity and viscosity of partially molten rock analogue: Toward seismic detection of small quantities of melt, Geophys. Res. Lett., 38, L18306, doi:10.1029/2011GL048776. [3]Takei, Y., F. Karasawa, and H. Yamauchi (2014), Temperature, grain size, and chemical controls on polycrystal anelasticity over a broad frequency range extending into the seismic range, J. Geophys. Res. Solid Earth, 119, doi:10.1002/2014JB011146. [4] Jackson, I., U. H. Faul, J. D. Fitz Gerald, and B. H. Tan (2004), Shear wave attenuation and dispersion in melt-bearing olivine polycrystals: 1. Specimen fabrication and mechanical testing, J. Geophys. Res., 109, B06201, doi:10.1029/2003JB002406. [5] Jackson, I., and U. H. Faul (2010), Grain size-sensitive viscoelastic relaxation in olivine: Towards a robust laboratory-based model for seismological application, Phys. Earth Planet. Inter., 183, 151–163.

Seismic discontinuities of the mantle transition zone beneath the northwestern Pacific Ocean

Daisuke Suetsugu[1], Hajime Shiobara[2], Takehi Isse[2],
Hiroko Sugioka[1], Aki Ito[1], and Hisashi Utada[2]

[1]Japan Agency for Marine-Earth Science and Technology
[2]Earthquake Research Institute, University of Tokyo, Japan,

We determined depths of the 410 and 660 discontinuities ('410' and '660') and thicknesses of the mantle transition zone (MTZ) with a P-wave receiver function analysis using data from the BBOBS and BBOBS-nx stations of the NOMAN network in the northwestern Pacific Ocean. We analyzed earthquake records from 2010 to 2014 for events of magnitude greater than 6 and epicentral distances between 30 and 90 degrees. Ocean bottom seismic stations in the area B and the western half of the area A provide earthquake records of a relatively high S/N, while those of eastern half of the area A have large reverberation after P-waves, which made it difficult to determine the discontinuity depths reliably. After visual inspection, we obtained about 430 receiver functions for the western area A and area B. The receiver functions were stacked for the western area A and the northern and southern regions of the area B. We applied a velocity correction for the depth determination using the tomographic model by Obayashi et al. (2015, this symposium).

The '410' and '660' depths and the MTZ thickness were determined to be 413km, 661km, and 248km km, respectively for the northern area B. Those of the southern area B are 416km, 657km, and 241 km, respectively. These values are close to the global averages (e.g., 418km, 660km, and 243km by Flanagan and Shearer (1998)) and the MTZ of the area B is regarded as 'normal', as we supposed in a planning of the NOMAN project. On the other hand, Those values beneath the southern area A is 406km, 676km, and 270km, respectively. These values suggest that the MTZ beneath the southern area A is significantly colder than that beneath the area B (and the global average). The area A may be 'anomalous' as opposed to the assumption of the NOMAN project. In the presentation, we try to interpret the 'anomaly' beneath the area A, by comparing the seismic results with electro-magnetic studies conducted in the project.

Is there a deep carbonatitic signature beneath the East African Rift ?

Pascal Tarits[1] , Sophie Hautot[2] , Fabrice Gaillard[3] & the Electrolith Team

[1]IUEM, Place Nicolas Copernic, F29280 Plouzané, France
[2]IMAGIR Sarl, 38 rue Jim Sévellec, F29200 Brest, France
[3]ISTO, Campus Geosciences, 1A rue de la Férolerie, F45071 Orléans, France

Fluids in the Earth's mantle concentrate many volatile species and greatly affect rock properties by favoring their melting, weakening their rigidity, and modifying their chemical status (redox state and metasomatic enrichment). It becomes increasingly clear that fluids fuel magmatism and plate tectonics, which are the two main manifestations of the Earth's geodynamics. Understanding the nature of those fluids, how their content and their nature vary within the mantle and whether they are dissolved in minerals or impregnated at grain boundaries is critical for our vision of mantle geodynamics and their consequences at the Earth's surface (volcanism, Earth's degassing into the atmosphere, earthquakes …). Volatile emissions from mantle-derived melts (MORB and Hotspot) indicate that water and carbon dioxide are present in nearly equal concentration in their mantle source regions, and sulfur constitutes the third most abundant volatile. Only subduction-related volatiles are dominated by water. Based on this evidence, geochemical estimations yield similar amount of hydrogen (water) and carbon in the average mantle (~ less than 0.1 wt%). All this might also indicate that carbon and hydrogen are conveyed in the mantle by the same process.

Experimental phase equilibrium at mantle conditions have provided a considerable dataset on the chemical nature of those fluids, which, combined to geochemical data on mantle derived melts and rocks, indicate that carbonatite fluids are present in the deep Earth (>60km), in most geodynamic settings excepted in the mantle wedge of subduction zones, which are clearly dominated by hydrous silicate fluids. Carbonatite fluids have been recognized to trigger several key geochemical processes such as mantle metasomatism, diamond formation, mantle melting, and they are probably involved in large-scale chemical transfers. In contrast, carbonatite fluid contributions to geophysical measures remain poorly explored.

Geophysical observations, particularly electrical conductivity as inverted from magnetotelluric sounding compared to laboratory measurements on mantle rocks, indicate the presence of fluids in several mantle regions. However, the nature of the fluids has been generally considered to be water and the related defects that it can introduce in mantle minerals. A considerable step forward has been realized by numerous studies on water in mantle minerals, essentially from the mineral physics point of view, but the chemical complexity of the fluids need to be increased in order to better represent their geochemical description.

In an effort to reconcile geochemical observations on the nature of mantle fluids and geophysical observations, it may be suggested that highly conductive zones of the Earth's mantle may reflect the presence of carbonatite fluids impregnating the rocks at grain boundaries. Hence several key questions need to be addressed. Can we see carbonatites melt

in the mantle by geo-electrical surveys? Can we see their depth of provenance? Does it vary from a geodynamic setting to another? Can we say how much carbonatite fluid is present at depth and can we resolve potential variations in carbonatites melt contents at depth? There is a need of large-scale probing of mantle fluids to complete and extend the above part.

In order to test the hypothesis that the construction of the oceanic lithosphere at MOR is deeply related to carbonatites flux from depth, we compared mantle conductivity models from active rifting and mature ocean ridge. The emission of carbonatites in the East African Rift (EAR) might then be the surface expression of the deep involvement of carbonatite fluid plumes infiltrating the mantle, which is however too cold to form basaltic melts. We investigated the mantle structure of the Tanzanian rift, performing and exploiting conductivity measurements of the mantle near the only active or subactive carbonatitic volcanoes on Earth, the Oldonyo Lengai volcano, Tanzania in the EAR. We attempted to image the extension of carbonatitic melt from the crustal magmatic activity of the volcano down to the upper mantle by performing a conductivity profile in the mantle underneath the volcano area. We carried out an experiment combining broadband (BBMT) and long period (LPMT) magnetotellurics. Six BBMT soundings were performed around the Oldonyo Lengai volcano and a LPMT was set for one year at a nearby site from 2013-2014. The 3-D inversion of the BBMT data provided clues about the crustal structure beneath the volcano down to lithospheric depth. The LPMT data was analysed to derive a deep 1-D conductivity profile. The crustal distortion was accounted for with the 3-D BBMT model. The results are compared to a revisited 3-D conductivity model from the MELT (East Pacific Rise) region and discussed in the framework of new petro-physical conductivity models of the mantle rocks containing melt.

Oceanic Mantle Structure from Global Tomography

Göran Ekström[1]

[1]Lamont-Doherty Earth Observatory, Columbia University, New York, USA

Several considerations suggest that, on a large scale, the seismic-velocity structure of the oceanic lithosphere and asthenosphere should be relatively simple. The basic notion of the oceanic lithosphere constituting a thermal boundary layer implies not only a direct connection to temperature, but also to the spatial scale of velocity variations. Except in the immediate vicinity of a ridge, temperatures are expected to vary smoothly, and seismic velocities should therefore, generally, vary over length scales comparable with the sizes of individual plates. Taken together with the simplicity and geographic homogeneity of the oceanic crust (as compared with continental crust), this sets up favorable conditions for imaging of the seismic velocity structure of the top few hundred kilometers of the mantle using surface waves, which have direct sensitivity to intrinsic elastic velocities with good resolution in depth, but with broad horizontal averaging. Similar conditions are not present for the imaging of continental plates, where heterogeneity of the crust, as well as tectonic fragmentation, make relevant horizontal spatial scales smaller and hence more difficult to resolve. While the last two decades have seen some convergence of tomographic models, there are still uncomfortably large differences between the models. These differences lead to remaining uncertainty about geophysical questions concerning the structure, state and dynamics of the lithosphere and asthenosphere. Many factors can be identified as responsible for the lack of a more rapid convergence. Some of these are related to data and modeling capabilities, and can in part be addressed by continued improvement of the quality and quantity of seismological data collected in ocean settings. Others are intrinsically linked to the complexity of the anisotropic elastic structure of Earth. Anisotropy demonstrably biases isotropic velocity estimates if it is not accounted for, but is in practice also not fully resolvable. Solving the objectively parameterized tomographic inverse problem may not be the most productive approach to providing better constraints on oceanic mantle structure. New methods of tomographic model parameterization and inversion that incorporate good prior seismological and non-seismological observations and model predictions may be a fruitful direction. In my talk, I will illustrate agreement and disagreement between recent seismological models and offer some thoughts on how the remaining differences may be explained and eventually reconciled.

Session 8-4

Oceanic boundary layer structure and dynamics from seismological imaging and geodynamic modeling

Thorsten W Becker

University of Southern California, Los Angeles

Seismic anisotropy in the Earth is strongest in the thermo-mechanical boundary layers of the mantle. There, observed variations in anisotropic patterns and strength should bestraightforward to relate to mantle flow, particularly for the lithosphere asthenosphere domain. However, both frozen-in and active mantle convection scenarios have been invoked to explain observations, and no simple, global relationships have yet been identified. Here, we show that paleo-spreading orientations provide a good proxy for the shallowest, lithospheric azimuthal anisotropy patterns. This is presumably due to frozen-in lattice preferred orientation (LPO) of olivine assemblages, for which we find a spreading rate and seafloor age dependent correlation. Further down, LPO inferred from mantle flow models and full texture computations, in fact, produces a valid global background model for asthenospheric anisotropy patterns, and to some extent, within the oceanic lithosphere. The same is not true for most simplified ("ISA") texture descriptions and absolute plate motion (APM) models, although a newly introduced, "ridge fixed reference" frame APM model provides a useful description. A ~200 km thick layer where flow model predicted LPO matches observations from tomography lies just below the ~1200 °C isotherm of half-space cooling, indicating a strong temperature dependence of the processes controlling development of azimuthal anisotropy. We infer that the depth extent of shear, and hence the thickness of a relatively strong oceanic lithosphere, can be mapped in this manner. These findings for the background model, and ocean-basin specific deviations from the half-space cooling pattern, are found in all of the three recent surface wave models we considered. Further exploration of deviations from the background model may be useful for general studies of oceanic plate formation and dynamics, as well as regional-scale tectonic analyses. We discuss our findings in light of other evidence including that from existing and ongoing radial anisotropy and receiver function studies.

BBOBS observations in the NOMan project and the future

Hajime Shiobara[1], Takehi Isse[1], Hiroko Sugioka[2], and Aki Ito[2]

[1]Earthquake Research Institute, University of Tokyo, Japan,
[2]Japan Agency for Marine-Earth Science and Technology

During the Normal Oceanic Mantle (NOMan) project, we have conducted several broadband seismic observations from June 2010 until Sep. 2014 (Figure 1). The numbers of deployments of the BBOBS [BB] and the BBOBS-NX [NX] are 27 and 8, respectively. The BB and NX at the seafloor are shown in Figure 2. Finally, all units have been retrieved, and the data recovery rate is about 90 % in total, so as to cover the whole study area for more than one year. The data quality is a standard level in this northwestern Pacific by using our BB, which is not so quiet as the noise at the middle of the Philippine Sea plate [PHS] in our previous stagnant slab project (2004–2008), as shown in two noise models of NM16 and NM21 for examples (Figure 3). A possible reason of this higher noise level in average seems existence of strong bottom currents (about 0.5 m/s or more) we met during ROV dives at several sites in 2012 even at this deep sea basin, which was not seen in several dives in the PHS. Figure 4 concisely shows noise level variations among all BBOBS sites, sampled at periods of 20 s and 100 s in the vertical (UD) and one horizontal (H1) component. Except for NM20 site, all UD noise levels are between the NLNM and the NHNM. H1 noise levels are generally high even at 5 NX sites, but it is clear that the NX worked well to reduce the horizontal noise level compared with those of BB. This graph also indicates that there is no clear relation between the noise levels and the area of sites (Figure 1). Our seismic observation in this project mainly consists of the passive survey using teleseismic signals, we also performed the controlled source survey by using large explosives in June 2014 to research the LAB as shown in the poster (P30, Isse et al.).

The BBOBS, which has high mobility due to a free-fall deployment and self pop-up recovery design, was developed in 1999 and has been used more than 120 times in several places not only around Japan but also in French Polynesia, New Zealand, etc. This compact and simple system of the BBOBS enables easy operation on a small boat with less limitations for the ship. But, the weakness lies in high horizontal noise level at periods longer than 20 s, which is inevitable for any OBS putting the sensor on the seafloor due to bottom currents. To avoid this problem, the BBOBS burial (Collins et al., 2001) demonstrated effectiveness of sensor penetration into the sediment, and the NX (Shiobara et al., 2013) was developed as a practical burial BBOBS system. The compaction of sediments surrounding the sensor package by the penetration makes better mechanical coupling, and the minimization of the package exposed into the seawater reduces the effect by the bottom current close to the boundary layer. Although the current NX looks already at a goal, but it lost the high mobility in the BB by necessity of the ROV. So, the next stage of the NX development will be started to realize the autonomous NX system like as the BB operation, although we still have some technical problems should be solved. This new NX system would be necessary to perform the global and dense BBOBS observations like as the "Pacific Array" in the future.

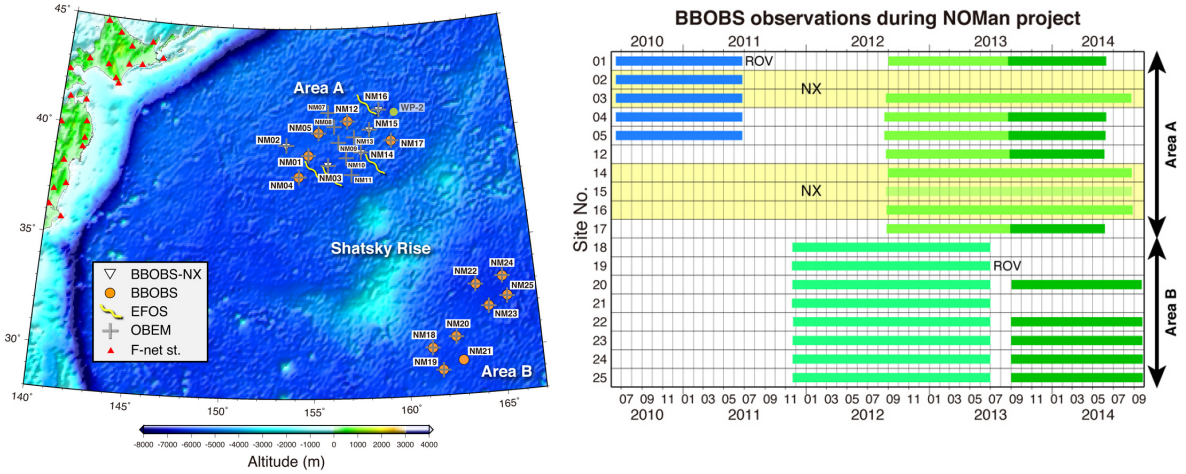

Figure 1. The NOMan project site map (left) and BBOBS observation terms (right). Thick horizontal bars indicate observation periods, and NX sites are hatched by yellow in the graph. Two BBOBSs (NM01/NM19) were recovered by the ROV (KAIKO7000II) in Sep. 2014.

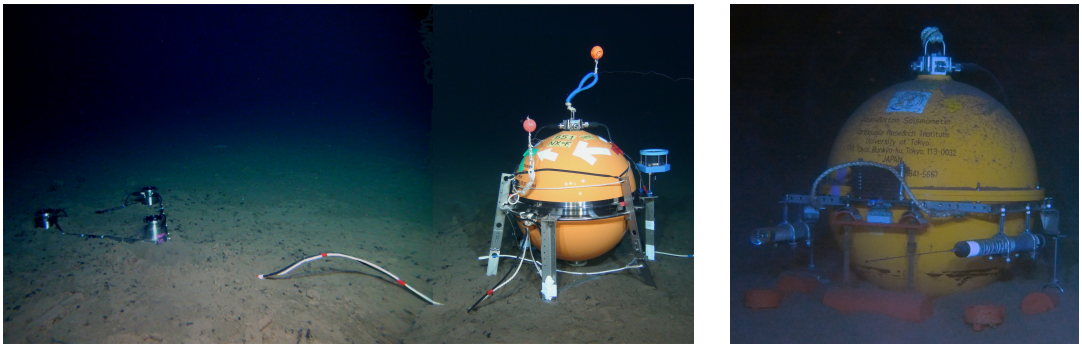

Figure 2. The BBOBS-NX (left, NM15) soon after the deployment ROV operation in Aug. 2012. The BBOBS (right, NM19) was rescued by the ROV, after 3 years-long stay at the seafloor from the deployment in Nov. 2011.

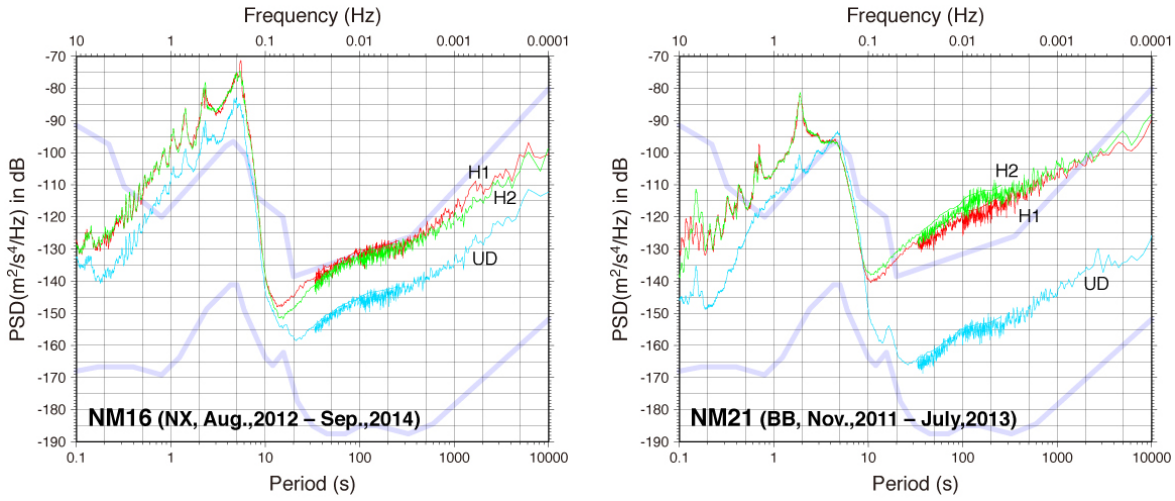

Figure 3. Typical noise models at NM16 (left, NX) and NM21 (right, BB). The NHNM and NLNM (Peterson, 1993) are indicated as two thick curves.

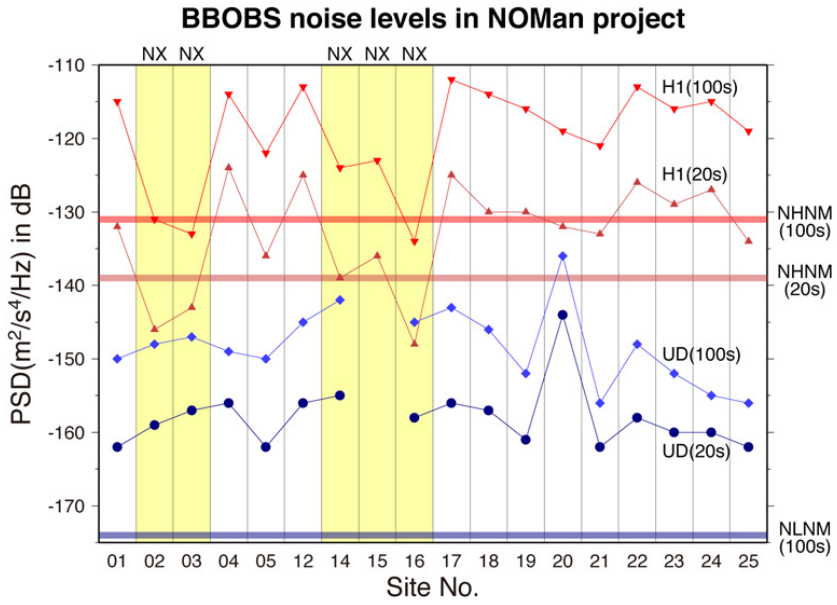

Figure 4. Variation of noise level among all BBOBS sites. Vertical (UD) and one horizontal (H1) component noise levels at periods of 20 s and 100 s are picked from noise models of all BBOBS sites. The NM15 has no vertical data. BBOBS noise levels at the WP-2 site, which was deployed between 2001 and 2002, were -156, -144, -137, and -122 in dB for UD at 20 s and 100 s, H2 at 20 s and 100 s, respectively.

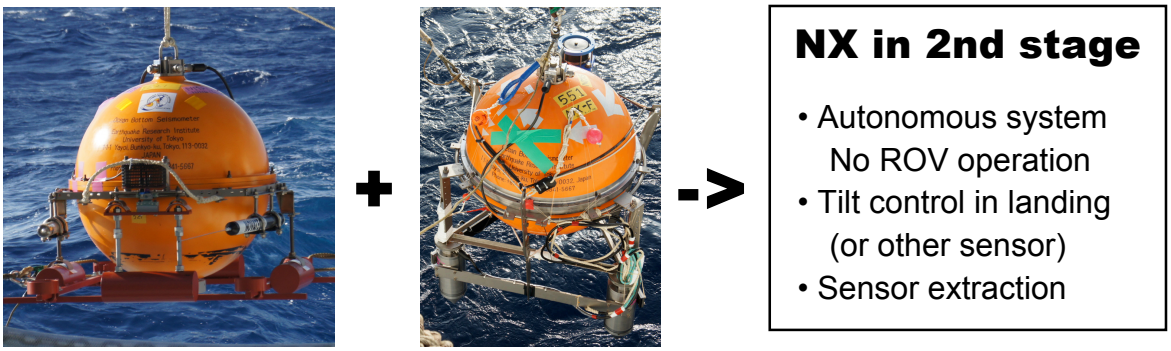

Figure 5. Concept of the BBOBS-NX in the future for the "Pacific Array".

Session 9-2

Pacific Array

H. Kawakatsu[1], A. Takeo[2], T. Isse[1], K. Nishida[1], H. Shiobara[1], D. Suetsugu[3], and H. Sugioka[3]

[1]Earthquake Research Institute, University of Tokyo, Japan
[2]Hokkaido University, Japan
[3]JAMSTEC, Japan

We propose a next generation large-scale array experiment in the ocean. Recent advances in ocean bottom broadband seismometry (e.g., Suetsugu & Shiobara, 2014, Annual Review EPS), together with advances in the seismic analysis methodology, have now enabled us to resolve the regional 1-D structure of the entire lithosphere/asthenosphere system, including seismic anisotropy (both radial and azimuthal), with deployments of ~10-15 broadband ocean bottom seismometers (BBOBSs) (namely "ocean-bottom broadband dispersion survey"; Takeo et al., 2013, JGR; Takeo, 2014, Ph.D. Thesis). Having ~15 BBOBSs as an array unit for 2-year deployment, and repeating such deployments in a leap-frog way (an array of arrays) for a decade or so would enable us to cover a large portion of the Pacific basin. Such efforts, not only by giving regional constraints on the 1-D structure, but also by sharing waveform data for global scale waveform tomography, would drastically increase our knowledge of how plate tectonics works on this planet, as well as how it worked for the past 200 million years. International collaborations might be essential, as if three countries/institutions participate this endeavor together, Pacific Array may be completed within five or so years.

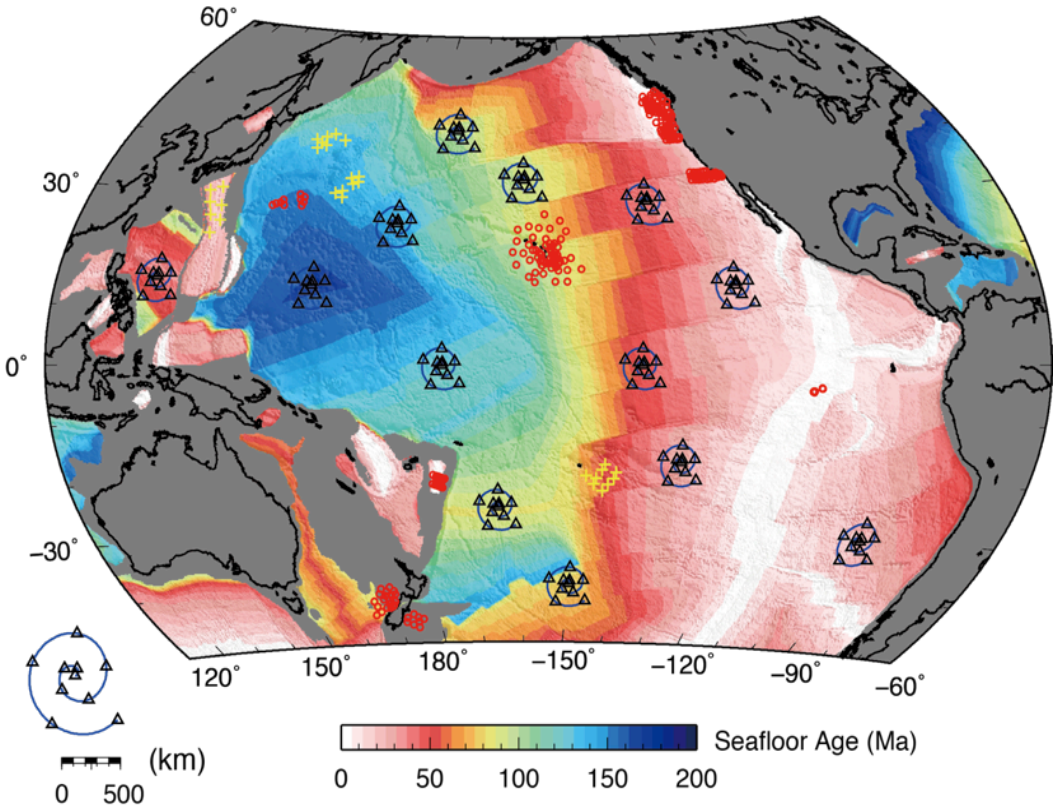

Poster Presentations

P2

A new type of 3D small-scale convection in the mantle wedge

Manabu Morishige[1]

[1]Institute for Geothermal Sciences, Kyoto University, Japan,

In subduction zones, we often observe a low surface heat flow and low seismic attenuation in the forearc region. It suggests that the forearc mantle is cold and rigid. To produce such a “cold corner”, the forearc mantle needs to be decoupled from the subducting slab down to a certain depth for geological time scales. One possible cause of the decoupling may be the existence of weak hydrous minerals at the plate interface including serpentine, talc, and chlorite. In this presentation, we investigate the effects of weak materials at the plate interface on the degree of coupling between the slab and forearc mantle and on 3D thermal structure in the subduction zones.

3D finite element models are used to compute the thermal and flow structure in subduction zones. The model domain is divided into four parts: the crust, a small portion of the mantle wedge tip which is rigid, the viscous mantle wedge, and the subducting slab. The model is exactly the same in the along-arc direction. The flow is computed only in the viscous mantle wedge, whereas temperature is computed for the whole model domain. In order to see the effects of weak materials at the plate interface, we set a thin, low viscosity layer (LVL) just above the slab surface for a certain depth range. The viscosity and the extent of LVL are treated as variable parameters.

We find that the viscosity in LVL has a strong impact on the 3D thermal and flow structure. When the viscosity in LVL is high, the slab and mantle are coupled and the development of the cold corner is limited to a small region near the corner of the mantle wedge. When the viscosity in LVL decreases, the slab and mantle are effectively decoupled and the cold corner is well developed above LVL. However, there are no along-arc variations in the thermal and flow structure in these cases. In contrast, a new type of 3D small-scale convection is observed when we assume a sufficiently low viscosity in LVL. It is a result of along-arc variation in the degree of coupling at the plate interface and it leads to along-arc temperature variation. Compared to the previous models, this new mechanism can produce the along-arc temperature variation in the mantle wedge based on an assumption which is simpler and better constrained by observations. As an example of the application of the model, we consider the observed distribution of Quaternary volcanoes in northeast Japan.

P3

Melt migration beneath thinning lithosphere

Chris Havlin[1,2], E.M. Parmentier[2] and G. Hirth[2]
1. Lamont-Doherty Earth Observatory, Columbia University,
New York, NY, USA
2. Dept. of Earth, Environmental and Planetary Sciences,
Brown University, Providence, RI, USA

In this study, we use numerical models to investigate (1) thermal erosion of the lithosphere due to melt infiltration at the lithosphere-asthenosphere boundary (LAB) and (2) the response of asthenosphere melt migration to evolving topography of the LAB. The model results may explain variations in the negative seismic velocity gradient imaged by receiver functions near the LAB above regions of melt production.

The model treats a simplified case in which melt is generated by adiabatic decompression in a mantle plume beneath thick lithosphere. We first construct a base state, in which the heat flux due to vertical migration of melt is applied as a spatially varying boundary condition along the LAB to calculate the thermal and mechanical evolution of the lithosphere. We then use the resulting LAB topography in 2-D calculations of melt migration in the asthenosphere subject to a diking flux (Havlin et al., 2013) along the LAB in order to evaluate the potential for 2-D geometrical focusing to modify lithosphere thinning and melt accumulation. We find that basal heating by melt infiltration thins the lithosphere faster than from solid state thermal erosion alone, resulting in significant LAB topography above regions of melting in the asthenosphere. In 2-D, geometrical focusing of melt can locally enhance lithosphere thinning rates and subsequent LAB topography.

Based on the model results, variations in the melting rate in the asthenosphere could explain differences between the negative velocity gradient (NVG) imaged by receiver functions in different tectonic settings. Because receiver functions have difficulty imaging steeply dipping boundaries, we suggest that the apparent disruption of the NVG beneath regions of recent volcanism could be due to large local topography along the LAB caused by melt infiltration. In regions of low or more uniform melt production, the NVG should be more continuous.

Synthesis and high-temperature creep experiments on polycrystalline Fe-bearing olivine

Kosuke Yabe[1] and Takehiko Hiraga[1]

[1]Earthquake Research Institute, University of Tokyo, Japan,

Experimental results of high-temperature creep of polycrystalline olivine have been used to understand the rheology of the upper mantle. Faul and Jackson (2007) showed that olivine aggregates prepared from reagents using sol-gel technique had 1 ~ 2 orders of magnitude lager strength compared to the naturally derived olivine aggregates, indicating a presence of significant but unknown factor that controls creep rate of olivine aggregate. One of the candidates for the factor is impurities in naturally derived olivine aggregates. It has been observed that a small amount of impurities such as CaO, Al_2O_3, TiO_2 were segregated at grain boundaries in naturally derived olivine aggregates. Such impurities segregated at grain boundaries have been found to have a large effect on the strength of polycrystalline oxides. In this study, we synthesized olivine aggregates with and without impurities by using new technique and conducted high-temperature creep experiment on the synthesized olivine aggregates.

The aggregates were prepared by applying vaccum sintering to nano-sized olivine powder synthesized from highly pure and fine-grained (<100 nm) raw powders (Koizumi et al 2010). Olivine aggregates with and without dopants of 0.1% Al_2O_3, CaO, NiO, TiO_2 were prepared. For creep test, we develop a deformation apparatus which can control the atmosphere. Deformation tests on these samples showed no major difference in their strength under diffusion creep. Further, the strength was essentially identical to the aggregates of Faul and Jackson (2007). Our results indicate that the some chemical species other than those investigated in this study has a significant effect on creep properties of polycrystalline olivine.

P5

Seismic structure of oceanic crust and sediment in the northwestern Pacific

Takashi Tonegawa[1], Hajime Shiobara[2], Takehi Isse[2], Hiroko Sugioka[1], Aki Ito[1], Akiko Takeo[3], Hitoshi Kawakatsu[2], Hisashi Utada[2]

[1]Japan Agency for Marine-Earth Science and Technology,
[2]Earthquake Research Institute, University of Tokyo,
[3]Hokkaido University

We present detections of Ps waves and their multiples converted from the basement and Moho, using records of earthquakes occurred during 2010–2014 with magnitudes greater than 5.5 and epicentral distances between 30º and 85º. These were observed at 18 broadband ocean bottom seismometers (OBSs) deployed by the NOMan project. We divided the observation area into two regions; Area A: a region at northwest of the Shatski Rise with 10 OBSs, Area B: another region at southeast of the rise with 8 OBSs. Since Ps converted waves are clearly observed at Area A, we only show RF results in Area A.

We totally collected 269 receiver function (RF) traces at a frequency band of 2–4 Hz with good S/N in the whole observation period at Area A. As a result, RFs show clear Ps, phases and their multiples from the basement and Moho. Using these converted phases emerged in RF, we examined H-κ stacking analysis with semblance function. The thickness and Vp/Vs for marine sediment at Area A were 0.2–0.4 km and 6–13, which are almost consistent with those in previous studies (Shinohara et al. 2008; Fujie et al. 2013; Tonegawa et al. 2013). Those parameters for oceanic crust were 5.5–7.5 km and 1.7–1.9. In particular, most of the estimated Vp/Vs for oceanic crust tends to be over 1.8.

Moreover, we examined Ps splitting analysis by using Ps phases coming from the basement and Moho. We first estimated splitting parameters for sediment layer by cross-correlation technique for Ps phase converted from the basement. Before estimating those for crust, we removed the effects of sediment anisotropy from Ps phase coming from the Moho by using stripping analysis (Oda, 2012). Finally, splitting parameters for oceanic crust were estimated by cross-correlation technique using the corrected Ps phase from the Moho. In particular, it seems that the fast axis tends to be oriented along ENE-WSW direction, which is almost parallel to magnetic lineation. However, the estimation of fast axis from Ps splitting analysis was slightly unstable. Therefore, waveform modeling analysis for Ps phases would be required to precisely estimate anisotropic structure within sediment and crust.

P6

Data and interpretation of the LAB beneath Wellington, New Zealand from the SAHKE experiment

Tim Stern[1], S.H. Henrys[2], D.A. Okaya[3], M.K. Savage[1], H. Sato[4], R. Sutherland[1,2], T. Iwasaki[4], J. Louie[5]

[1]Institute of Geophysics, Victoria University, Wellington, 6140, New Zealand

(tim.stern@vuw.ac.nz)

[2]Institute of Geological and Nuclear Sciences, Lower Hutt, 5010, New Zealand

[3]Department of Earth Sciences, University of Southern California, Los Angeles, CA 90210, USA

[4]Department of Earth Sciences, Tokyo University, Tokyo, 12345, Japan

[5]Seismological Laboratory, University of Nevada, Reno, NV 89557, USA

In this poster we present data from the SAHKE experiment that managed to image the base of the Pacific oceanic plate beneath Wellington, New Zealand. We show shot gathers , a ray tracing solution for selected shot gathers and a multichannel seismic stack for the ~ 80 km long line that crossed the lower North Island. A so called Median filter was used to enhance the multichannel seismic section. This filter is borrowed technology from industry that is used to sharpen photographic images. It's a digital filter that is a form of two-way running average similtaneously in both space and time.

P7

Thermal structure and melt fraction distribution in a mantle wedge determined from the 3-D electrical conductivity structure beneath Kyushu in the Southwest Japan Arc

Maki Hata[1] and Makoto Uyeshima[1]

[1]Earthquake Research Institute, University of Tokyo, Japan,

We determine temperature and melt fraction distributions in a mantle wedge by combining a subsurface electrical conductivity structure with laboratory-derived results. The laboratory-derived results are relation between electrical conductivity and temperature for four nominally anhydrous minerals (Olivine, Orthopyroxene, Clinopyroxene, and Garnet) [*Dai and Karato*, 2009; *Yoshino et al.*, 2009; *Yang et al.*, 2011; *Zhang et al.*, 2012], relation between electrical conductivity and temperature for hydrous basaltic melt [*Ni et al.*, 2011; *Sifre et al.*, 2014], and a parameterization result of isobaric hydrous mantle melting [*Katz et al.*, 2003]. In this presentation, we will show our approach to determine temperature and melt fraction as a function of the water contents among the four nominally anhydrous minerals and the hydrous basaltic melt, which integrate laboratory-derived conductivity and field-derived conductivity. We will also show the results of adopting our approach, which are thermal structure profiles and melt fraction distribution profiles of the mantle wedge beneath one non-volcanic region and two volcanic regions of the Kyushu Island. The Kyushu Island in the Southwest Japan Arc has many Quaternary active volcanoes, which exist along the volcanic front of N30°E-S30°W, in relation to the subduction of the Philippine Sea Plate. The volcanoes are located in northern and southern regions of the island, and no volcano is located in the central region (the non-volcanic region) between the two volcanic regions of the island. We have performed three-dimensional inversion analyses to obtain a lithospheric-scale electrical conductivity structure (model) beneath the entire Kyushu Island using the Network-Magnetotelluric data [*Hata et al.*, 2015]. One of two major findings from a distribution of conductive anomalies in the model is that the volcanoes in the northern and southern volcanic regions have two different origins bordering the non-volcanic region at deep depths. Secondly, the degrees of magmatism and the relative contributions of slab-derived fluids to the magmatism vary spatially in the one non-volcanic and two volcanic regions. Thus, in this study, we try to verify whether the respective conductivity anomalies impart a different effect on temperature and melt fraction.

P8

Synthesis of textured olivine aggregate using colloidal processing under high magnetic field

Sanae Koizumi[1], Tohru S. Suzuki[2], Yoshio Sakka[2], Takehiko Hiraga[1]

[1]Earthquake Research Institute, University of Tokyo, Japan,
[2]National Institute for Material Science

Crystallographic preferred orientation (CPO) of olivine is considered to be widely developed in the upper mantle via its plastic deformation. Due to the presence of anisotropic physical properties such as elasticity, plasticity, electron conductivity and etc... of single crystal olivine, their bulk rock properties can significantly be affected by the presence of CPO. To measure CPO effect on the bulk rock properties by room experiments, it is required to prepare polycrystalline materials with ideally controlled CPO.

Magnetic field was applied to fine-grained (~120 nm) equigranular Fe-free and Fe-bearing olivine particles, which were dispersed in ethanol (solvent). To enhance the dispersibility of particles in solution, we applied various types and amount of polymer dispersant finding that the dispersibility was enhanced by an addition of ≧2wt% polyethyleneimine. The applied magnetic field strength for Fe-free olivine was 12T and for Fe-bearing olivine was up to 8T. We expected the particles to align with respect to magnetic direction due to their magnetic anisotropy. Aligned particles were gradually deposited on a solid-liquid separation filter by ethanol drainage. The directions of magnetic field and particle deposition were parallel. The dried particles were then densified isostatically at 200 MPa for 10 min and sintered using the alumina tube furnace with vacuum pump.

The a-axis oriented Fe-free olivine and the c-axis oriented Fe-bearing olivine aggregates were obtained. We could achieve highly orientated and highly dense (≧99%) and fine grained (<1 μm) at the same time. We found that the degree of orientation was enhanced by grain growth and the magnetic field strength. . Such synthesized aggregates will allow us to measure CPO effect on the physical properties of olivine aggregate.

P9

Tomographic slabs and simulated slabs

Satoru Honda[1]

[1]Earthquake Research Institute, University of Tokyo, Japan,

I try to combine the results and knowledge of seismic tomography, geodynamic modeling and geologic history of the subduction zone around the Japanese Islands to understand the tectonics their. For this purpose, I estimate the cold temperature anomaly by converting the fast velocity anomaly of recent tomographic model [Obayashi, et al., 2011] to the temperature anomaly using the recent estimate of d(ln Vp)/dT by Karato [2008] with the constraint from the relation between the theoretical estimate of temperature and the observed seismicity in the subducting slab [Emmerson & McKenzie, 2007]. I find that, the estimated temperature shows fairly continuous cold anomaly from the upper to the lower mantle, that is consistent with the results of geodynamic modeling of the subducting slab with the temperature-dependent viscosity included. However, there is still a significant thinning or an absence of the slab just below the stagnated slab in the transition zone. Geodynamic modeling of subduction, especially, the stagnation of the slab in the transition zone shows that the slab behavior strongly depends on the geological settings of subduction zone such as the rollback of trench. To understand the present feature of the slab revealed by the seismic tomography, I construct a simple half-kinematic model of subduction by taking into account the geological settings including the opening of the Japan Sea. Two possibilities, that is, the opening of the Japan Sea and the subduction of old ridge, are suggested for the origin of the gap and the absence of the slab.

A part of this presentation is from T33B-4675 presented at AGU Fall Meeting 2014.

P10

Elasticity, anelasticity, and viscosity of a polycrystalline material at near-solidus temperatures

Hatsuki Yamauchi[1] and Yasuko Takei[1]

[1]Earthquake Research Institute, the University of Tokyo, Japan,

For a quantitative interpretation of seismic structures in the earth's interior, understanding of rock viscoelasticity over a broad frequency range is needed. There are high-Q^{-1} and low-V regions in the upper mantle. To understand the cause of those anomalies, we investigated the effects of partial melting on anelasticity. Particularly, temperature effect on anelasticity just below the solidus temperature is examined in detail. By using polycrystalline aggregates of borneol + diphenylamine binary eutectic system (solidus temperature T_m = 43°C) as rock analogue, we accurately measured elastic, anelastic, and viscous properties at near-solidus temperatures.

We prepared 4 samples with different grain sizes and melt fractions. Young's modulus and attenuation of these samples were measured from 100 Hz to 0.2 mHz by forced oscillation tests at near-solidus temperatures ($0.88 \leq T/T_m \leq 1.01$). Ultrasonic tests and creep tests were conducted to measure elasticity and viscosity, respectively, at the same temperature conditions.

By using the obtained data, we examined how elasticity, anelasticity, and viscosity behave at the onset of melting. We found that although the ultrasonic velocities are discontinuously reduced by the poroelastic effect of melt, anelasticity and viscosity changed continuously with temperature even at the onset of melting. Based on these data, an empirical formula of the relaxation spectrum X was obtained as a function of dimensionless variables f/f_M (f_M: Maxwell frequency) and T/T_m. A preliminary application of the formula to the upper mantle suggests that high Q^{-1} and low V can occur at near-solidus temperatures even without melt. It also suggests that seismic attenuation changes continuously even at the onset of melting, whereas seismic velocity changes discontinuously due to the poroelastic effect of melt.

In this study, the temperature dependence of anelasticity could be captured at near-solidus temperatures, but dependences on the grain size and melt fraction couldn't be captured. This is because the samples that experienced partial melting show various hysteresis effects, and the hysteresis effects masked these effects. We are planning to investigate effects of grain size and melt fraction on anelasticity by using samples that do not experience partial melting and hence are free from the hysteresis effects.

P11

Three-dimensional electrical conductivity structure in the upper mantle in the French Polynesia

Noriko Tada[1,3], Pascal Tarits[2], Kiyoshi Baba[3], Takafumi Kasaya[1], Daisuke Suetsugu[1], and Hisashi Utada[3]

[1]Japan Agency for Marine-Earth Science and Technology, Japan
[2]Institut Universitaire Europeen de la Mer, France
[3]Earthquake Research Institute, University of Tokyo, Japan

The mantle upwellings are one of the most important features for understanding the mantle dynamics. A large-scale mantle upwelling beneath the French Polynesia region in the South Pacific has been suggested from seismic studies, which is called the South Pacific superplume. Nolasco et al. (1998) carried out magnetotelluric (MT) survey around the Society hotspot, which is one of the hotspots in the French Polynesia region, in order to estimate electrical conductivity structure beneath and the vicinity of the Society hotspot in two-dimension. This previous study is not enough to understand the geometry of the hotspot, because the hotspot seems to be cylindrical form according to the results from the seismic study. Moreover, Suetsugu et al. (2009) suggested that the slow velocity anomaly continues from the lower mantle to the uppermost upper mantle just beneath the Society hotspot. The geometry, temperature, and composition of the Society hotspot remain controversial, however, due to still insufficient accumulation of the geophysical data.

Then, we carried out the TIARES project that composed of multi-sensor stations that include broadband ocean bottom seismometers, ocean bottom electromagnetometers (OBEMs), and differential pressure gauges from 2009 to 2010. To obtain three-dimensional (3-D) image of the upwelling of the Society hotspot in terms of electrical conductivity, we newly settled eleven OBEMs and obtained MT responses at 20 sites in total. A 3-D marine MT inversion program, which can treat topographic change distorting electromagnetic data, was applied to these MT responses to estimate a 3-D electrical conductivity image.

The result detected a high electrical conductive anomaly elongating from the mantle transition zone to the uppermost upper mantle just below and the east side of the Society hotspot. In general, high conductivity indicates high temperature and/or the existence of partial melt or volatiles. This feature is consistent with the slow velocity anomaly obtained from the surface wave tomography (Suetsugu et al., 2009) in terms of high temperature.

P12

Experimental Determination of the H_2O-undersaturated Peridotite Solidus

Emily Sarafian[1], Glenn Gaetani[2], Erik Hauri[3], Adam Sarafian[1]

[1]MIT-WHOI Joint Program, Woods Hole Oceanographic Institution, Woods Hole, MA
[2]Geology and Geophysics, Woods Hole Oceanographic Institution, Woods Hole, MA
[3]Department of Terrestrial Magnetism, Carnegie Institution of Washington, Washington D.C.

Knowledge of the H_2O-undersaturated lherzolite solidus places important constraints on the process of melt generation and mantle potential temperatures beneath oceanic spreading centers. Nominally anhydrous minerals (NAMs) in the mantle, such as olivine, pyroxene, and garnet, are capable of accommodating 10-100s of μg/g H_2O into their structures at upper mantle conditions (e.g., Hirschmann et al., 2005). Small amounts of H_2O dissolved in NAMs drastically decreases the temperature at which the upper mantle melts as a function of pressure, i.e., the solidus, thereby increasing the depth of melting relative to the anhydrous solidus. The small concentration of H_2O (~50-200 μg/g) dissolved in the oceanic mantle is thought to exert a strong influence on the peridotite solidus, but this effect has not been directly determined. The utility of existing experimental data is limited by a lack of information on the concentration of H_2O dissolved in the peridotite and uncertainties involved with identifying small amounts of partial melt. In this study, we use new experimental results to quantitatively define the H_2O-undersaturated solidus at 1.5 GPa for oceanic upper mantle with 170 μg/g H_2O dissolved.

To determine the peridotite solidus at low H_2O contents, we carried out partial melting experiments on a synthetic depleted mid-ocean ridge basalt mantle peridotite composition (Workman and Hart, 2005) with San Carlos olivine spheres roughly 300 μm in diameter mixed in at 95:5 proportions by weight. Experiments were conducted at 1.5 GPa using a solid-medium piston-cylinder device with 12.7 mm assemblies. Volume diffusion of H_2O in olivine is rapid (e.g., Demouchy and Mackwell, 2006) such that spheres of San Carlos olivine roughly 500 μm in diameter embedded in a matrix of fine-grained peridotite will diffusively equilibrate with the water fugacity imposed by the peridotite within 2 hours. Therefore, the measured olivine sphere H_2O content should equilibrate with the surrounding peridotite and follow a predicted melting curve with increasing temperature. At subsolidus temperatures the olivine sphere H_2O content remain constant, but at temperatures above the solidus H_2O strongly partitions into the melt and the measured H_2O content of the olivine sphere drops. After the experiment, the concentration of H_2O dissolved in the olivine spheres is determined by secondary ion mass spectrometry.

Melting experiments, spaced 20 °C apart, were performed from 1250 to 1430°C. The concentration of H_2O in the olivine spheres remains constant up to 1330 °C, and then decreases systematically with increasing temperature. This indicates a solidus temperature of ~1390 °C, which is ~55-80 °C above the existing estimates for anhydrous solidus. The H_2O-undersaturated solidus indicated by our experimental results provide important constraints on the melt generation processes including the depth of melting at a mid-ocean ridge.

Demouchy, S., Mackwell, S., 2006. Mechanisms of hydrogen incorporation and diffusion in iron-bearing olivine. Physics and Chemistry of Minerals 33, 347-355.
Hirschmann, M.M., Aubaud, C., Withers, A.C., 2005. Storage capacity of H2O in nominally anhydrous minerals in the upper mantle. Earth and Planetary Science Letters 236, 167-181.

Workman, R.K., Hart, S.R., 2005. Major and trace element composition of the depleted MORB mantle (DMM). Earth and Planetary Science Letters 231, 53-72.

P13

The Electrical Structure of the Central Pacific Upper Mantle Constrained by the NoMelt Experiment

Emily Sarafian[1], Rob. L. Evans[2], John Collins[2], Jimmy Elsenbeck[2], Glenn Gaetani[2], James B. Gaherty[3], Greg Hirth[4], Daniel Lizarralde[2]

[1]MIT-WHOI Joint Program, Woods Hole Oceanographic Institution, Woods Hole, MA
[2]Geology and Geophysics, Woods Hole Oceanographic Institution, Woods Hole, MA
[3]Lamont-Doherty Earth Observatory of Columbia University, Palisades, NY
[4]Geological Sciences Department, Brown University, Providence, RI

The NoMelt Experiment imaged the mantle beneath 70 Ma Pacific seafloor with the aim of understanding the transition from the lithosphere to the underlying convecting asthenosphere. Seafloor magnetotelluric data from four stations were analyzed using 2-D regularized inverse modeling. The preferred electrical model for the region contains an 80 km thick resistive (>10^3 Ωm) lithosphere with a less resistive (~50 Ωm) underlying asthenosphere. The preferred model is isotropic and lacks a highly conductive (≤10 Ωm) layer under the resistive lithosphere that would be indicative of partial melt. We first examine temperature profiles that are consistent with the observed conductivity profile. Our profile is consistent with a mantle adiabat ranging from 0.3 °C/km-0.5°C/km. A choice of the higher adiabatic gradient means that the observed conductivity can be explained solely by temperature. In contrast, a 0.3°C/km adiabat requires an additional mechanism to explain the observed conductivity profile. Of the plausible mechanisms, H_2O, in the form of hydrogen dissolved in olivine, is the most likely explanation for this additional conductivity. Our profile is consistent with a mostly dry lithosphere to 80 km depth, with bulk H_2O contents increasing to between 25 and 400 ppm by weight in the asthenosphere with specific values dependent on the choice of laboratory dataset of hydrous olivine conductivity and the value of mantle oxygen fugacity. The estimated H_2O contents support the theory that the rheological lithosphere is a result of dehydration during melting at a mid-ocean ridge.

The poster presentation of the NoMelt Experiment will critically examine the data from the four usable stations, the model fits to the data, and the interpretation of the observed conductivity. This will provide a more detailed description of the NoMelt investigation.

Electromagnetic investigation into the mantle transition zone by using the NOMan project data

Tetsuo Matsuno[1], Hisashi Utada[1], Kiyoshi Baba[1], Hisayoshi Shimizu[1], and Noriko Tada[1,2]

[1]Earthquake Research Institute, University of Tokyo, Japan
[2]Japan Agency for Marine-Earth Science and Technology, Japan

We report a result of an analysis of marine electromagnetic field data obtained under the Normal Oceanic Mantle (NOMan) project for elucidating an electrical conductivity structure of the mantle transition zone in the northwestern Pacific. A primary aim of this study is to answer one of the fundamental questions tackled in the project "Is the mantle transition zone a major water reservoir of the Earth?" from observations for the electrical conductivity structure by using our new and latest ocean bottom instruments. To elucidate the electrical conductivity structure of the mantle transition zone, periods of electromagnetic response functions should be long as more than 10^5 s (approximately 1 day) due to the response sensitivity to a plausible electrical conductivity profile of the mantle [Fukao et al., 2004]. To obtain electromagnetic response functions at the target period range with high accuracy, we used the electric field observation system (EFOS). The EFOS has better signal-to-noise ratio than the ocean bottom electromagnetometer (OBEM) in measurement of electric field fluctuation at the period range with much higher portability than the submarine cable [Utada et al., 2013]. In addition to utilizing the EFOS, we conducted multi-year observations with EFOSs and OBEMs (up to 2 years with EFOSs and up to 4 years with OBEMs).

Long-period MT response functions are estimated at 3 sites in Area A (northwest of the Shatsky Rise) by using EFOS electric field data and OBEM magnetic field data. Long-period GDS response functions are estimated at 15 sites in Area A and at 7 sites in Area B (southeast of the Shatsky Rise) by using OBEM magnetic field data. MT response functions are estimated at 10^5 - $5*10^5$ s, and GDS response functions are estimated at 10^5 - $2*10^6$ s. The estimated response functions are compared with a prediction from a known 1-D electrical conductivity model under the north Pacific with land-ocean conductance distribution in a surface layer [Shimizu et al., 2010] and with predictions from models based on laboratory measurements of mantle materials having several different water contents in the mantle transition zone [e.g., Yoshino and Katsura, 2013]. The response functions observed in Area A are predicted well by a model with 0.1 wt.% or less water content in the wadsleyite and ringwoodite layers, if temperature in the mantle transition zone is lower than a standard adiabatic temperature profile [Katsura et al., 2010] by approximately 150 K as inferred by a seismic receiver function and tomography study [Suetsugu et al., this symposium].

Continuous measurements of electrical conductivity and viscosity of synthesized lherzorite samples during partial melting under gradual temperature change

Kenta Sueyoshi[1] and Takehiko Hiraga[1]

[1]Earthquake Research Institute, University of Tokyo, Japan,

It is considered that transport properties of the mantle (ex. electrical conductivity, viscosity, and seismic attenuation) changes during ascend of the mantle by partial melting. To understand how partial melting changes the physical properties of ascending mantle (ex. beneath mid-ocean ridge), we measured the electrical conductivity and viscosity of the synthesized peridotite samples under atmospheric pressure during slow increases and decreases in temperature reproducing the mantle crossing its solidus.

Samples of forsterite (50%) + enstatite (40%) + diopside (10%) with addition of 0.5% spinel, were synthesized from $Mg(OH)_2$, SiO_2, $CaCO_3$ and $MgAl_2O_4$ powders with particle size of <50 nm. They were expected to exhibit the gradual partial melting with temperature increase above solidus. In addition, two types of the samples, forsterite (80%) + diopside (20%) and forsterite (95%) + diopside (5%), which were expected to exhibit different manners in initiation of partial melt and amount of melt during the temperature change, were also prepared by the same process. We continuously measured electrical conductivity of these samples at every temperature during gradual temperature change, which crosses the sample solidus (~1200˚C and 1380˚C for spinel-added samples and forsterite + diopside samples, respectively). Sample viscosity were measured under constant loads of 0.5~50 MPa. Microstructures of the samples quenched from above solidus were observed by scanning electron microscopy (SEM) in order to measure the melt fraction.

In the spinel-added samples, the melt fraction was changed from ~0 to 0.09 during the temperature increase from 1200˚C to 1390˚C. The electrical conductivity at below solidus exhibited linear distributions in their Arrhenius plots indicating that a single mechanism controls for each transport property within the experimental temperature ranges. Such linear relationship was no longer observed at higher temperature regime and changed to an exponential increase of the conductivity until the temperature reached to produce a phase assembly of forsterite + enstatite + melt. Arrhenius plots of viscosity also showed a change in (apparent) activation energy from ~700 kJ/mol to ~900 kJ/mol across around solidus. Stress-strain rate relationship showed a stress exponent of 1.3~1.5 at both temperature below and above solidus indicating that the samples deformed by diffusion creep mechanism.

P16

High precision measurement of activation energy of creep of polycrystalline forsterite

Tadashi Nakakoji[1] and Takehiko Hiraga[1]
[1]Earthquake Research Institute, University of Tokyo, Japan

Flow property of the upper mantle has been studied by conducting deformation experiments on olivine aggregate. Extrapolation of the experimental results to nature requires highly-precise flow parameters such as activation energy (Q), stress exponent (n) and grain size exponent (p), which can be changed by different flow mechanisms. The purpose of this study is to obtain such parameters with small error range, which helps to minimize uncertainties in the extrapolation. For this purpose, we investigated a dependence of the viscosity of iron-free olivine on temperature. The deformation experiment was conducted under atmospheric pressure and high temperature, with constant load by using Shimadzu AG-X50kN and change in temperature with a very low rate (10min./^{o}C) by furnace attached to the instrument. The deformation sample was synthetic olivine composed of forsterite (90Vol %) and enstatite (10Vol %). After the experiment, the samples were observed by scanning electron microscope (SEM) and the grain size was measured by the SEM image. The sample viscosity was obtained by calculating strain rate at every temperature with least square fit. The grain size exponent, p was obtained from the relation of grain size and sample viscosity for the same temperatures exhibiting the values of ~3. This value is used to correct viscosities for constant grain size of 1 micron. The relation of logarithmic reciprocal viscosity and reciprocal temperature shows linearity in each experiment. The obtained activation energy ranges from 478 ± 3 kJ/mol to 694 ± 7 kJ/mol which can be attributed to the transition of deformation mechanism from grain boundary diffusion control to lattice diffusion control depending on temperature and grain size.

P17

Crustal and upper mantle structure in southeast of Shatsky Rise in the northwestern Pacific revealed from seismic reflection and refraction data

Akane Ohira[1], Shuichi Kodaira[1,2], Yasuyuki Nakamura[2],
Gou Fujie[2], Ryuta Arai[2], Seiichi Miura[2]

[1]Yokohama National University, Japan, [2]JAMSTEC

In the theory of plate tectonics the outer shell of the Earth is considered to be composed of moving plates of rigid lithosphere which overlie the warm ductile asthenosphere. It is well known that physical and chemical properties create the rheological contrast between the lithosphere and asthenosphere. In previous studies the lithosphere-asthenosphere boundary (LAB) has been confirmed by using surface waves (e.g. Nettles and Dziewonski, 2008), sea-floor magnetotelluric data (Naif et al., 2013) and converted teleseismic waves (e.g. Kawakatsu et al., 2009). More recently, an active-source seismic method is used to obtain high-resolution image for the LAB (Stern et al., 2015). However, there is little information of seismic images of the LAB in typical oceanic areas, which is an important clue to understand the dynamics of plate tectonics comprehensively.

Here we show results of an active-source refraction/reflection survey at southeast of the Shatsky Rise, northwestern Pacific, with R/V Kairei of JAMSTEC in 2014. Five ocean bottom seismometers (OBSs) were deployed and recovered along a 1130-km-long survey line which covers the old Pacific plate formed from the Late Jurassic to the Early Cretaceous (Nakanishi et al., 1989). We used an airgun array with a total volume of 7,800 cubic inches (approximately 130 L) with firing at intervals of 200 m as controlled sources. Multi-channel seismic reflection (MCS) data were also collected with a 444-channel, 6,000-m-long streamer cable.

On OBS records, we identified refractions from the oceanic crust (Pg), reflections from the Moho (PmP), refractions from the uppermost mantle (Pn), and deep reflections from within the upper mantle (DR). The apparent velocity of Pn phases was about <8.6 km/sec. DR phases were visible at offsets 170-250 km and 250-380 km, 260-350 km, 290-380 km, 350-440 km in OBS5, OBS4, OBS3, OBS2 (Fig.), respectively. In order to obtain the P-wave velocity structure of the crust and to estimate depths of deep reflectors in the upper mantle, we conducted forward modeling (Zelt and Smith, 1992; Fujie et al., 2008). As a result, the P-wave velocity structure of the crust was generally typical oceanic crust divided into oceanic layer 2 of Vp =5.0-6.5 km/sec and oceanic layer 3 of Vp =6.8-7.0 km/sec, and depths of reflectors in the upper mantle were about 40-65 km. We will make further processing of the OBS data, in particular amplitude data, to examine if the observed reflectors correspond to the LAB.

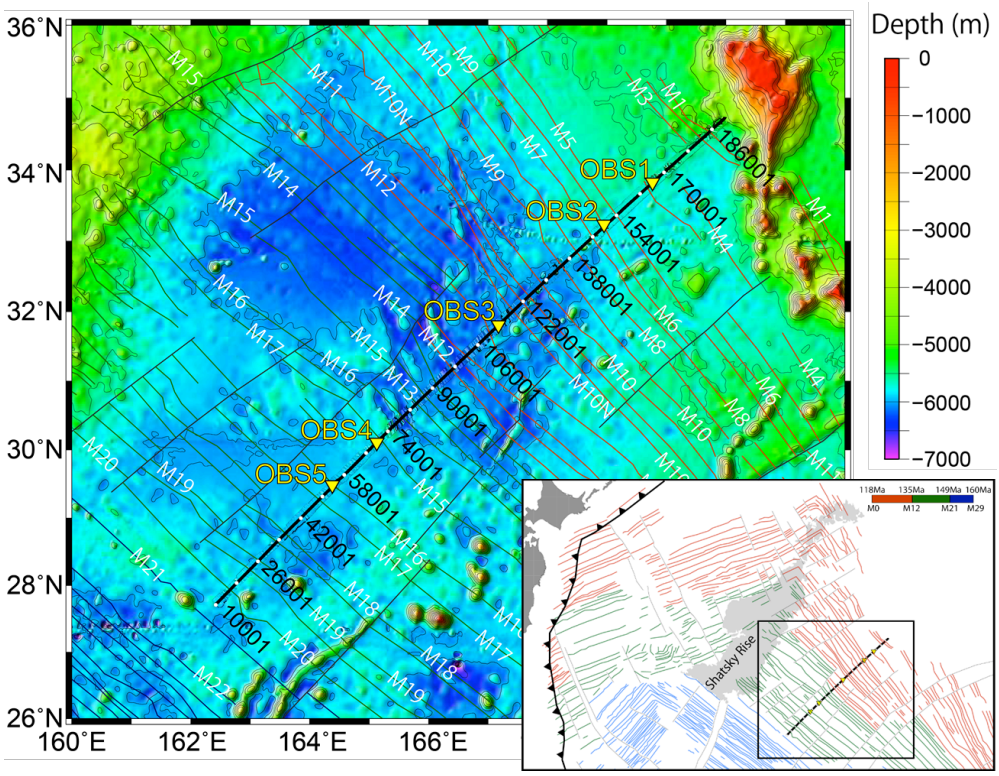

Fig. Bathymetric map of the study area. The thick black line shows a seismic refraction/reflection survey line. The yellow triangles represent OBSs. Color lines show magnetic lineations (Nakanishi et al., 1989).

P18

Observations of Grain- to Multi-Grain Scale Deformation to Elucidate the Development of Crystal Preferred Orientation during Diffusion Creep

Genta Maruyama[1] and Takehiko Hiraga[1]

[1]Earthquake Research Institute, University of Tokyo, Japan,

The seismic anisotropy in Earth's upper mantle has been explained by the crystallographic preferred orientation (CPO) of rock-forming minerals, which have anisotropic elasticity. Our team showed that the CPO of forsterite is produced even during diffusion creep and proposed its mechanism by a rigid-body like grain rotation (Miyazaki et al. 2013). We considered that grain boundary sliding selectively occurs at a low-index plane grain boundary, which is parallel to a long axis of grain controlled by crystallography. Such sliding forces grains to rotate toward specific tensile direction. The purpose of this study is to examine this hypothesis by observations of samples surface after the sample deformation where fine-scale strain markers were imposed.

We deformed cylindrical polycrystalline samples of synthesized forsterite plus 20 vol. % diopside and monomineralic anorthite, both of which develop low index plane grain boundaries, at their diffusion creep regime. We polished the lateral side of the sample where we imposed grooves parallel to the compression axis of the sample using a focused ion beam. These marker lines allow us to observe grain rotation due to a plastic deformation of the sample. After the high temperature 1 atmosphere compression experiment, we observed the marker lines under scanning electron microscope.

We succeeded to observe the marker lines after the deformation (Fig. 1a). Strain of bulk sample and of the marker line exhibited the similar values indicating the similar deformation proceeded both at bulk and surface regions of the samples. Grain rotation, which was identified by a rotation of intra-granular markers, was observed in all the samples. No distortion of the markers within the grains was found indicating the absence of intragranular deformation process such as a glide of dislocations; however, in the samples deformed at high stress (~300 MPa), curved intra-granular markers were observed, which is consistent with dislocation activity at high stress condition. Quantification of the grain rotation revealed that (1) the rotation angle increases with increasing strain, (2) the direction of grain rotation depends on the direction of long-axis of the grains (Fig. 1b) and (3) the grain rotation rate is largest at ~45º and smallest ~0º and ~90º against compression axis (Fig. 1b). Such observations were also found in anorthite aggregate.

Our experimental results showed not only the ability of identification of the deformation mechanism by the observation of the sample surface but also significant operation of grain rotation, which is necessary process for the development of CPO, during diffusion creep. With an assumption of the grain rotation rate to be proportional to shear stress

on the low-index plane grain boundary, we successfully reproduced variations of grain rotation rate with respect to the boundary orientation and alignment of long axis of the grains against compressional axis with increasing strain. Such results indicate that CPO can easily develop during diffusion creep as long as low-viscous low-index plane grain boundaries are present in polycrystalline aggregate (Fig. 1c).

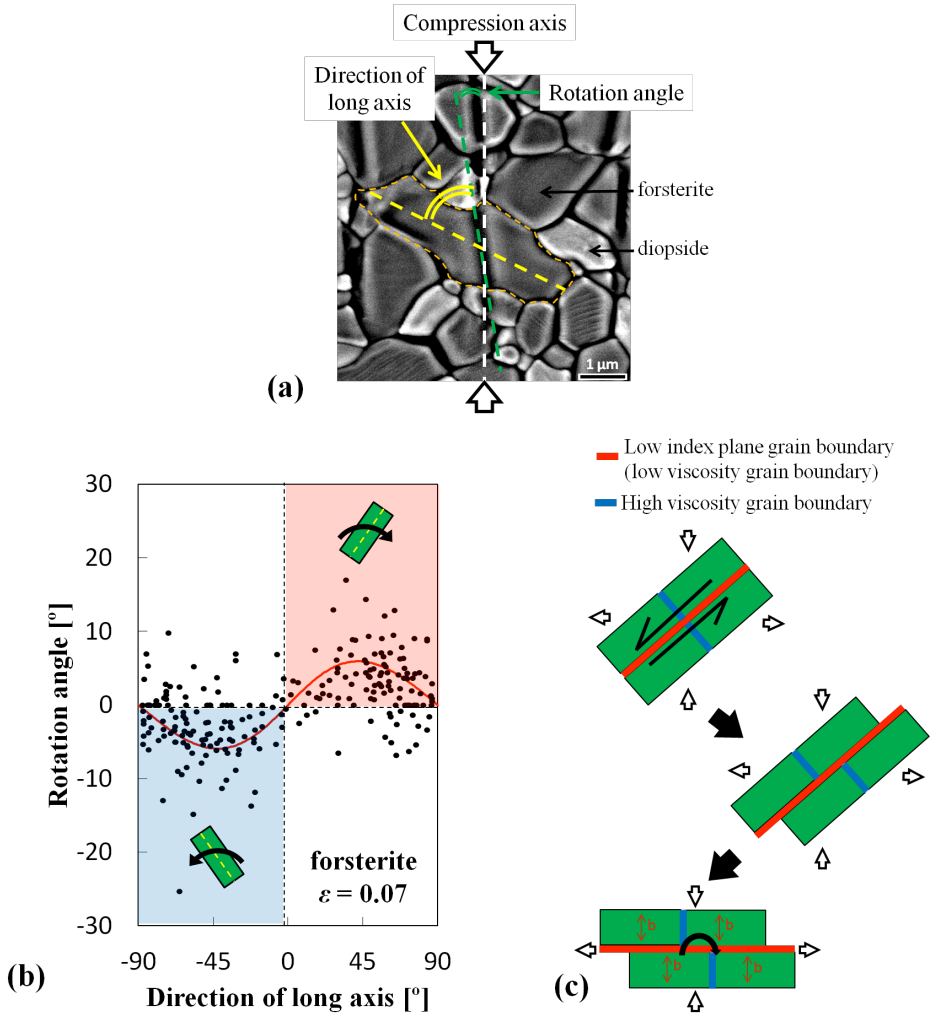

Fig. 1 (a) SEM image of the sample surface after deformation. (b) Direction of long axis of forsterite grain versus rotation angle of the grain measured from tilting angle of an intragranular line marker. The red line represents a calculated curve. (c) Our model of CPO development by a selective grain boundary sliding on low-index plane boundary.

P19

Anisotropic shear-velocity structure of the lithosphere-asthenosphere system in the central Pacific from the NoMelt experiment

P.Y. Lin[1], J. B. Gaherty[1], G. Jin[1], J.A. Collins[2], D. Lizarralde[2], R. Evans[2], G. Hirth[3] and H. F. Mark[2]

[1]Lamont-Doherty Earth Observatory of Columbia University
[2]Woods Hole Oceanographic Institution
[3]Brown University

The Recent theoretical models of the seismic properties of mantle rocks predict seismic velocity profiles for mature oceanic lithosphere that are fundamentally inconsistent with the best observations of seismic velocities in two ways. Observations of strong positive velocity gradients with depth, and a very sharp and very shallow low-velocity asthenosphere boundary (LAB), both suggest that non-thermal factors such as bulk composition, mineral fabric, grain size, and dehydration play important roles in controlling the formation of the lithosphere, and thus the underlying LAB. There is little consensus on which of these factors are dominant, in part because observations of detailed lithosphere structure are limited. To address this discrepancy, we conducted the NoMelt experiment on ~70 Ma Pacific lithosphere between the Clarion & Clipperton fracture zones. The experiment consists of a 600x400 km array of broad-band ocean bottom seismometers (OBS) and magnetotelluric instruments, and an active-source reflection/refraction experiment. Here we characterize the shear-velocity structure and its seismic anisotropy across the lithosphere-asthenosphere system beneath the array using surface-wave dispersion from ambient noise and earthquake-generated Rayleigh waves. Of the 27 deployed instruments, 21 were recovered, all of which produced useful data on the seismometer and the differential pressure gauge in the 20-200 s period band. Energetic, high S/N Rayleigh waves and useful love waves are observed from over 19 and 7 events with Mw > 6.5 respectively. Models of shear velocity as a function of depth derived from intra-array Rayleigh-wave phase velocities are characterized by a thin lid with high velocity overlying a modest low velocity zone and can pretty well fit the dry-olivine with a simple cooling model with no melt adding in. The Rayleigh-wave phase velocities show remarkable strong and clear evidence of azimuthal anisotropy with fast-directions parallel to fossil spreading (78^{o} azimuth) at periods of 14-60 seconds. The anisotropy appears to weaken slightly at intermediate periods, before strengthening and rotating slightly towards a more EW direction at the longest periods. The model of seismic anisotropy as a function of depth suggests strong seafloor-spreading fabric in the upper 60 km and the strength is relatively week in the asthenosphere. In addition to azimuthal anisotropy from shear velocity variations, the result from P-wave refraction data suggest that the upper 10-15 km of the mantle are strongly anisotropic, with velocities in the direction of fossil seafloor-spreading ~8% faster

than in the ridge-parallel direction. Love waves are difficult to observe on OBS data due to the higher noise levels generated observed on the horizontal components. We have measured the average phase velocity in the frequency band between 20-60 sec. Love-wave propagation in the ocean basins produces a complex multi-mode wavefield. The relatively contributions of fundamental and higher modes are strongly frequency dependent for the oceanic upper mantle.

P20

Anisotropy in the Pacific Upper Mantle from Inversion of a Surface-wave Dispersion Dataset

Celia L. Eddy[1], Göran Ekström[1], Meredith Nettles[1], and James B. Gaherty[1]
[1]Department of Earth and Environmental Sciences, Lamont-Doherty Earth Observatory, Columbia University

Models of seismic anisotropy in oceanic regions provide information about the geometry of strain and flow in the mantle, the specific nature of the lithosphere-asthenosphere boundary, and the possible presence of partial melt in the asthenosphere. In order to investigate these and other questions, we are developing a three-dimensional model of the anisotropic velocity structure of the Pacific upper mantle. We use measurements of fundamental-mode dispersion for Rayleigh and Love waves traversing oceanic paths. The observations are drawn from the waveform dataset used to construct the global dispersion model GDM52. To supplement this dataset, we make additional measurements of surface-wave dispersion on waveform data from the NoMelt experiment, a deployment of broadband ocean-bottom seismometers on ~70 Ma lithosphere between the Clarion and Clipperton fracture zones in the central Pacific. The shorter oceanic paths sampled by this dataset help improve the resolution of the velocity model in the Pacific by providing a regional constraint on the larger plate-scale model. We invert phase-velocity maps for the combined dataset for the anisotropic velocity structure at depth at several different locations in the Pacific basin. An oceanic reference model is used to compute the sensitivity of phase velocity to the elastic parameters. We find a clear distinction between lithosphere and asthenosphere in the central and western Pacific as defined by both v_S and anisotropy. We will incorporate waveform data into our three-dimensional modeling that contains higher-mode signals sensitive to deeper elastic structure; waveforms will help constrain both the average structure of the basin and potentially variations in the anisotropic parameter η. The goal of this work is to produce a three-dimensional model of isotropic and anisotropic velocities in the Pacific, which will improve constraints on olivine fabrics and strain geometries in the oceanic upper mantle.

P21

Electrical conductivity structure beneath backarc side of Chubu District, Central Japan, revealed by the Network-MT survey

Makoto Uyeshima[1] and Research Group of Network-MT Survey in Chubu District

[1]Earthquake Research Institute, University of Tokyo, Japan,

In order to elucidate regional scale deep resistivity structure, we performed series of the Network-MT surveys in backarc side of the Chubu District, Central Japan. In order to realize electric measurements relatively free from the static effect, we measured electrical potential differences with dipoles whose lengths range from several to several 10s kilometers by using telephone line networks (Uyeshima et al., 2001, Uyeshima, 2007). Six geomagnetic stations were installed in the target area for references and remote-references. Response functions in the frequency domain were estimated between each voltage differences and the magnetic field with the aid of a robust MT processing codes by Chave and Thomson, 1989 or Chave and Thomson, 2003, and they were inverted to obtain resistivity structures.

The first Network-MT campaign, was done in 2005-2008 in the vicinity of the Atotsugawa Fault (ATF), which runs along the Niigata-Kobe Tectonic Zone (NKTZ), where the most significant strain-rate accumulation in the inland area in Japan was detected by the dense GPS observation Network (GEONET). We obtained 2-D images beneath two lines in the back-arc area across the ATF. Both of the 2-D images contained conductive anomaly in the mantle wedge just above the Philippine Sea Plate (PHI) (Usui et al., 2010, Mogami et al., 2010) and the anomaly was interpreted as dehydrated fluid phase (melts or hydrous melts). Since the mid-crust conductors are located just beneath the main strike slip faults in the NKTZ, and are connected to the deep seated conductor just above the slab, we interpreted that the dehydrated fluids cause the strain accumulation in the narrow area of NKTZ.

In the western part of the Chubu district, in addition to undulation of the PHI (Hirose et al., 2008), dehydrations from both PHI and the deep seated Pacific Plate (PAC) may contribute generation of the Quaternary volcanoes and the NKTZ. Start point of the rupture for one of the largest inland earthquakes in Japan, the 1891 Noubi Earthquake (M8.0), was also located on the NKTZ. Thus, we did another Network-MT survey to the west of the first target area in 2011-2013. In wide area facing the Japan sea, we detected out of quadrant phases in the principal (off-diagonal) components of the impedance tensors, which cannot be explained by 2-D structure (Ichihara and Mogi, 2009). Then we applied a 3-D DASOCC inversion scheme (Siripunvaraporn et al., 2005) to obtain a 3-D resistivity structure. Along the Noubi Earthquake (M=8.0) seismic fault zone, a shallow and narrow conductive zone was located, and in the mid-crust beneath the zone, a rather resistive layer (higher than 1k Ohm m) was distributed. Just on the interface of the subducted Philippine Sea slab and beneath the rupture starting area, conductive anomaly is detected. In addition, another deep seated conductive zone was detected along the NKTZ. The conductive zone indicates existence of dehydration also from the Pacific Plate, as was pointed out by the geo-chemical investigation (Nakamura et al., 2008), and the fluids may cause the back-arc volcanism and strain rate accumulation.

P22

Upper mantle electrical resistivity structures beneath the Indian Ocean and back-arc basins

Nobukazu Seama[1] and Tetsuo Matsuno[2]

[1]Department of Earth and Planetary Sciences, Kobe University, Japan
[2]Earthquake Research Institute, University of Tokyo, Japan

We present preliminary or final results of upper mantle electrical resistivity structures beneath three areas in the Indian Ocean and beneath two back-arc basins; the Southwest Indian Ridge (SWIR) at 37ºE, the Southeast Indian Ridges (SEIR) near the Rodriguez Triple Junction, the western Cosmonauts Sea at the continental margin of East Antarctica, the Lau Basin, and the Mariana Trough. The magnetotelluric (MT) method is a base to estimate upper mantle resistivity structures. We conducted a series of marine MT experiments to obtain the electromagnetic variation data on the ocean bottom using OBEM (Ocean Bottom Electro-Magnetometer), and OBM (ocean bottom magnetometer) that is attached to ocean bottom seismograph (we can call this OBSM). We carried out the time-series data analysis to estimate the MT responses and corrected topographic distortions in the MT responses. We have basically performed a smooth model inversion analysis using the processed MT responses to estimate a resistivity structure with minimum model smoothness. As for the back-arc basins, we also have considered a prior constraint in the inversion analysis for the subducting slab inferred from a seismic research. For the SWIR, we conducted a marine MT experiment across the spreading axis at 37ºE using 7 OBEMs along a ~110 km profile for almost one year. These data were used to derive 2-D upper mantle resistivity structures beneath the observation line. Near the Rodriguez Triple Junction, we conducted a marine MT experiment across the central and southeast Indian Ridges for two months using 15 OBEMs and one OBM. Iizuka (2015) analyzed the data at three sites on the observation line across the SEIR to derive 1-D upper mantle resistivity structures beneath the sites. In the western Cosmonauts Sea, 2 OBEMs were used to obtain the time variation of the electromagnetic field on the old seafloor (likely >90 Ma) for two months during the 47th Japanese Antarctic Research Expedition. Three-dimensional forward modeling indicates 1-D structure of a thin conductive layer immediately under the sites (mostly sediment), an upper resistive layer (≥300 Ω-m) with less than 100 km thickness, and an underlying conductive structure (~10 Ω-m). In the Lau back-arc basin, we obtained 12 months length data by 2 OBEMs and 7-9 months length data by 11 OBMs along 2 observation lines across eastern Lau spreading center at 19.7ºS and 21.3ºS; the length of both observation lines are 150 km. It is worth noting that it is the first experiment to use OBSMs. Matsukura (2014) analyzed these data to derive 2-D upper mantle resistivity structures beneath the two observation lines. In the southern Mariana Trough back-arc basin, we conducted a marine MT experiment along a 120 km length observation line across the spreading axis, and we obtained 60-85 days length data by eight OBEMs. Shindo (2013) reported preliminary results from these data, and we reanalyzed the data to derive a 2-D upper mantle resistivity structure beneath the observation line. We will show all these results, which are compared with results from previous studies.

P23

Thermal conductivity of omphacite, jadeite and diopside under pressure : Implication for the role of eclogite in subduction slab

Masahiro Osako[1], Chao Wang[2] and Akira Yoneda[3]

[1]National Museum of Science and Nature, Tsukuba, Ibaraki, Japan
[2]China University of Geosciences, Wuhan, China
[3]Institute for Study of the Earth's Interior, Okayama University, Misasa, Tottori, Japan

Eclogite is one of the major rocks in subducted oceanic crust and the lowermost part of thickened continental crust. Thus, the thermal properties of eclogite are important in the control of various tectonic processes. The thermal property of eclogite can be constrained from those of its major components of garnet and omphacite by applying a rule of mixtures. We investigated the thermal properties of three pyroxenes: omphacite, diopside and jadeite. The thermal diffusivity and the thermal conductivity at high pressure were determined simultaneously up to 14 GPa and 1000 K in the Kawai-type multianvil apparatus using a pulse heating method. The heat capacity can be also obtained form these two properties. Polycrystalline samples of omphacite and diopside were synthesized from glasses with stoichiometric compositions, and natural jadeite from Itoigawa, Japan, was used in the present study. Measurements for omphacite are characterized by much lower thermal conductivity and thermal diffusivity than those of its two end-members of jadeite and diopside. Combining our result with thermal property data of garnet, the thermal structure of the subduction zone is addressed. The thermal conductivity of eclogite is much smaller than that of harzburgite, which is assumed to compose of 80% olivine and 20% enstatite, implying that subducted oceanic crust impedes thermal conduction from the hotter wedge mantle to the subducting slab. A simulation of the thermal structure shows that temperature of the subduction zone is about 50 K decreased when the effect of oceanic crust is included. This consequence means that the location of dehydration reactions of hydrous minerals should be about 50–100 km deeper in the central part of the slab and therefore can reach the area of dense hydrous minerals (such as phase A). This overlap consequently enables water to transport into the mantle transition zone.

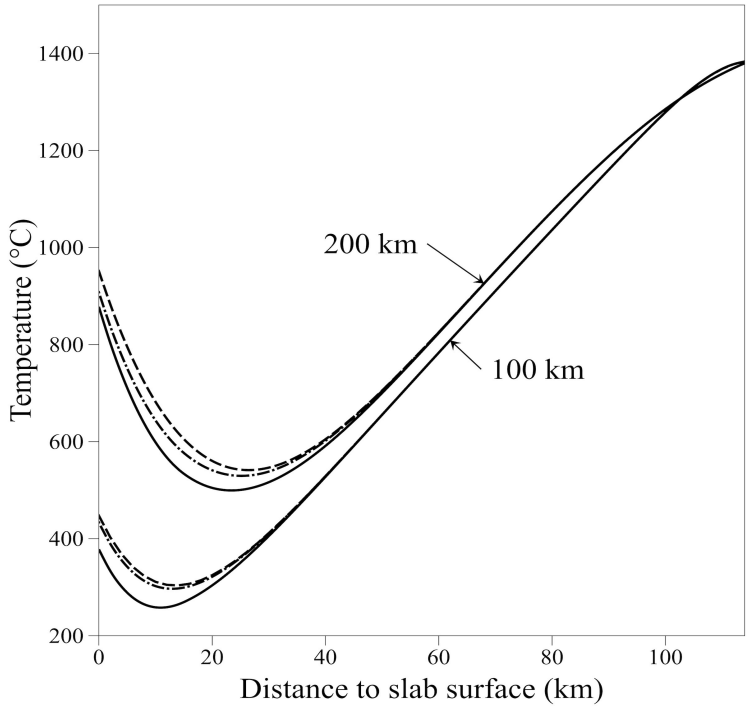

Fig. Thermal models for subducting slab. Modeled with a 120 Ma incoming lithosphere. Solid line: using eclogite (this study) for oceanic crust and harzburgite for lithospheric mantle; dashed line: using harzburgite for whole subducting slab; dash-dotted line: using eclogite [Dobson et al., 2010] for oceanic crust and harzburgite for lithospheric mantle. The thermal conductivity of the mantle wedge is assumed to be that of harzburgite.

References

Dobson, D. P. et al., (2010), High Press. Res., 30, 406–414.
Osako, M., E. Ito, and A. Yoneda (2004), Phys. Earth Planet. Inter., 143–144, 311–320.
Wang, C. et al. (2014), J. Geophys. Res., Solid Earth, 119, 6277–6287.

P24

Multiple-scale heat flow anomalies seaward of the Japan Trench associated with deformation of the incoming Pacific plate

Makoto Yamano[1], Yoshifumi Kawada[2] and Hideki Hamamoto[3]

[1]Earthquake Research Institute, University of Tokyo, Japan
[2]Japan Agency for Marine-Earth Science and Technology, Japan
[3]Research Institute, Center for Environmental Science in Saitama, Japan

The Pacific plate subducting along the Japan Trench is very old, over 130 m.y., and thus supposed to be cold. Extensive heat flow measurements conducted in the northern Japan Trench area, however, showed that high and variable heat flow values are pervasively distributed seaward of the trench and within about 150 km of the trench axis. In this anomalous zone, the average heat flow is 60 to 70 mW/m^2, appreciably higher than the value typical for the seafloor age (Yamano et al., 2014). The occurrence of the anomalous heat flow along the trench indicates that it results from processes closely related to deformation of the incoming plate. The seismic velocity structure of the oceanic crust also shows anomaly on the seaward side of the trench, attributable to fracturing and water infiltration due to plate bending (Fujie et al., 2013). Based on these observations, Kawada et al. (2014) proposed that thickening of the permeable layer in the oceanic crust due to fracturing leads to development of pore fluid circulation, which efficiently pumps up heat from the underlying impermeable basement. Numerical modeling showed that this process can yield a broad high heat flow anomaly at a scale of 100 km, as observed in the Japan Trench area. Similar high anomalies on the seaward side of the trench may exist in other subduction zones.

Overlapping the broad anomaly, local variations at a scale of a few kilometers were detected through concentrated measurements at some sites. Such local anomalies may arise from heterogeneity of the oceanic crust, e.g., basement topography and high-permeability faults. For investigation of the origin of the local anomalies, we conducted a dense heat flow survey along an E-W line around 39°N in an area 60 to 80 km from the trench axis, where immature horst and graben structures are found. The obtained 20-km detailed profile shows a prominent sawtooth-like variation (60 to 110 mW/m^2) at a scale of 3 to 5 km. This peculiar heat flow variation has no apparent correlation either with the basement topography or faults and might result from local variation in the permeability structure in deeper part of the oceanic crust.

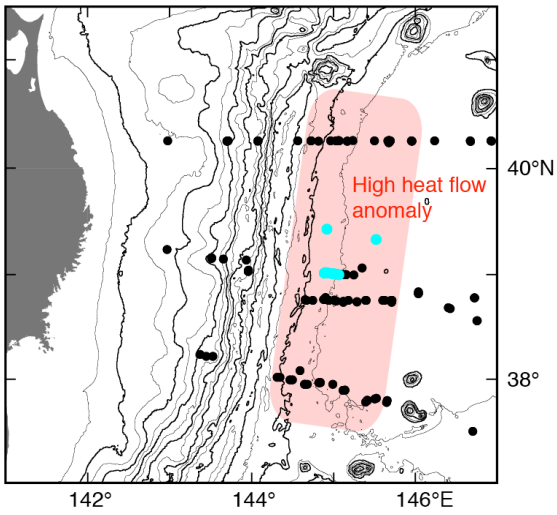

Broad high heat flow zone (reddish shade) seaward of the Japan Trench revealed by extensive measurements (black dots). Blue dots represent measurements made in 2014.

P25

Single Crystal Elasticity of Iron Bearing Perovskite and Post Perovskite Analog

Akira Yoneda[1]

[1]ISEI, Okayama Univ., Japan,

We measured single crystal elasticity of (1) pure and iron bearing $MgSiO_3$ perovskite, and (2) *Pbnm*-$CaIrO_3$ and *Cmcm*-$CaIrO_3$, a representative analog of $MgSiO_3$ perovskite and post perovskite, respectively, by means of inelastic X ray scattering at BL35XU, SPring-8. The present results for $MgSiO_3$ perovskite demonstrate that elastic anisotropy of magnesium perovskite is highly enhanced by iron incorporation. Furthermore anti-correlation between bulk sound velocity and shear wave velocity was confirmed with iron content, which is against the theoretical prediction. The anti-correlation found in this study is important, because it enables us to interpret the recent seismological observation of the anti-correlation in the deep lower mantle by means of iron content difference in perovskite. On the other hand, we can learn difference of elasticity between perovskite and post perovskite thorough measurement on $CaIrO_3$, as analog of $MgSiO_3$ perovskite and post perovskite. From a characteristics of the single crystal elasticity of $CaIrO_3$ compounds, we interpreted the texture pattern in the D" layer consistent with recent seismic observation.

P26

Observation and modeling of SKS splitting parameters measured in Japan with Hi-net

Naoto OGAWA[1], Hitoshi KAWAKATSU[1], Nozomu TAKEUCHI[1], and Katsuhiko SHIOMI[2]

[1]Earthquake Research Institute, University of Tokyo, Japan
[2]National Research Institute for Earth Science and Disaster Prevention, Japan

The interpretation of the splitting parameters (fast polarization direction φ and delay time δt) observed in subduction zones is rather difficult because anisotropic structures, such as mantle wedge, subducting slab, and asthenosphere, all contribute to them. Here we focus on the splitting intensity (SI) measurement introduced by Chevrot (2000). The SI method is based on cross-correlation of polarized waveforms, and has a potential to extend the finite-frequency tomography (Dahlen, 2000) for anisotropic structures.

In this study, to systematically investigate the spatial variation of seismic anisotropy around Japanese islands, we measured splitting parameters of teleseismic SKS phases using the dense seismic array Hi-net in Japan by two different methods: SI method and Wolfe & Silver (1998)'s method (based on Silver & Chan (1991)). We applied two band-pass filters between (1) 8-20 seconds and (2) 20-100 seconds. We selected ten seismic events which have good S/N ratio. The results indicate regional scale variations of splitting parameters that are apparently related to subduction systems, especially in Hokkaido, Tohoku, Kyushu, and Chugoku region.

In order to investigate detailed anisotropic structures (fabric in mantle wedge, subducting slab, and asthenosphere), we made forward modeling using synthetic seismograms. We modeled the SKS phases by the ray theory, and assumed that the SKS ray is straight and that each region has homogenous anisotropy. We calculated the phase velocity in each region by solving the Christoffel matrix. The preliminary analysis indicates that the measured splitting parameters appear to be primarily affected by the fast directions observed by surface waves using our OBS data (Takeo, 2014).

P27

On the effects of parameterization for radial anisotropy constrained by Love and Rayleigh waves

Kazunori Yoshizawa[1]

[1]Earth & Planetary Dynamics, Faculty of Science, Hokkaido University, Japan

The radial anisotropy of shear wave speed represents the differences between a vertically-polarized SV wave speed (Vsv) and horizontally-polarized SH wave speed (Vsh), and can be a key to understanding the dynamic processes and rheological properties in the upper mantle. Seismic surface waves are the most powerful tool to determine the spatial distribution of the radial anisotropy in the lithosphere and asthenosphere. Some recent studies have revealed the existence of a layer with strong radial anisotropy (Vsh > Vsv) beneath the lithosphere; e.g., under the Pacific plate (Nettles & Dziewonski, 2008, JGR) and the Australian continent (Yoshizawa, 2014, PEPI). This is, however, not always the case and there are also some earlier studies on radial anisotropy that do not show clearly such a layer with anomalous radial anisotropy underneath the lithosphere. The differences in model parameterization for surface wave inversions may attribute to the different estimates of radial anisotropy.

For the inversions of multi-mode phase speeds of Love and Rayleigh waves for S-wave radial anisotropy, we can use either set of model parameterization for anisotropic S wave speeds; i.e., (A) [Vsv, Vsh] or (B) [Vsv, ξ], where ξ is a radial anisotropy parameter $\xi=(Vsh/Vsv)^2$. The choice of the set of model parameters for inversion is arbitrary, and both parameterizations have been widely used in earlier studies. In this study, through synthetic experiments, we have confirmed that this difference causes non-negligible effects on the reconstruction of S-wave radial anisotropy. This is primarily caused by the differences in the sensitivity kernels of Love-wave phase speeds to the structural parameters; Vsv, Vsh and ξ.

For the set of parameters (B) [Vsv, ξ], Love waves always have the largest sensitivity to Vsv with suppressed sensitivity to ξ, and the kernel shapes for both Vsv and ξ are nearly identical, which imposes a strong correlation between the resultant SV and SH wave speeds. On the other hand, with the parameterization (A) [Vsv, Vsh], Love wave phase speeds are controlled primarily by Vsh, to which Love wave phase speeds have the largest sensitivity with little influence from Vsv, and, in this case, Vsv can be constrained almost independently by Rayleigh waves.

Such intrinsic differences in the sensitivities of surface waves can lead to somewhat different results in the estimated radial anisotropy. Our synthetic experiments suggest that the parameterization using [Vsv, Vsh] would be preferable, particularly when the strong radial anisotropy (SH>SV) is caused by anomalously “slower Vsv” (rather than faster Vsh), which is consistent with the recent anisotropy models of the fast moving Pacific and Australian plates. We have also found that the retrieved anisotropy using the [Vsv, ξ] parameterization tends to be dependent more strongly on the initial model.

P28

A preliminary resistivity model of the back arc region in the NE Japan arc based on marine and island MT data

Hiroshi Ichihara[1], Noriko Tada[1], Kiyoshi Baba[2], Takafumi Kasaya[1], Masahiro Ichiki[3], Toshiki Kaida[3] and Yasuo Ogawa[4]

[1]Japan Agency for Marine-Earth Science and Technology, Japan, [2]Earthquake Research Institute, University of Tokyo, Japan, [3]Tohoku University, Japan, [4]Tokyo Institute of Technology, Japan

The NE Japan arc is important research field to understand dynamics of mantle wedge. However, distribution of physical properties has not been understood especially beneath the back-arc region because the region is mostly located on the sea floor. In this study, we estimated electrical resistivity distribution in this area based on electromagnetic data obtained on the seafloor and islands in the eastern part of Japan Sea. The ocean bottom EM data were acquired with 6 ocean bottom electro-magnetometers (OBEMs) between April and August 2013 by MR13-02A and NT13-18 JAMSTEC scientific cruises. The island data were acquired in the 3 islands in the Japan Sea (Tobishima, Awashima and Sado islands) between April and October 2013. These recorded time-series data were converted to a frequency-domain impedance tensor based on the BIRRP program (Chave and Thomson, 2004). As results, high-quality MT responses and geomagnetic tippers in both the trench and back-arc areas. Then we estimated resistivity distribution based on the 3-D inversion code (Tada et al., 2012) after the correction local topographic effect. The inversion result shows a significant conductor above the subducting Pacific plate. Although depth and precise resistivity of the conductor is not well constrained in the present analyses, high phase tensor values (Phi2 >60 degree at period >8000 sec) estimated from the MT impedances support existence of the conductor. The deep conductor may be related to dehydration in subducting Pacific Plate and convention in the mantle wedge.

P29

A new parameter characterizing radial anisotropy

Hitoshi Kawakatsu

Earthquake Research Institute, University of Tokyo, Japan,

Kawakatsu et al. (2015) recently proposed a new parameter, η_κ, that properly characterizes the incidence angle dependency of seismic bodywaves in VTI system (radial anisotropy). While the commonly used parameter to describe VTI system, $\eta=F/(A-2L)$, has no simple physical meaning, the newly defined parameter,

$$\eta_\kappa = \frac{F+L}{(A-L)^{1/2}(C-L)^{1/2}}$$

where A, C, F and L denote the Love's elastic constants for transverse isotropy, measures the departure from the "elliptic condition" (Thomsen, 1986) when η_κ is not equal to unity, and characterizes nicely the incidence angle dependency of bodywaves (Figure 1). I suggest (and hope) this parameter to be used in future surface wave and bodywave modelings, rather than the conventional η.

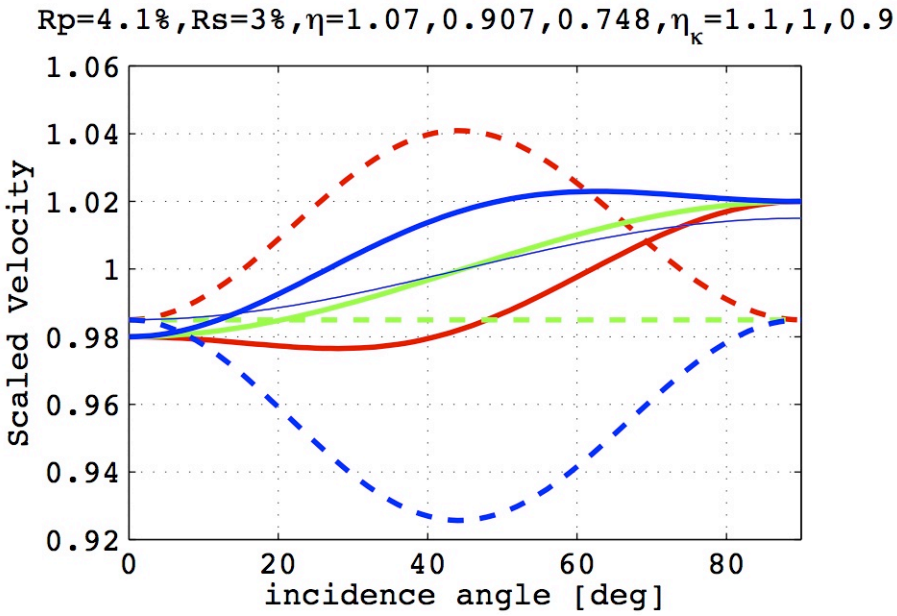

Fig. 1. Incidence angle dependency of bodywaves in three VTI systems that have the same P- and S-wave anisotropy (i.e. same ξ and ϕ). Red, green and blue colors are for η_κ=1.1, 1.0, 0.9, respectively (corresponding η values are indicated at top). Solid lines are for Vp, broken lines are for Vsv, and thin lines are for Vsh (same for all models). P and S anisotropy are 4% and 3%, respectively

Reference:

Kawakatsu, H, J-P Montagner, and T-R A Song, On DLA's h, in *The Interdisciplinary Earth: A volume in honor of Don L. Anderson*, edited by Foulger et al., GSA, in press (2015).

P30

Oceanic plate structures beneath the northwestern Pacific Ocean revealed by explosion experiments

T. Isse[1], H. Shiobara[1], M. Shinohara[1], T. Yamada[1], T. Yagi[1], H. Sugioka[2], H. Utada[1]

[1]Earthquake Research Institute, University of Tokyo, Japan,
[2]Japan Agency for Marine-Earth Science and Technology, Japan

Plate tectonics is based on a concept that a rigid lithosphere moves over a weaker asthenosphere. Understanding of the plate tectonics is important to understand the Earth's system. However, the nature of the lithosphere and asthenosphere boundary (LAB) is not yet well determined. To understand the physical condition for the LAB, we have conduct a seafloor observation called " Normal Oceanic Mantle (NOMan) Project". We focused on the oceanic plate because the nature and evolution history of the oceanic plate is simpler than the continental plate so that it is easier to investigate its nature.

To analyze the upper mantle structures around the LAB, we conducted a seismic explosion experiments as a part of NOMan project.

Seismic explosion experiments were conducted at four shot sites with ten broadband ocean bottom seismometers and the size of explosions is 400 kg at two sites, and 200 kg at other sites. The profile lengths are about 700 and 400 km, respectively.

Previous studies in this area revealed the azimuthal anisotropy in the uppermost lithosphere (Shinohara et al., 2008), a sharp LAB at a depth of ~ 80 km (Kawakatsu et al. 2009), small-scale heterogeneities in the lithosphere (Shito et al., 2013).

The results show the azimuthal anisotropy whose amplitude is about 4% and whose fast axis is nearly perpendicular to the magnetic lineations. Some Pn waveforms at ~ 300 km is complicated although some others are simple, which may suggest the existence of the heterogeneities in the lithosphere.

P31

Possibility of anisotropic structure in electrical conductivity for the upper mantle beneath northwestern Pacific Ocean

Kiyoshi Baba[1] and Hisashi Utada[1]

[1]Earthquake Research Institute, The University of Tokyo, Japan

We have estimated isotropic one-dimensional (1-D) structure in electrical conductivity beneath the northwestern Pacific through Normal Oceanic Mantle Project. However, the model did not explain observed magnetotelluric (MT) responses perfectly. The misfits should be attributed to the lateral heterogeneity and/or anisotropic structure. In this study, we examined if some possible anisotropic structures can explain the observed MT responses better or not. We consider anisotropic structures that the conductivity in the asthenospheric mantle is higher in the direction parallel to the current plate motion (~N63°W) and that the conductivity in the lithospheric mantle is higher in the direction parallel to the past plate spreading direction (~N22°W). We also consider the effect on surface heterogeneity due to ocean-land distribution and bathymetric change. We simulated MT responses in the survey area A (northwest of the Shatsky Rise) to the 3-D surface heterogeneity over 1-D anisotropic structures and compared with the MT responses observed and simulated to the isotropic model. The result showed that any models considered in this study did not improve the misfit to the data, suggesting that rather laterally heterogeneous structure is more likely.

Program committee:
Hitoshi Kawakatsu (chair), Kiyoshi Baba, Thorsten Becker, Donald Forsyth,
Takehiko Hiraga, Jean-Paul Montagner, Pascal Tarits

Local Organizing committee:
Hisashi Utada (chair), Daisuke Suetsugu (co-chair), Hajime Shiobara, Nozomu Takeuchi,
Hisayoshi Shimizu, Takehi Isse, Kiyoshi Baba;
Junko Odawara, Hitomi Umeda (Secretariat)